Master's thesis

NTNU
Norwegian University of Science and Technology
Faculty of Information Technology and Electrical Engineering
Department of Electric Power Engineering

Eirik Ivarsøy

Optimal planning of fast charging stations for EVs – A Norwegian case study

Master's thesis in Energy and Environmental Engineering
Supervisor: Magnus Korpås NTNU and Bendikk Nybakk Trosæter
SINTEF Energy Research

June 2020

NTNU
Norwegian University of Science and Technology

Eirik Ivarsøy

Optimal planning of fast charging stations for EVs – A Norwegian case study

Master's thesis in Energy and Environmental Engineering
Supervisor: Magnus Korpås NTNU and Bendikk Nybakk Trosæter
SINTEF Energy Research
June 2020

Norwegian University of Science and Technology
Faculty of Information Technology and Electrical Engineering
Department of Electric Power Engineering

NTNU
Norwegian University of
Science and Technology

Abstract

The integration of electric vehicles (EVs) plays an integral part in reducing GHG emissions from the transport sector. In recent years, the number of EVs has increased rapidly. Due to government policies and technological advancement, the growth is expected to continue. The EVs have a limited range, but it will often be sufficient for daily routines. However, to enable long-distance travel, a network of fast charging stations (FCSs) is needed. Fast charging of EVs is characterized by its stochastic nature, high power, and short charging time. This can potentially result in bottlenecks in the grid.

To face the challenges that come with the integration of FCSs into the distribution grid, an optimal planning scheme is needed. The main objective of this master thesis was to develop a model to decide the optimal planning of an FCS network. In this thesis, an EV mobility model, FCS load model and distribution grid model are combined in an optimization model to decide the optimal planning of FCSs.

The FCS load model is developed to determine the load profile at different FCSs. The FCS load model includes the EV traffic flow, EV charging curves and temperature-dependent driving consumption. The available traffic data was inadequate. Hence, a mobility model was developed to create a more detailed traffic flow of EVs in the system. The EV mobility model determines the route of each EV. The FCS load model determines the charging need of the different EVs and which FCS they will charge at. Then, by aggregating the charging needs of the EVs, the charging demand at each FCSs is determined.

The data about the Norwegian distribution grid is not open to the public. Thus, a novel distribution grid model was developed, which creates and dimension distribution grids. The proposed distribution grid model is based on power system planning principles, taking into consideration both economic and power system aspects.

The aforementioned models are combined in the optimization model. The optimal planning of FCSs is a nonlinear problem and a particle swarm optimization (PSO) algorithm is implemented to solve the problem. The proposed optimization model is a two-step model, the first step determines the location of the FCSs, and the second step determines the number of charging points.

The performance of the developed optimization model was tested on a 74 km stretch of highway between Gardermoen and Hamar. There are many aspects to consider when planning an FCS network. Thus, different objective functions were used in the optimization model. The first case study minimized the additional energy losses in the distribution grid due to the integration of FCS. For the second case study, the cost of FCSs was added to the objective function. For the final case, the perspective of EV owners was taken into consideration, by assigning a cost to EV detours. Thus, for the last objective function, the perspective of the DSO, FCS operator and EV owners were included.

The results illuminate how the optimal number of FCSs and their location is highly dependent on the objective function. For the three case studies performed, all got a different optimal number of FCSs. The proposed optimization model was able to find the optimum solution with all the three objective functions. To compare the different objective functions, the social cost was computed for all three cases. The results showed that the social cost was highest for case 2, which only considers the DSO and FCS operator perspective. This resulted in a 25.2% higher social cost for case 2 than case 3, with most of the increase due to a 5400% increase in the detour cost. Thus, emphasizing the importance of considering the perspective of all the interested parties when planning an FCS network. The effects on the serviceability of an FCS when reducing its peak power were investigated. This showed promising results as the peak power of the FCS could be reduced significantly, with little impact on the serviceability of the FCS.

Sammendrag

Elektriske biler spiller en sentral rolle for å redusere utslippene av drivhusgasser fra transport sektoren. Antall elbiler har vokst raskt i løpet av de siste årene. Denne er veksten er forvente å fortsette, grunnet teknologiske fremskritt og statlige insentiver. Elektriske biler har en begrenset rekkevidde, men den vi som oftest være tilstrekkelig for daglig bruk. For lengre kjøreturer er elbilene avhengig av er nettverk av hurtigladestasjoner. Hurtiglading av elbiler kjennetegnes ved høy effekt, kort ladetid og uforutsigbart ladetidspunkt. Dette kan potensielt føre til problemer for distribusjonsnettet.

For å minimere ulempene som kan forekomme ved utbygging av hurtigladestasjoner trengs det et planleggings verktøy. Hovedfokuset i denne masteroppgaven er å bestemme den optimale plasseringen til hurtigladestasjoner. Dette er gjort ved å lage en trafikkmodell, en hurtigladestasjon lastmodell og en modell som dimensjonerer distribusjonsnettet. Disse tre modellene gir informasjon til en optimeringsmodell, som bestemmer posisjonen og størrelsen til hurtigladestasjonene.

Lastmodellen kalkulerer lasten til de ulike hurtigladestasjonene. Dette gjøres ved hjelp av trafikkflyten til elbilene, ladekurvene til elbilene og temperaturavhengig energiforbruk. En trafikkmodell ble utviklet siden den tilgjengelige trafikkdataen ikke var nøyaktig nok. Trafikkmodellen bestemmer kjøreruten til hver eneste elbil. Lastmodellen bestemmer først lasten til hver elbil og hvilken hurtigladestasjon den skal lade på. Før lasten til en hurtigladestasjon beregnes ved å legge sammen lasten fra alle elbilene som skal lade på den samme hurtigladestasjonen.

Data om distribusjonsnettene i Norge, er ikke tilgjengelig for allmennheten. Dette gjorde at en nettmodell ble utviklet, som generere og dimensjonerer distribusjonsnett. Distribusjonsnettene er dimensjonert ved bruk av økonomisk optimalt tverrsnitt.

De nevnte modellen er til sammen kombinert inn i optimeringsmodellen. Optimal plassering av hurtigladestasjoner er et ikke-lineært optimeringsproblem og partikkelsverm optimering er tatt i bruk. Den forslåtte optimeringsmodellen er todelt, hvor den første steget bestemmer posisjonen til hurtigladestasjonene og steg nummer to bestemmer antall ladepunkt.

Optimeringsmodellen ble brukt til å designe et ladenettverk langs 74 km motorvei mellom Gardermoen og Hamar. Det er mange aktører som har en interesse av hvor hurtigladestasjonene plasseres. Det ble derfor brukt flere objektivfunksjoner. I det første scenarioet var målet å minimere tapene i distribusjonsnettet som følge av integrasjon av hurtigladestasjoner. I scenario nummer 2 ble kostnaden av hurtigladestasjoner lagt til objektivfunksjonen. I det siste scenarioet ble interessene til elbil eierne lagt til objektivfunksjonen. Dette ble gjort ved legge til en kostnad til omveiskjøring for å komme til en hurtigladestasjon. Dermed er interessene til både hurtigladestasjonsoperatør, nettoperatør og elbil eier inkludert i den siste objektivfunksjonen.

Resultatene viser den optimale løsningen varierer med både antall ladestasjoner og ladestasjonenes posisjon. De tre scenarioene fikk alle ulikt antall ladestasjoner for den optimale løsningen. Den samfunnsøkonomiske kostnaden ble beregne for alle de tre scenarioene. Resultatene viste at den samfunnsøkonomiske kostnaden ble høyest ved objektivfunksjon 2, som bare inkluderer interessene hurtigladestasjonsoperatør og nettoperatør. Da var den samfunnsøkonomiske kostnaden 25.2 % høyere enn i scenario 3 som var billigst. Mesteparten av økningen var på grunn av omkjøringskostnaden var 5400 % høyere i scenario 2 enn i scenario 3. Dette understreker viktigheten ved å inkludere interessene til alle involverte parter når et hurtigladestasjonsnettverk skal designes.

Preface

This master thesis is submitted as final work for the degree of master of science at the Norwegian University of Science and Technology. This master thesis is written in collaboration with and is a part of KPN FuChar[1]. FuChar is a KPN project funded by The Research Council of Norway and industry partners (grant no. 295133/E20). The FuChar project aims to minimise investment and operating costs related to the grid integration of electric transport.

The master thesis builds on the work presented in the specialization projected that was delivered in December 2019 [1]. As it should be possible to read the master thesis without reading the specialization project, parts of chapter 2, 3 and 5 has been reused. Chapter 2 covers the background for the work, and as the master thesis is continuation of the work presented in the specialization project, some parts are reused. However, its been modified and a section about the FCS development in Norway has been added. In chapter 3, the literature review about demand modelling has been reused and a section has been added about the state-of-the-art research on optimal planning of FCSs. In Chapter 5, the FCS load model developed in the specialization project is modified and extended from one to multiple FCS.

I would like to thank my supervisor, Professor Magnus Korpås, for your guidance throughout the process of writing this thesis. I'm grateful for your availability for discussions and thoughtful supervision. I would also like to thank my co-supervisor Bendik Nybakk Torsæter at SINTEF Energy Research. I'm grateful for your valuable help and guidance. Finally, I wish to thank my family for their continuous support during my education.

Trondheim, June 2020

Eirik Ivarsøy

[1] https://www.sintef.no/projectweb/fuchar/

Contents

List of Tables

List of Figures

Abbreviations

EV	-	Electric vehicle
PHEV	-	Plug-in hybrid electric vehicle
BEV	-	Battery electric vehicle
ICE	-	Internal combustion engine
FCS	-	Fast charging station
MCS	-	Monte Carlo simulation
BESS	-	Battery energy storage system
SOC	-	State of charge
PSO	-	Particle swarm optimization
IPSO	-	Integer particle swarm optimization
BPSO	-	Binary particle swarm optimization
DSO	-	Distribution system operator

1 Introduction

1.1 Motivation

The transport sector accounts for 25% of the world's CO2-emissions [2] and road vehicles are responsible for the majority of these emissions. They are also accountable for 80% of the rise in GHG-emission from the transport sector from 1970-2020 [3]. The situation in the EU is similar, with more than 60% of the CO2-emission from the transport sectors coming from road vehicles [4]. The Paris agreement, which 187 states have ratified, aims to keep "*a global temperature rise this century well below 2 degrees Celsius above pre-industrial levels and to pursue efforts to limit the temperature increase even further to 1.5 degrees Celsius*"[5].

Electrification of the transport sector will play an important role in reaching the goal of the Paris Agreement. A transition away from ICE to EVs, will lower the dependency on fossil fuels and lower the emissions. However, there are some barriers to overcome. EVs have less range, slower charging time and are more expensive, compared to their ICE equivalents. With technology advancements within power electronics and battery technology, the range is increasing. Also, batteries are becoming cheaper and governments are adding incentives to switch to EVs. Thus, helping with the economic aspect of the transition from ICE to EVs.

Even though the range is increasing, an FCS network is necessary for long-distance travel. High power at the charging points of the FCSs is necessary to compete with the fulling time of ICE vehicles. From a distribution grid perspective, the integration of FCS presents a potential problem. With its stochastic nature, short charging time and high power, it can present a potential grid capacity issue. Thus, it can potentially reduce the quality of supply or costly investments to upgrade the distribution grid is needed. The placement of FCSs is therefore of great interest from the distribution system operator's perspective (DSO). However, the DSO is not the only interested party. FCSs operator wants to locate their FCSs to maximize profitability. Lastly, EV owners wants a high density of FCSs with many charging points to avoid range anxiety and long waiting time.

1.2 Objective

This thesis aims to develop an optimization model to decide the location and number of charging points for each FCS in an FCS network. The model should ensure grid stability and take into account the interests of the DSO, FCS operator and EV owners. Investigate how different objective functions impact the optimal planning of FCSs. Furthermore, the effects on the serviceability of an FCS when reducing its peak power is investigated.

1.3 Report outline

The thesis is divided into 11 chapters. In the first chapter, the motivation and aim of thesis are covered. In chapter 2, the background and current trends of EV integration and FCS deployment are presented. Chapter 3, contains a literature review of the current state-of-the-art research on FCS demand modeling and optimal planning of FCSs. In chapter 4, the relevant theory is presented. Then, in chapter 5, the different models used in the thesis are described. In chapter 6, the system and input to the different models are described, also some subresults are presented. Chapter 7, describes the different cases that are studied and the main results are presented in section 8. Then, in chapter 9, the developed models, subresults and main results are discussed. Lastly, the conclusion is drawn in chapter 10, with further work presented in chapter 11.

2 Background

2.1 Global EV status

EV sales are increasing rapidly. In 2018, over 2 million EVs were sold, adding to a total of over 5 million EVs worldwide [6]. The main contributor to this growth is China with over 1 million EVs, followed by Europe and the United States. The market share and EV sales of the biggest EV markets are depicted in figure 1. The light-shaded part of the bar plot represents the PHEVs, while the darker represent BEVs. PHEVs are cars with an ICE and a battery that can either be charged by the engine or from a charger. BEVs are purely electric, only containing a battery. The EV market in China is dominated by BEVs, while in Europe its a more equal share between BEVs and PHEVs, as seen from figure 1.

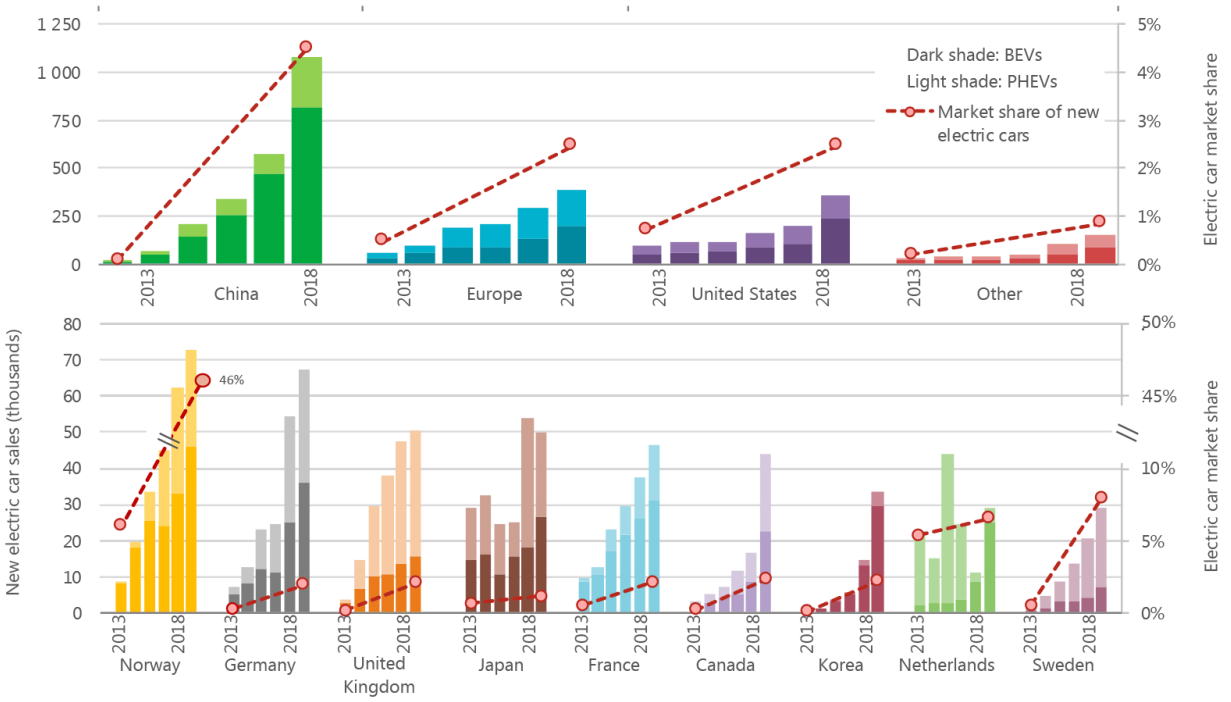

Figure 1: EV sales and market share in the period 2013-2018. Figure from [2]

Despite the rapid growth in global EV sales, the global market share is still low. So action is needed to further increase the growth of EVs. The EU has committed to a 37.5% C02 reduction from new cars by 2030 [7], compared to 2019 levels. To reach this goal, it's proposed that 35% of new car sales from 2030, should be PHEVs or BEVs. Various countries in the EU has taken action to transition away from ICE vehicles. Both the UK [8] and France [9] has set goals targeting no new ICE sales after 2040, with the UK including hybrid vehicles as well. The UK also aims to see at least 50% of new car sales in 2030 to be either EV or PHEV. Ireland wants to face out ICE cars faster, aiming to stop selling new ICE cars after 2030 [10]. Major cities have also taken action towards reducing its GHG-emission from transport. Paris is aiming to ban ICE cars by 2030 and only allowing EVs to drive in the city [11]. These are all important actions towards increasing the share of EVs and lowering the GHG-emission. However, with current EU regulation, member countries are not allowed to ban ICE [12].

IEA has developed two future scenarios for the growth of the global EV stock, illustrated in figure 2. Both scenarios include more than passenger light-duty vehicles, such as buses or trucks. However, passenger light-duty vehicles have a dominating share of the global stock in both scenarios. The New Policies Scenario

is based on the current policies from various countries along with an extension of the current technology advancement. This scenario predicts the global EV stock to be slightly below 150 million vehicles in 2030. The second scenario is based on the goal of the EV30@30 campaign [13]. The campaign's goal is that EV sales will stand for 30% market share by 2030. There are currently only 11 participating countries, this includes China, India, Japan, Norway, and France, among others. If this goal is reached, the scenario predicts that by 2030 there will be more than 250 million EVs globally. In the rest of this thesis EV reefers to BEV.

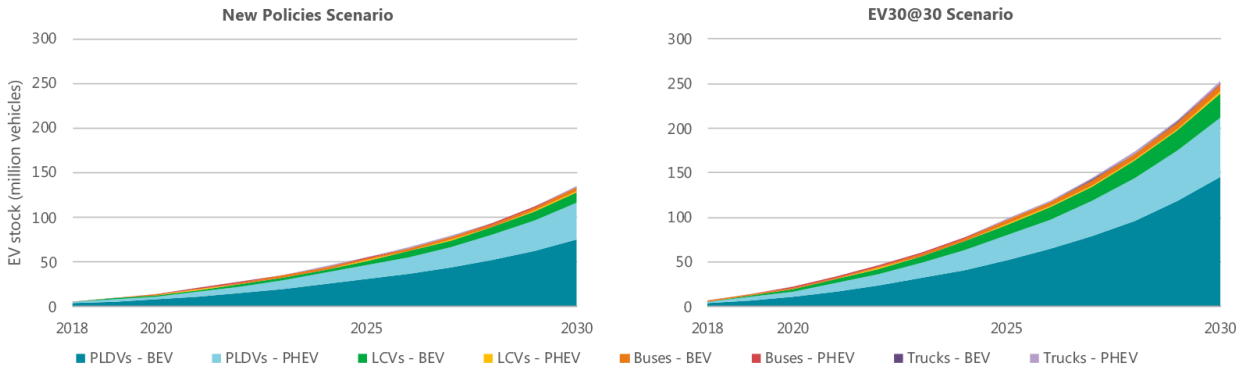

Figure 2: Future EV sales. Figure from [2]

2.2 EVs in Norway

Norway is the world-leading nation in EV integration, with EVs accounting for 42.4% of the sales of new cars in 2019 [14]. The evolution of the Norwegian EV sale is illustrated in figure 3. Even though the EV sales have increased rapidly in the last few years, EVs only account for 9.3% of the total number of cars in Norway [15] at the start of 2020. Nonetheless, Norway is way ahead of the rest of the world. This has been achieved by national polices to stimulate EV sales, among them VAT exemption on EV and registration tax exemptions. Many cities have also given incentives to purchase of EVs, with access to bus lanes, free parking, and free toll roads, among a few benefits.

Norway is, through "klimaloven", committed to reducing its GHG-emissions with a least 40% in 2030 compared to 1990 [17]. Norway also has a target of becoming a low-emission society by 2050, reducing its emissions by 80-95%. These policies and targets have resulted in Norway aiming to have all new cars be zero-emission vehicles by 2025, through "Nasjonal transportplan 2018-2029" [18]. With the current development in Norway, it's clear that if the target is to be reached, EVs will account for the vast majority of the zero-emission vehicles.

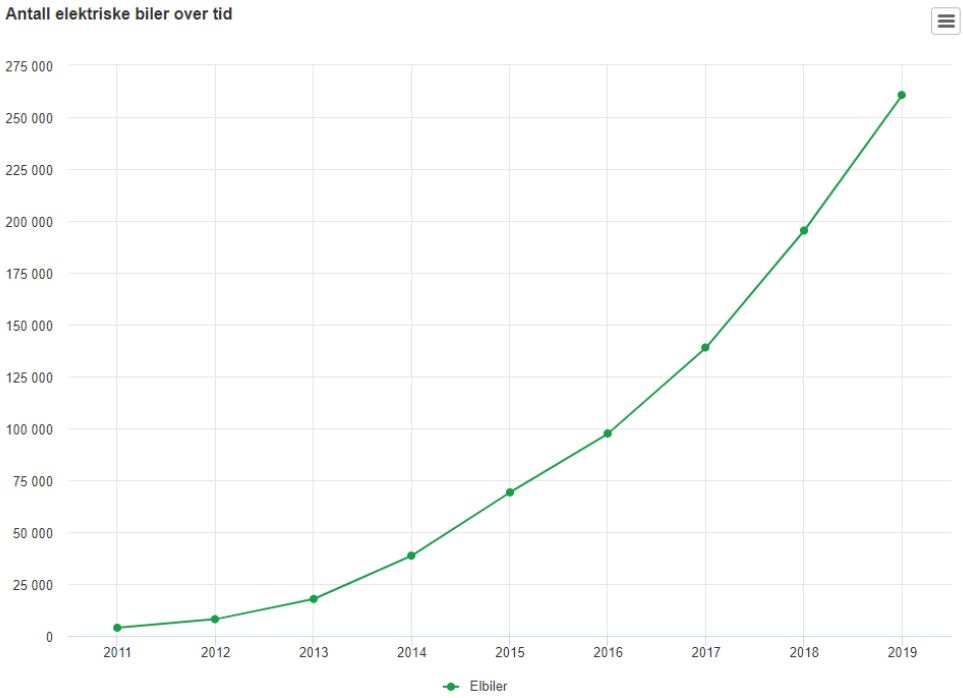

Figure 3: Number of EVs in Norway from 2011-2019. Figure from [16]

2.3 Fast charging

EV charging can either be done with AC or DC. The main difference is that for AC charging, the current is converted to DC inside the EV. For fast charging purposes, DC is used, due to the limitation of the on-board AC/DC converter. Fast charging is defined as charging at or above 50 kW. There are two main charging systems for fast charging CHAdeMO and CCS. CHAdeMO was the first charging system to enter the market and is primarily used by Nissan and Mitsubishi. CHAdeMO was the preferred charging system, but in recent years CCS has gained more traction and the majority of the new EV entering the marked supports CCS [19].

At an FCS, there can be one or several charging points. Most of the current FCS only offer charging at 50 kW. However, to close the gap between fuelling time for ICE vehicles and charging time of EVs, charging points that support charging at higher powers are being installed. Charging points with a charging power of 350 kW have been installed [20]. Charging with this power would substantially reduce the charging time of EVs. Still, there are currently not any commercially available EVs that can charger at this speed. Some automobile companies have announced that they are in the process of releasing EVs that charge with 350kW, but this is expensive high-end EVs. Still, this development will put automobile companies and customers at ease, because when EVs are capable of charging at such high power, there will be existing infrastructure. It's also important to note, that even though EVs are not capable to charge at 350 kW, they can still use the charging point. The EV's own battery management system will limit the power drawn from the charging point.

2.4 FCS development in Norway

By the beginning of 2020, there were a total of 2362 fast charging points in Norway [22]. The number is rapidly increasing, with 713 new fast charging points being installed in 2019 [23]. There was also a massive increase in ultra fast charging points[2], going from 25 in 2018 to 226 by the end of 2019. To close the gap between fuelling time for ICE vehicles and charging time of EVs, charging points that support ultra fast charging is important. Tesla was one of the pioneers in the Norwegian market, with all its V2 Supercharger allowing peak power of 120 kW, and later 150kW. The first V3 Supercharger FCS was opened in June 2019, which allows for peak charging up to 250kW [24], but only for select models. Though Tesla is the biggest FCS operator in Norway, there are plenty of other operators such as Fortum, Grønn kontakt and Ionity.

Even though the FCS network in Norway is growing rapidly, there are still parts of Norway were the exist no FCS network[25]. However, an FCS network consisting of 25 FCSs in the most northern part of Norway is expected to be ready in late 2020[26]. To reach the goal of all new cars be zero-emission vehicles by 2025, it's estimated that 8000 new fast charging points are needed [27]. This is 1100 fast charging points per year, which is nearly twice the number of fast charging points being installed in 2019.

[2]Ultra fast charging points is here defined as charging points delivering 150kW or more

3 Literature Review

3.1 Demand modeling

Accurate models for the load of the FCS are necessary to study its impact on the distribution grid, as well as to determine the optimal placing and sizing of new FCS. The arrival of the EVs to the FCS is one of the key factors in modeling the load of an FCS.

There is limited data available for the arrival of EVs to FCS, and it's also highly dependent on the location of the FCS. Therefore, a lot of research papers use other approaches to model the arrival rate at the FCS. In [28] - [35], a mobility model of the EVs is built on statistical data or local traffic flow. Based on the mobility model, the arrival of the EVs at the FCS is determined. A simpler approach is used in [36] - [39], where a predefined arrival rate is used.

Data from the National Highway Transport Survey is used to build a mobility model in [28] - [32]. This is a US-wide survey, recording information about the number of trips each day, departure and arrival time of each trip and length of each trip. Based on the statistical data, a mobility model is built. The EVs are initialized with a SOC and battery capacity, and the driving data is generated. Two approaches are used, either directly sampling from the distribution [28] - [32] or building a statistical distribution [28]. The EV will charge at the FCS if the SOC goes below a certain limit before a trip is completed. By adding the demand from each EV that visits the FCS, the load profile for the FCS is constructed. Due to the low market share of EVs in the US, the use of the NHTS data builds on the assumption that the driving pattern is the same for EVs as for ICE cars. A drawback of using the NHTS data set is that it's based on driving data for the whole US, which doesn't necessarily reflect local mobility patterns in the area where the FCS is located.

Local mobility patterns were included in [29], where the distribution of vehicles on the road was used to determine the load profile of the FCS. The percentage of vehicles on the road was divided into intervals, and each interval corresponded to an arrival rate of EVs at the FCS. In [33], the traffic flow from the highway where the FCSs were placed was used to determine the arrival of the EVs. Since the EVs arrived into a system, the daily driving distance was not of interest but the SOC when they entered the highway. SOC, driving efficiency and battery size were varied in between limits. Monte Carlo Simulation was then used to get aggregated and individual load curves for the FCSs.

Predefined arrival rates are used in [36] - [38]. Both [36] and [37] uses a predefined arrival rate based on arrival time distribution of ICE vehicles at gas stations. The daily expected number of EVs visiting the FCS is then used with the hourly arrival rate, to determined the hourly expected number of EVs. The expected number of EVs is then used as an input in a Poisson algorithm, to get the actual number of visiting EVs and the time of their arrival. A simpler approach is used in [39], where the number of visiting EVs each hour is predefined.

As the popularity of EVs increases, the usage of the FCS will follow. This will cause queues at FCS, especially in peak charging hours. Queuing will affect the load profiles and its therefore important to implement queuing models. A $M_1/M_2/\text{c}$ queuing model is implemented in [28, 29, 31, 33]. Where M_1 is the arrival rate at the FCS, M_2 is the service rate(charging time + wait) and c is the number of charging points. This queuing model doesn't have any limitations on the length of the queue. In the case of long queues, EV owners might choose to leave the FCS to charge elsewhere. Therefore, a $M_1/M_2/\text{c/k}$ queuing model is implemented in [37]. This is a loss system where the queue is limited to k EVs. A similar queuing model is used in [36], but the queue is limited in waiting time, instead of the number of EVs. All these queuing models follow the first-come, first-served principle and assume full transparency when it comes to the length of the queue.

The charging power selected in the simulations impacts the demand profile of the FCS. The power that the EVs charge with, affects both the shape and peak of the demand profile. The majority of the research papers assumes 50 kW as the charging power [28, 29, 31, 35, 38]. However, there is already a considerable

amount of EVs on the market that supports charging above 50 kW and market share is growing. Therefore, studies with charging power above 50 kW are important, both to look at the current and future demand profiles. Different charging powers between 50-250 kW is used in [33], but only 100 kW is used for the simulation results. In [39], it's assumed that the EV charges at 2C of its battery capacity. With the battery capacity of the EVs in the model, this results in charging between 66 - 200 kW. The charging curves of EVs with a maximum charging power of 50kW, 125kW and 350 kW are presented in [30]. The curves show that constant charging power is a good approximation when charging at 50 kW. However, when charging at the higher charging powers it's no longer constant and the charging curves have to be taken into account when calculating demand profiles. A simple charging curve is implemented in [36]. The maximum charging power is 150 kW, but for the last four minutes of charging a linear decrease from 150 kW to 50 kW is assumed.

Outside temperature affects the demand profile. The driving efficiency, and thereby the driving range of the EVs, is affected by the outside temperature. In [40], different EVs is tested at a temperature of -6.5°C and 35°C, and compared to the performance in 24°C. With an outside temperature of -6.5°C the range is reduced with 12 percent, and 41 percent when the HVAC is used. When the temperature is 35°C, the driving range is reduced by 4 percent and 17 percent when using the HVAC. Similar results can also be found when using Nissan's range calculator for Nissan Leaf [41] and Opel's range calculator for Opel Ampera-e [42]. However, it's not only the driving range that's affected by the outside temperature. An empirical analysis of fast-charging events in different temperatures was performed in [43]. When the charging was done at 0°C compared to 25°C, the analysis showed that the SOC after a 30-min charge could be 36 percent lower.

Partial charging at FCS is another factor that will affect the demand profile. Many EV owners can charge at home and home-charging is cheaper than fast-charging. Therefore, they might only partially charge the EV at the FCS and then charge the rest at home. Taken partial charging into account, will result in changes in the demand profile for FCS, as shown in[44].

3.2 Optimal planning of FCSs

The siting and size of FCS are important since it will affect both the traffic flow and the distribution network, as well as present a social cost. Multiple different optimization problems have been formulated to determine the placement and size of FCS.

The FCSs were placed to minimize the voltage stability index in [45]. A simple charging demand model is created based on a PDF for daily driving distances and only one type of EV. The solution is constrained by power-flow constraints, capacity constraints of the FCS, and lines and voltage limits. The optimization is solved by a version of particle swarm optimization (PSO), called adaptive particle swarm optimization (APSO). The lowest VSI is achieved for a high number of FCS, which is natural since the solution is not penalized for the number of FCS. The proposed model doesn't take into account the traffic flow.

The aim of [46] is to minimize the social cost associated with building an FCS infrastructure. The social cost consists of investment and operation cost of the FCSs, charging the cost of EV users and a wastage cost if a detour is needed to get to the FCS. Limits for the number of FCS, power-flow equations, and voltage limits are among the constraints. To solve the non-linear problem a gravitational search algorithm is proposed and the optimal solution is in the lower part of the interval of the number of FCS constraints. This is as expected since only the wastage cost is reduced by adding more FCS, while the other cost increases. Even though network constraints are considered, the additional power loss is not added to the social cost.

In [47], initial candidate sites for FCS are determined by considering convenience for EV owners, price of land, close to proximity to existing electricity grid and the traffic flow. The objective is to minimize the total cost associated with the FCS. The cost includes investment cost, operation cost, maintenance cost and cost of increased distribution system losses. The constraint for the optimization model is power-flow equations and other distribution grid constraints such as voltage limits and minimal load power factor. The mathematical model developed is solved with a modified primal-dual interior point algorithm (MPDIPA). Although the traffic flow was included in the screening process, its not used to determine the placing of the FCS station.

The model doesn't size the FCS either, nor account for EV fleet distribution and charging demand pattern.

A two-stage model for location and sizing of FCS is proposed in [48]. The first model aims to determine the location of the FCSs, while maximizing the captured EV flow of the FCSs. The first model is solved with a binary particle swarm algorithm (BPSO). The second model determines the number of charging points for each of the FCSs determined in step one. The objective is to minimize the number of charging points constrained by a maximum allowed waiting time for the EVs. This is a nonlinear integer programming problem and is solved with an integer particle swarm optimization (IPSO) technique. The proposed design of the FCS results in voltage levels beyond permissible values at some of the buses. This is due to the effects of the FCS load on the distribution grid is not considered in the proposed model.

In [49], an innovating approach is used to determine the location and size of FCSs. A multi-objective function is proposed minimizing the EV transportation energy loss, FCS build-up cost and grid effects. The EV transportation loss is calculated by the use of a Google API, which calculates the time to all the potential FCSs locations. The EV will select the FCS that is the shortest time away and use it to calculate the energy that EV loses on its way to the FCS. The grid effects that are accounted for in the model are extra grid power losses taking into account the increased harmonics.

Different demand response programs are added to the optimal siting and sizing of FCS in [50]. The objective is to minimize the investment cost of the FCS, connection cost, cost of power losses, and demand response cost. A PSO algorithm is used to solve the problem MILP. The results show that with the implementation of a demand response program the total cost is reduced.

4 Theory

4.1 Particle Swarm Optimization

Particle Swarm Optimization is a heuristic optimization method first introduced in [51]. The optimization method is inspired by bird flocking and swarm theory to find the solution to nonlinear functions. PSO has become popular due to its simple concept, being computationally cheap and fast convergence compared to similar methods [52]. However, due to its heuristic nature, a global optimum solution is not guaranteed.

PSO finds its solution by initializing a population of random solutions, called particles, in the solution space. Each particle is assigned a random velocity to go along with its random solution (position). The position and velocity both are vectors in D dimension. After the initial solution is tested, the velocity of particle i is given by equation 1. Each particle's movement is affected by the population's best solution g_{best}, its personal best solution p_{best} and its current velocity. Its trade-off between exploration, trying to find new solutions, and exploitation, improving existing solutions. The weighting of between exploration and exploitation are determine by tuning the parameters w, c_1 and c_2. The variables r_1, r_2, r_3 are assigned randomly independent values between 0 and 1 for each iteration.

$$v_i^{t+1} = wr_1v_i^t + c_1r_2(p_{best,i} - x_i^t) + c_2r_3(g_{best} - x_i^t) \tag{1}$$

The absolute values of the velocity vectors are constrained by V_{max}. A too high V_{max} can result in particle flying out of the solution space, while a too low limits the search. After the velocity of the particle for the new time step $t + 1$ is determined, its position is updated according to equation 2.

$$x_i^{t+1} = x_i^t + v_i^{t+1} \tag{2}$$

The pseudo code in algorithm 1 describes the PSO. The fitness is the value of the function in its current position.

Algorithm 1 Particle Swarm Optimization

```
while Stop criterion is not met do
    for Each particle i do
        Evaluate the fitness
        Update personal and global solution
        Update the velocity with equation 1
        Update the position with equation 2
Return Best solution
```

4.2 Integer Particle Swarm Optimization

The first version of PSO introduced in [51] operated in continuous space. Thus, changes have to be made in the original PSO algorithm to solve problems with a discrete integer solutions space. The new optimization is called integer particle swarm optimization (IPSO). The adjustments are made when the position is updated. The position is calculated as shown in equation 2, but is then rounded off to its nearest integer. The rest of the algorithm is identical to the original PSO illustrated in algorithm 1.

4.3 Binary Particle Swarm Optimization

Many optimization problems are in a discrete space with qualitative variables. Binary particle swarm optimization (BPSO) was introduced to solve those optimization problems [53]. Alterations are made to the existing PSO to be able to handle binary vectors.

In the continuous space, the particles have a velocity that is used to search the solution space. In binary space, the velocity vector is changed to a probability vector. The probability vector represents the probability that a bit of the position vector X, is taking the value 1. The probability vector is calculated by equation 1, in the same way as the velocity vector. Where $p_{best,i}$, g_{best} and X_i are now binary vectors. According to equation 1 v_i^{t+1} can take values outside the interval [0.0, 1.0]. Since V is a probability vector, a logistic transformation, $S(V_i)$, is used to constrain its value in the interval [0.0, 1.0]. For particle i, in dimension d, the position is determined by rule seen in algorithm 2. Where r is a random uniformly generated number between 0 and 1.

Algorithm 2 Determining position BPSO

1: $r \leftarrow rand()$
2: **if** $r < S(v_{i,d}^t)$ **then**
3: $\quad x_{i,d}^t \leftarrow 1$
4: **else**
5: $\quad x_{i,d}^t \leftarrow 0$

A high or low $v_{i,d}$ will result in a very high or low probability of a bit being 1. This can stall the BPSO and limit the search. Therefore, a maximum limit V_{max} is introduced and $\left|v_{i,d}^t\right| < V_{max}$. The maximum limit is a tuning parameter. To illustrate selecting $V_{max} = 5$ the probability is limited between 0.007 and 0.993. With these alterations, the algorithm for the BPSO is the same as the algorithm for PSO shown in 1.

4.4 Optimum cross section

The optimum cross section for overhead lines is a trade-off between investment cost and cost of power losses. The investment cost of an overhead line is in cost per length of the line. An increased cross section results in a higher cost per km line. The theory in this section is based on the theory presented in [54]. The investment cost of a line is given by equation 3. Where c_o is the cross section independent cost, c_{cs} is the cross section dependent, A is the cross section of the line and L is the length of the line.

$$C_L = (c_0 + c_{cs}A) \cdot L \tag{3}$$

For a three phase system, the power loss in a line is given by equation 4. Where I is the current of the line and R is the resistance.

$$\Delta P = 3I^2R \tag{4}$$

The resistance of the line can be calculated according to equation 5. Where ρ is the specific resistance of the conductor.

$$R = \rho \cdot \frac{L}{A} \tag{5}$$

The power loss is proportional to R and R is inversely proportional to the cross section. Therefore, the cost of power loss is inversely proportional to the cross section. The cost of power loss is calculated by equation 6. Where C_{pekv} is the capitalized equivalent cost of power losses.

$$C_{\Delta P} = \Delta P \cdot C_pekv \tag{6}$$

The total cost for a line is given by equation 7.

$$C_{tot} = (3I^2 \cdot \frac{\rho}{A} + c_0 + c_{cs}A) \cdot L \tag{7}$$

The optimum cross section is given by equation 8 and minimizes the cost in equation 7. Where U_L is the line voltage, P is the power and $\cos\varphi$ is the power factor.

$$A_{opt} = \frac{P}{U_L \cdot \cos\varphi}\sqrt{\frac{\rho \cdot C_{pekv}}{c_{cs}}} \tag{8}$$

5 Modeling approach

The proposed modeling approach determines the optimal siting and size of FCS. The modeling approach consists of a mobility model, demand model, and a grid model, which together is incorporated in the optimization model. The main contribution of the work presented is two-step optimization algorithm taking into account both distribution grid effects and traffic flow, and a novel distribution grid model to create and dimension distribution grids from limited data.

5.1 EV mobility model

To be able to determine the load at the FCS, and the travel patterns of the EVs is a requirement. To get an accurate traffic flow of the EVs in the system, a mobility model is created. The mobility model is based on traffic flow measurements.

5.1.1 Traffic nodes

The mobility model determines the traffic flow of EVs in the system and consists of multiple traffic flow measurements. Each measuring point is considered a traffic node in the system. For each traffic node, there are four flows that have to be determined, the flow into the node, flow out of the node, flow into the system and flow out of the system. There is also a fifth flow that is used in some of the traffic nodes to calculate the other four flows. The different traffic flows are seen in Figure 4.

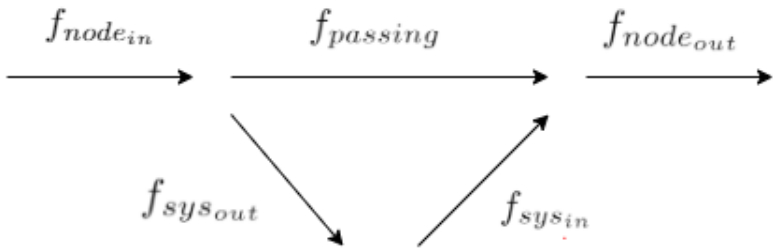

Figure 4: The different types of traffic flows at a traffic node

Flow into a node is defined as the traffic flow exiting the previous node and entering into the current node. Flow into the system and out of the system is defined as the flow entering and leaving the node from outside the system. There are four different types of traffic nodes, each based on one or two measured traffic flows. The different types of nodes are:

1. Passing flow.
2. Passing flow and flow out of the system.
3. Passing flow and flow into the system.
4. Flow into the system and flow out of the system

For node type 1 the flow into and out of the node is equal, as seen in equation 9, and there is no flow out or into the system.

$$f_{node_{in}} = f_{node_{out}} = f_{passing} \tag{9}$$

If the node is of type 2, the flow into the node can be calculated by equation 10.

$$f_{node_{in}} = f_{passing} + f_{sys_{out}} \tag{10}$$

For nodes of type 3 the flow out of the node, $f_{node_{out}}$, can be calculated by equation 11.

$$f_{node_{out}} = f_{passing} + f_{sys_{in}} \tag{11}$$

If the node is of type 4, only the flow of EVs to the node from outside the system are known.

5.1.2 Traffic flow

The flow of the system can't be determined by looking at the traffic nodes individually, since not all the desired flows being measured at each traffic node. To get the total traffic flow, the traffic nodes have to be sorted after geographical location and a system boundary defined were the traffic flow out of the starting node is known. Then flows for the connecting nodes are determined iteratively.

If the traffic flow is to be calculated for the direction 1, northbound traffic, the algorithm 3 is used. Since in this direction all the traffic nodes are either type 1, 3 or 4, and the $f_{node_{out},n}$ is either known for type 1 and 3 or can easily be determined according to equation 12. By assuming that $f_{node_{out},n-1}$, since $f_{node_{out},n-1} = f_{node_{in},n}$, where n is the node index.

$$f_{node_{out},n} = f_{node_{out},n-1} + f_{sys_{in},n} - f_{sys_{out},n} \tag{12}$$

The iterative algorithm to determine the traffic flow in direction 1 is shown in 3. It starts with the first node, $n = 0$, and the traffic flow is in the same direction as the node indexing.

Algorithm 3 Calculating the north bound traffic flow

```
for Hours h in a day do
    for For the nodes, n, in the system do
        if For the first node n = 0 then
            Record f_{node_{out},n,h}
        else
            if Traffic node is type = 1 then
                Equation 9
                Record f_{node_{in},n,h} and f_{node_{out},n,h}
                if f_{node_{out},n-1,h} ≠ f_{node_{in},n,h} then
                    Assing EVs leaving to f_{sys_{out},n,h}
                    Assing EVs arriving to f_{sys_{in},n,h}
            else if Traffic node is type = 3 then
                Equation 11
                Record f_{node_{out},n,h} and f_{sys_{in},n,h}
                f_{node_{in},n,h} ← f_{node_{out},n-1,h}
                if f_{node_{out},n-1,h} ≠ f_{node_{out},n,h} − f_{sys_{in},n,h} then
                    Assing EVs leaving to f_{sys_{out},n,h}
                    Assing EVs arriving to f_{sys_{in},n,h}
            else if Traffic node is type = 4 then
                Recordf_{sys_{in},n,h} and f_{sys_{out},n,h}
                f_{node_{in},n,h} ← f_{node_{out},n-1,h}
                f_{node_{out},n,h} ← f_{node_{in},n-1,h} + f_{sys_{in},n,h} − f_{sys_{out},n,h}
```

When calculating the traffic flow going in the opposite direction, southbound, algorithm 4 is used. Since for southbound traffic, all the traffic nodes are either type 1, 2 or 4. For type 2 nodes $f_{node_{in}}$ is known and not $f_{node_{out}}$ as for type 3 nodes. Therefore, the algorithm 4 starts with calculating the traffic flow exiting the

last node in the direction of the flow $f_{node_{in},n=0,d=2}$ and then iterating backwards against the flow of traffic. Since the numeration of the nodes is kept the same for both directions, iterating backwards is starting at $n = 0$ and stopping at $n = N$

Algorithm 4 Calculating the south bound traffic flow

for Hours h in a day **do**
  for For the nodes, n, in the system **do**
    if For the first node $n = 0$ **then**
      Record $f_{node_{out,n,h}}$
    else
      if Traffic node is type = 1 **then**
        Equation 9
        Record $f_{node_{in,n,h}}$
        $f_{node_{out,n,h}} \leftarrow f_{node_{in,n-1,h}}$
        if $f_{node_{in,n-1,h}} \neq f_{node_{in,n,h}}$ **then**
          Assing EVs leaving to $f_{sys_{out,n,h}}$
          Assing EVs arriving to $f_{sys_{in,n,h}}$
      else if Traffic node is type = 2 **then**
        Equation 10
        Record $f_{node_{in,n,h}}$ and $f_{sys_{out,n,h}}$
        $f_{node_{out,n,h}} \leftarrow f_{node_{in,n-1,h}}$
        if $f_{node_{out,n,h}} \neq f_{node_{in,n,h}} - f_{sys_{out,n,h}}$ **then**
          Assing EVs leaving to $f_{sys_{out,n,h}}$
          Assing EVs arriving to $f_{sys_{in,n,h}}$
      else if Traffic node is type = 4 **then**
        Record$f_{sys_{in,n,h}}$ and $f_{sys_{out,n,h}}$
        $f_{node_{out,n,h}} \leftarrow f_{node_{in,n-1,h}}$
        $f_{node_{in,n,h}} \leftarrow f_{node_{out,n,h}} - f_{sys_{in,n,h}} + f_{sys_{out,n,h}}$

5.1.3 Determining route of EVs

The traffic flow for the system is determined as described in 5.1.2. However, the route of the individual EVs is not decided. EVs arrive at the system either at the ends of the system or at the traffic nodes with $f_{sys_{in,n}} \neq 0$. The methodology to determine the number of arriving EVs is described in 5.2.1. When an EV has entered at a node, n_{entry}, the node in which the EVs exist the system has to be determined. EVs can only exit the system at the end of the system or at traffic nodes with $f_{sys_{out,n}} \neq 0$. The probability that the EV will exit the system at node n, at hour h, is given by equation 13.

$$p_{exit,n,h} = \frac{f_{sys_{out,n,h}}}{f_{node_{in,n,h}}} \tag{13}$$

Algorithm 5 illustrates how the exit node for an EV is decided, when the EV enters the system at node n at hour h.

Algorithm 5 Determining the exit node for an EV

$ev_{exit} \leftarrow false$ ▷ To determine if EVs leaves inside the system or at the end
for Iterating from $n = n_{entry} + 1$ to end of system **do**
    if $f_{sys_{out,n,h}} \neq 0$ **then** ▷ EVs are exiting at the node
        $u \leftarrow rand(0, 1)$ ▷ Generate random number between 0 and 1
        $p_{exit} \leftarrow$ Equation 13
        if $u < p_{exit}$ **then**
            $n_{exit} \leftarrow n$
            $ev_{exit} \leftarrow true$
if ev_{exit} = True **then** ▷ EV exits the system inside the system
    Return n_{exit}
else ▷ EV leaves at the end of the system
    Return end node

5.2 FCS load model

To model the FCS demand, a mobility model of the EVs is used together with temperature-dependent driving efficiency, EV charging curves for the EV and EV fleet representation. The proposed modeling approach models the arrival of the EVs at the FCS and their load profile, to ultimately get an aggregated load profile for the FCS. The objective is to get an accurate model for the load profile of FCS. The following subsections 5.2.1 - 5.2.6 is based on the specializing project [1], but is extended from 1 to multiple FCS.

5.2.1 Arrival of EVs

The traffic flow in the model is assumed to be free flow and not congested. Then, the distance between the cars on the road is uncorrelated. Therefore, the distance and time between cars follow a Poisson distribution [55]. The Poisson process is used to determine the entering of the EVs to the system. The waiting time, in minutes, until the next EV enters is given by equation 14. The variable u is a random variable, uniformly distributed between 0 and 1. λ is the expected number of EV entering per minute, for a given hour, and found by equation 15, where $q(t)$ is the traffic flow.

$$w = -\frac{1}{\lambda} ln(1-u) \tag{14}$$

$$\lambda(h) = percentage_{EV} \cdot q(t) \tag{15}$$

Therefore, the first EV for a given hour, h, will arrive at the h hour and w minute. The n^{th} EV will arrive according to equation 16

$$t_n = t_{n-1} + w \tag{16}$$

The Poisson process for each hour continues until equation 17 is fulfilled. his equation states that EV number $n+1$ arrives in the next hour of the simulation

$$t_{n+1} >= 60 \tag{17}$$

Algorithm 6 illustrates how equations 14, 15, 16 and 17 is used, to determine the arrival of the EVs.

Algorithm 6 EV arrivals

```
1:  arrival                                  ▷ Matrix to store the arrival time of the EVs for a day
2:  for For the hours, h, in a day do
3:      λ ← q[hour]                          ▷ Getting the expected number of arriving EVs for hour h
4:      counter ← 0                          ▷ Counter for the number of arriving EVs for hour h
5:      time ← 0
6:      while time < 60 do
7:          u ← random.uniform(0, 1)         ▷ Random Uniform value between 0 and 1
8:          Equation 14
9:          Equation 16
10:         arrival[h][counter] ← time       ▷ Recording the arrival time for the n'th EV in hour h
11:         counter[h] ← counter[h] + 1
```

5.2.2 Generate EVs

When the exact number of EVs is determined using algorithm 6, the EVs have to be created in the model. The EVs are created randomly based on EV data input. The EV data contains information about a select number of EV models. This is used to represent the EV fleet. For each EV model in the input the battery size, maximum charging power, driving efficiency, charging curve, and the probability of selecting each specific EV model are known. The EVs will not always charge at maximum power, but will charge according to its charging curve. The probability of each EV model is added together to a cumulative probability. A uniform random variable between 0 and 1 is then used to select the type of EV. Each EV is also given a SOC when they enter the system. The EVs the arrive in the system throughout the day are initialized by algorithm 7.

Algorithm 7 Initialize EVs

```
1: cdf ← Input                                   ▷ cumulative probability function of the different types of EVs
2: for the hours, h, in a day do
3:     for The number, n, of arriving EVs in hour h do
4:         u ← random.uniform(0, 1)                                   ▷ To determine the type of EV
5:         for The number of EVs, i, in the input EV data do
6:             if u is in between cdf[i-1] and cdf[i] then                          ▷ If its the i^th EV
7:                 The n^th EV in hour h will be of type i          ▷ Assigning it values of the i^th EV
8:
```

5.2.3 Temperature dependency

As mentioned in section 3.1, the outside temperature affects the driving range of EVs. Nissan [41] and Opel [42] are the only car manufactures, to the best of the author's knowledge, to have a range calculator dependent on temperature. Their range calculators are for the models Nissan Leaf and Opel Ampera-e. Figure 5 shows the comparison between the models. It's important to note that the scaling factor can be higher than 1, due to the reference driving efficiency might not be for the most optimal conditions. The relationship between efficiency and temperature shows the same tendencies for both EVs, with Opel Ampera-e having a slightly scaling factor for all temperatures. The difference is likely caused by the Opel's range assumed too low, or Nissan's too high. Nissan's range calculator is used in this model.

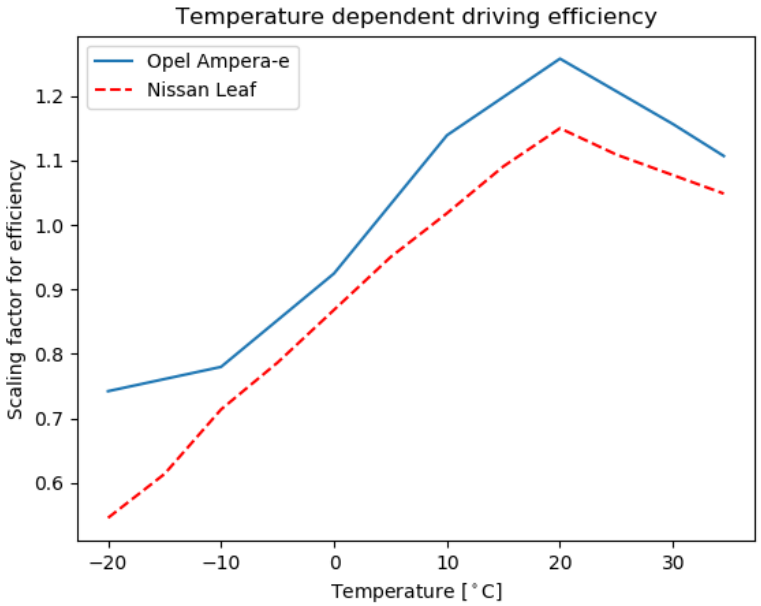

Figure 5: Temperature dependent scaling factor for the EVs driving efficiency

The input to Nissan's range calculator is the number of passengers, average speed and outside temperature. Thus, the range, $D(n_{pas}, v, T)$, can then be calculated dependent on the temperature, where n_{pas} is the number of passengers, v is the speed of the EV and T is the outside temperature. Further, using the size of the Nissan Leaf battery, the temperature-dependent driving efficiency, η_T, can be calculated, as shown in equation 18. Where, E_{bat}, is the battery size of the EV in kWh.

$$\eta_T = \frac{D(n_{pas}, v, T)}{E_{bat}} \tag{18}$$

A scaling factor, β, is calculated for the normal Nissan Leaf driving efficiency, as seen in equation 19. In this equation, η is the driving efficiency published by the manufacturer.

$$\beta = \frac{\eta}{\eta_T} \tag{19}$$

It is assumed that the temperature and range relationship is the same for all the other EVs in the model. Therefore, the β that is calculated for Nissan Leaf can be used to calculate the temperature-dependent efficiency for all EVs, as shown in equation 20.

$$\eta_T = \frac{\eta}{\beta} \tag{20}$$

5.2.4 Charging

An EV has an arrival SOC, SOC_{arr}, when it enters in the system. The EV will decide to charge at an FCS if the SOC goes below a certain limit, SOC_l, before the EV leaves the system. SOC_l is drawn randomly from a normal distribution with $\mu = 0.30$ and $\sigma = 0.05$ for each EV. Equation 21 shows whether an EV will charge or not.

$$SOC_l > SOC_{arr} - SOC_{loss} \tag{21}$$

SOC_{loss} is the reduction in SOC of the EV when it drives through the system, which is given by equation 22. In this equation, l_{route} is the length of the route the EV drives, which is based on its entry node and exit node.

$$SOC_{loss} = \frac{l_{route} \cdot \eta_T}{E_{bat}} \tag{22}$$

If the inequality in equation 21 holds, the EV will decide to charge and the SOC when it arrives at the FCS must be calculated. This is calculated with equation 23, where l_{FCS} is the length from the entry point of the EV to the FCS.

$$SOC_{FCS} = \frac{l_{FCS} \cdot \eta_T}{E_{bat}} \tag{23}$$

As there are multiple FCSs in the system, which FCS an EV will charge at, must be decided. The EV will always want to charge at an FCS along its original route. If the original route contains multiple FCSs, then FCSs that gives an $SOC_{FCS} \in [0.3, 0.5]$ is the first choice. However, if this is not possible, an $SOC_{FCS} > 0.5$ is selected above an $SOC_{FCS} < 0.3$. In the case that there are multiple FCSs within the same interval, then the FCS is selected randomly between the FCSs in question, except for when there are multiple FCSs that gives an $SOC_{FCS} < 0.3$. Then the FCSs that give the highest SOC_{FCS} are selected. However, it's possible that there are no FCSs along the original route. Then, the EV needs to drive a detour to be able to charge. The EV will charge at FCS that requires the shortest detour. This can either be driving in the opposite direction when entering the system or driving past its exit point to be able to charge at an FCS.

The amount of energy, E, the EV needs to charge is given by equation 24. SOC_{upper} is the battery percentage the EV will charge to, which is assumed to 80 % SOC. This value for the SOC_{upper} is chosen because the charging power that an EV can charge with usually drops after 80 % SOC. Therefore, it becomes less favorable to charge at an FCS. SOC_{FCS} is the SOC of the EV when it arrives at the FCS.

$$E = (SOC_{upper} - SOC_{FCS}) \cdot E_{bat} \tag{24}$$

The charging time of the EVs is determined by equation 25. P_{EV} is the maximal charging power for the given EV. The function α is a representation of the charging curve of the EV. Each EV model will have a unique α, which models the specific charging curve of each EV model. The EVs will not always charge at maximum power. This is controlled by the EVs battery management system and depends on many different factors, such as SOC, outside temperature, the batteries state of health and more. To make it less complex, it's assumed in the charging model that the charging power is only a function of SOC. The data for the charging curves used in this paper is from a Dutch charging network company Fastned [60]. They have tested different EV models on their FCSs and measured the charging power as a function of SOC. Therefore, α

takes the SOC as an input and returns a value between 0 and 1, which determines how much of its maximum charging power the EV can charge with.

$$E = \frac{1}{60} \int_0^t Power \cdot \alpha(soc) dt \tag{25}$$

Equation 25 has to be solved numerically to determine the charging time, t. Algorithm 8 is used to solve the equation and getting the charging time. It also finds the demand for the EV and returns the power the EV charges with during the stay. It's assumed that the EV charges with constant power for each time increment t, which is 1 minute. As mentioned in section 2.3, the capacity of the charging point can limit the power the EV can charge with. This is implemented in line 6 of algorithm 8. Its also assumed that charging points has an efficiency, $\eta_{charger}$, of 90%. Therefore, if an EV charges with 50kW, the charging point presents a load of 55.56kW to the grid.

Algorithm 8 Charging Time

1: *Needed Energy* $\leftarrow$ *(*SOC_{upper} *-* SOC_{FCS}*)*battery*
2: *Charged Energy* $\leftarrow 0$
3: $SOC \leftarrow SOC_{arrival}$
4: $time \leftarrow 0$
5: $\eta_{charger} \leftarrow 0.90$ ▷ The efficiency of the charging point
6: **while** *Needed Energy* $>$ *Charged Energy* **do**
7: **if** Charging point limits the charging power **then**
8: $P_{EV} \leftarrow P_{Charging,point}$
9: *Charged Energy* $\leftarrow$ *Charged Energy* $+ \frac{1}{60} P_{Charging,point}$
10: $SOC \leftarrow SOC + \frac{ChargedEnergy}{Battery}$
11: $time \leftarrow time + 1$
12: **else**
13: $P_{EV} \leftarrow P_{max} \cdot \alpha(SOC)$
14: *Charged Energy* $\leftarrow$ *Charged Energy* $+ \frac{1}{60} P_{max} \cdot \alpha(SOC)$
15: $SOC \leftarrow SOC + \frac{ChargedEnergy}{Battery}$
16: $time \leftarrow time + 1$
17: **Return** *time,* $\frac{P_{EV}}{\eta_{charger}}$

5.2.5 Queuing model

The arrival time of the EV at the FCS is calculated according to equation 26. Where v is the speed of the EV.

$$t_{arrival,FCS} = t_{charging,start} = t_{arrival,system} + \frac{l_{system}}{v} \tag{26}$$

Then by using the charging time found in algorithm 8, the departure time of the EV can be calculated.

$$t_{departure,FCS} = t_{charging,stop} = t_{arrival,FCS} + t_{charging} \tag{27}$$

However, there can be queues forming and resulting in EVs not being able to charge straight away. If there is a waiting time due to queue, then the charging start time will be according to equation 28.

$$t_{charging,start} = t_{arrival,FCS} + wait \tag{28}$$

The departure time will be according to equation 29.

$$t_{departure,FCS} = t_{charging,stop} = t_{charging,start} + t_{charging} \tag{29}$$

In this model a variation of the $M_1/M_2/c/k$ queuing model is implemented, where k is a time restriction in the length of the queue, rather than the number of EVs. Full transparency is assumed, meaning that the customers know how long the wait is in the queue for each charging point. The customer will always choose the queue with the shortest waiting time and will leave if the waiting time exceeds k for all the queues. In the model, the maximum waiting time in the queue is assumed to be 15 minutes.

Algorithm 9 Queuing model

```
for the minutes, m,in a day do
    if a EV/EVs is arriving then
        for how many EVs arriving in the m_th minute do
            if No queue then
                Equation 26
                Equation 27
            else if Wait is less than or equal to 15 then
                Equation 28
                Equation 29
            else                                  ▷ The queue is longer than 15
                EV will leave the FCS
```

5.2.6 Monte Carlo Simulation

There a lot of stochastic elements in the modeling of the load profile of the FCS. Therefore, Monte Carlo Simulation (MCS) is performed in the model, with a flow chart as shown in figure 6. The deterministic input data to model a representation of the EV fleet, the percentage of cars that are EVs and the number of charging points and its corresponding rated power. MCS is then performed for a predefined number of iteration. For each iteration, traffic flow and temperature profile for the system is chosen. This is drawn randomly from a predefined data set of traffic flows and temperature profiles. The load profile for an FCS is then simulated for a day with the use of algorithms 6, 7, 8 and 9. For each iteration, the load profile for the FCS is recorded.

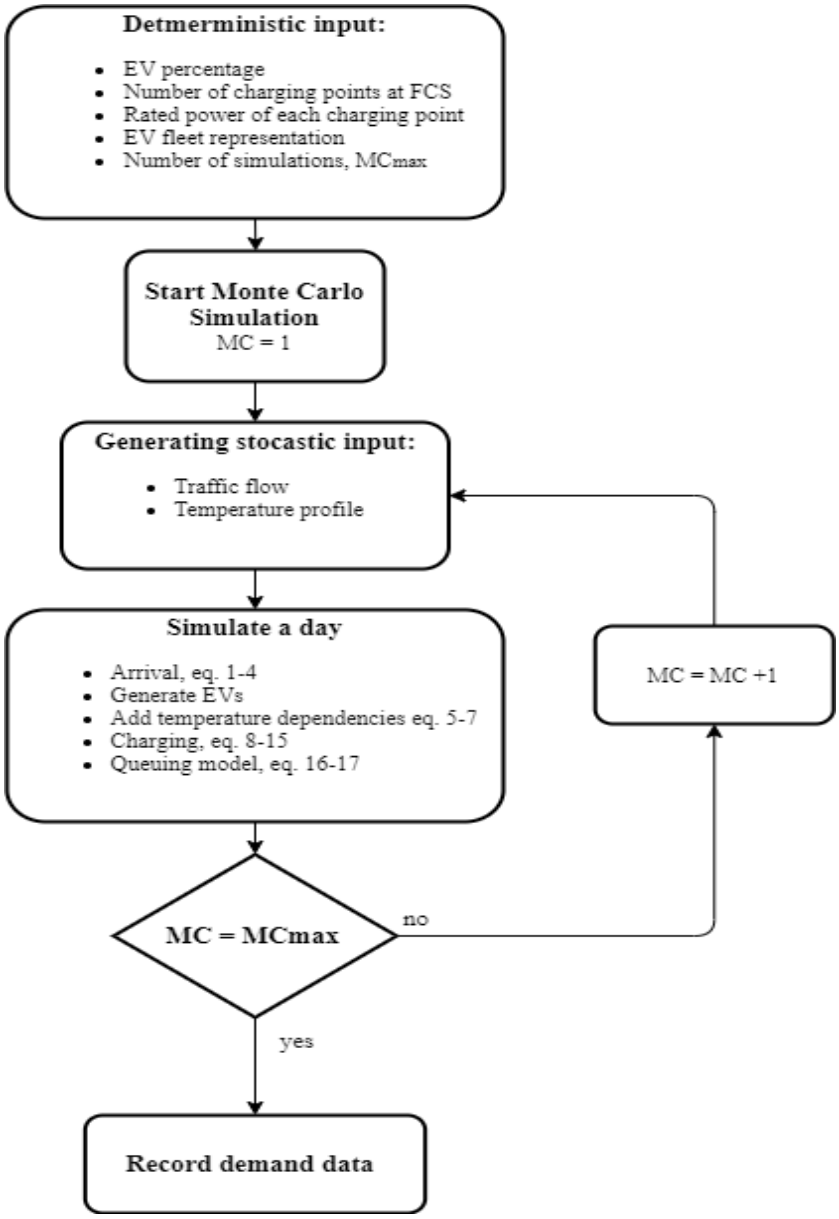

Figure 6: Flow chart of the FCS load model

5.2.7 Reduction of peak load at an FCS

It can be desirable to let the allowed peak load of an FCS be lower than the sum of the rated power of all the charging points. When the load at the FCS exceeds its maximum limit, each active charging point gets the power it can deliver adjusted by equation 30. Where $P_{fcs,max}$ is the maximum power the FCS can draw from the grid and $n_{active,ch}$ is the number of charging points currently charging an EV.

$$P_{ch,adj} = \frac{P_{fcs,max}}{n_{active,ch}} \tag{30}$$

This reduction in power the charging points can deliver is then fed to the algorithm 8, which recalculates the charging time. This is an iterative process and described by algorithm 10. This algorithm is placed inside the queuing algorithm 9. Thus, the increased charging time, due to the reduction of the maximum FCS power, affects the queuing at the FCS.

Algorithm 10 Reduction of peak load at an FCS

1: **while** $P_{fcs} > P_{fcs,max}$ **do**
2: $P_{ch,adj} \leftarrow$ equation 30
3: Update charging time of EVs with 8

5.3 Electricity grid model

The distribution grid in Norway, regarding types of lines and its length, is not public information. Furthermore, the amount of customers at each bus, and their respective load profile is not known. Thus, a methodology for creating and dimensioning distribution grids was developed.

5.3.1 Determining the topology of the distribution grid

The Norwegian Water Resources and Energy Directorate have a map tool, NVE Atlas [56], which shows where overhead distribution lines down to 11 kV are located. Figure 7 shows a segment of the distribution grid at Minnesund. The location of the grid is given and the length of each line can be measured manually, with the NVE Atlas measuring tool. Buses are placed where the distribution grid splits into branches and along lines with a high density of customers. Thus, the topology of the distribution grid is determined.

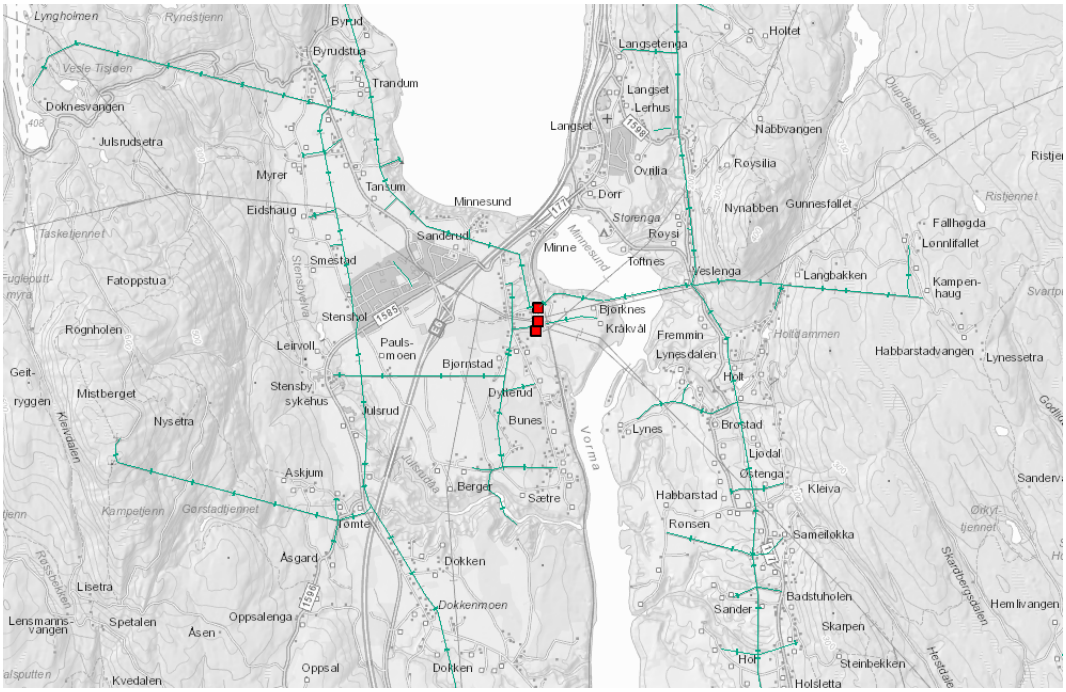

Figure 7: Map of the distribution grid from NVE Atlas at Minnesund. The green lines are 22 kV lines and the red squares are transformers.

5.3.2 Determining the base load of the distribution grid

SINTEF Energy Research has created general demand profiles for 11 different customer groups [57]. All the different load profiles are in appendix A. Some of the customer groups are households, offices, agriculture and school. Each building is assigned to its closest customer group. To illustrate, a kindergarten will be given assigned a school demand profile. The general load profiles are on the form illustrated in equation 31. Where h is the hour, T is outside temperature and l is the customer group. $a_l(h)$ is a temperature-dependent variable and $b_l(h)$ is a temperature-independent variable, both are dependent on the type of customer group l and the time h. There are four different load profiles, high load weekdays and high load weekends, and the same for the low load profiles.

$$P_l(h,T) = a_l(h) \cdot T + b_l(h) \tag{31}$$

The load in the distribution system has to be determined. NVE Atlas map tool is detailed enough to distinguish houses from commercial buildings. Google Maps [58] street viewer functionality is used to determine which customer group the building belongs to. Each load is connected to its closest bus. If there is a lot of consumers along a line, the line is split into two and a bus is placed at the load, else the load is put at the closest bus.

When all the customers in the system are assigned to a bus, the peak load of each bus needs to be calculated. This is due to the peak load through a line is the dimensioning factor for the cross section of the line. The peak load from households at a bus is calculated by Velanders formula, shown in equation 32. Where n_{hh} is the number of households at a bus and E_{hh} is the average yearly energy consumption for a household. The average energy consumption for a household is calculated by using equation 31 and a monthly temperature average, with the assumption that 9 months of the year is low load and 3 months of the year is high load. The two other variable k_1 and k_2 are empirical coefficients dependent on the location of the households.

$$P_{hh,max} = k_1 \cdot E_{hh} \cdot n_{hh} + k_2 \sqrt{W \cdot n_{hh}} \tag{32}$$

The general load profiles are used to determine the peak load of the non-households customer groups. The worst-case temperature profile is used in equation 31 for the high load weekday profile. The peak load throughout the day is then set to be the peak load for its customer group l. The peak load is multiplied with the number of customers from the specific customer group connected to that bus. The peak load from customer group l at bus i is calculated by equation 33. Where $N_{l,i}$ is the number of customers at the bus from customer group l.

$$P_{i,l,max} = N_{l,i} \cdot \mathbf{Max}(P_l(h, T_{min})) \tag{33}$$

The maximum load for a bus is calculated by equation 34. Where N_{cg} is the number of customer groups and the customer group $l = N_{cg}$ is households.

$$P_{i,max} = k_1 \cdot E_{hh} \cdot n_{hh} + k_2 \sqrt{W \cdot n_{hh}} + \sum_{l=1}^{N_{cg}-1} (N_{l,i} \cdot \mathbf{Max}(P_l(h, T_{min}))) \tag{34}$$

5.3.3 Dimensioning the lines of the distribution grid

When the base load has been determined the distribution grid has to be dimensioned. The first step is to determine the peak load through each line in the distribution system. The peak load through each line is calculated by equation 35. Where z_j, i is a binary variable determining if the power to bus i is flowing through line j.

$$P_{j,max} = \sum_{i=1}^{N_{bus}} z_{j,i} \cdot P_{i,max} \tag{35}$$

After the peak load through each line is calculated, the cross section of each line can be decided by equation 8 from section 4.4. After the lines are dimensioned, a power flow has to be performed to check if the voltage levels of the system are within allowed limits. The voltage limits are shown in equation 36

$$V_{min} \leq V_i \leq V_{max},\ i = 1, \ldots N_{bus} \tag{36}$$

5.4 Optimization model

To determine the optimal location and sizing of the FCS network, a two-step optimization model is developed. A two-step approach is selected to make the optimization problem more transparent and less computationally expensive. The impacts of this choice are discussed in section 9.2. The first optimization model decides the optimal location, while the second selects the number of charging points at each FCS.

5.4.1 Optimal location of FCSs

To decide the optimal location of the FCSs, a BPSO algorithm is used. Since the siting of an FCS is a qualitative variable, either an FCS is placed in a location or not. The FCS selection vector V_{fcs} is of length N_{fcs}, which is the number of potential locations for to place an FCS. Each particle in the swarm, represent a potential design for the FCS network. The load profile for each of the selected FCSs is calculated by the FCS load model. The load of each of the selected FCSs is then connected to its respective distribution gird bus. Power flow calculations are then performed with the distribution grid and base load from the grid model, with the added FCSs load. It's not possible to add formal constraints, as the PSO is a heuristic optimization method. Thus, the penalty method is used. With the penalty method, the objective function is evaluated, and if some constraints are breached a penalty is added to the objective function. The penalty is set higher than any value a no-penalized objective function can take.

Algorithm 11 Particle Swarm Optimization

```
1:  while Stop criterion is not met do
2:      for Each particle i do
3:          if Solution not tested before then
4:              for N times do                                  ▷ Evaluate the fitness
5:                  1. Calculate demand for each of the FCSs
6:                  2. Run power flow simulation with the FCS load
7:                  3. Evaluate the objective function
8:                  4. Evaluate constraints
9:          else
10:             Use the fitness from the first time the solution was tested
11:         Update personal and global solution
12:         Update the velocity 1
13:         Update the position alg. 2
14: Return Best solution
```

The PSO is a search algorithm, and by its design, it's likely that some of the solutions will be tested multiple times. To evaluated the fitness of a particle the EV fast charging demand model has to be simulated, a power flow is performed and then, the objective function and constraints are evaluated. To increase the speed of the algorithm there is implemented a ledger that records each tested solution and its fitness level. Therefore, if a particle has a position vector that has been evaluated previously, it can drop the simulations and use the fitness level from the first time the position vector was tested. There is a lot of stochasticity in the EV fast charging demand model. Thus, the fitness is evaluated N times and the average fitness is used to decrease the stochastic impact. Therefore, increasing the probability that the solution found by the PSO algorithm is the optimum solution.

To make the optimization less computationally expensive, the power flow is performed with a time step of 1 hour. Since the FCS load has a granularity of 1 minute, its hourly average value is used in the optimization. Then, for the final solution, the power flow is performed with a time step of 1 minute. To make sure that the solution is valid and no constraints are breached.

The distance between the FCSs or between system ends and the first FCS, has to be less than $d_{fcs,max}$, to prevent EVs from running out of energy. The limit $d_{fcs,max}$, is determined by the EV in the EV fleet

with the shortest range, the lower limit for SOC_l and the lowest SOC an EV can arrive to the system with $SOC_{arr,min}$. The distance d_fcs, max is calculated by equation 37.

$$d_{fcs,max} = \frac{SOC_{arr,min} - SOC_l}{\eta_T} E_{bat} \tag{37}$$

Thus, the distance between the FCSs d_{fcs} is constraint by coverage constraint in equation 38.

$$d_{fcs} \leq d_{fcs,max} \tag{38}$$

In addition to the position constraint in equation 38, there are some constraints on the distribution system. Firstly, there is the voltage limit constraint described in equation 36. There is also the nonlinear power balance constraint presented in equation 39 and 40.

$$P_{\mathrm{i}} = \sum_{k=1}^{N_{bus}} (|Y_{\mathrm{ik}}||V_{\mathrm{i}}||V_{\mathrm{k}}| \cos(\delta_{\mathrm{i}} - \delta_{\mathrm{k}} - \theta_{\mathrm{ik}}),\ i = 1, \ldots N_{bus} \tag{39}$$

$$Q_{\mathrm{i}} = \sum_{k=1}^{N_{bus}} (|Y_{\mathrm{ik}}||V_{\mathrm{i}}||V_{\mathrm{k}}| \sin(\delta_{\mathrm{i}} - \delta_{\mathrm{k}} - \theta_{\mathrm{ik}}),\ i = 1, \ldots N_{bus} \tag{40}$$

δ_i is the angle of the voltage V_i, δ_k is the angle of the voltage V_k, θ_{ik} is the angle of the line admittance Y_{ik} and N_{bus} is the number of buses in the distribution system.

The power flow through any transmission line is constraint by equation 41

$$S_j \leq S_{j,max},\ j = 1, \ldots N_{lines} \tag{41}$$

5.4.2 Optimal size of FCSs

Deciding the number of charging points at each FCS is a discrete integer problem. Thus, an IPSO algorithm is used as described in section 4.2. The objective is to minimize the number of chargers at for each of the N_{fcs}. Its constrain by a maximum daily average waiting time for the EVs. The optimization problem is also constrained the maximum percentage of EVs leaving the FCS due to excessive waiting time. If a constrained is breached a penalty is added in the same way as for the BPSO. It's assumed that the size of the individual FCS doesn't affect each other. Therefore, the size of each FCS can be optimized separately. The impact of this will be discussed in section 9.2. The optimization problem is illustrated in 42, with the constraints for the waiting time and the percentage of rejected EVs presented in 43 and 44.

$$\begin{aligned} \min \quad & n_{l,chargers} \quad \forall l = 1, .., N_{fcs} && (42) \\ \text{subject to:} \quad & W_l \leq W_{max} && (43) \\ & R_l \leq R_{max} && (44) \end{aligned}$$

6 System description and models

6.1 System

The studied system is 74 km of the highway E6, between Gardermoen and Hamar. An overview of the system is shown in figure 8 [58]. The system limits are placed due to a good density of traffic flow measuring point from Statens Vegvesen [59]. The distribution grid in the system is overhead lines and not cables, so they appear in NVE Atlas. Thus, the distribution grids can be created and dimensioned as described in 5.3.

The red circles in figure 8 indicates the potential locations for FCSs. There are 12 different locations, but one location has two different distribution grids it can be connected to. Thus, there are 13 potential locations to connect an FCS.

Figure 8: An overview of the system, 72 km of the highway E6, between Gardermoen and Stange. The red circles indicates the potential locations for FCSs. The map is rotated with north being to the right.

A more detailed description of the potential FCS locations are given in table 1. The table describes the geographical location and the closest bus in the distribution system for the potential FCS locations.

Table 1: Overview of the potential FCSs geographical location and location in the distribution grids

Potential FCS location	Distribution grid	Bus	Distance to system end north	Distance to system end south
1	1	12	71	3
2	1	2	65	9
3	2	15	55	19
4	2	3	50	24
5	3	9	43	31
6	4	6	40	34
7	5	2	28	46
8	5	5	22	52
9	5	7	17	57
10	6	15	16	58
11	6	3	12	62
12	7	9	7	67
13	7	2	2	72

6.2 Mobility model

The proposed mobility model from section 5.1 has been implemented in Python. There is a total of 10 traffic nodes in the system and the position of each node is illustrated in figure 9. The traffic data for each node is from Statens Vegvesen [59], with different information depending on the type of traffic node. The traffic data is filtered to only contain vehicles less than 5.6 meters, which is assumed to all be cars. Two traffic flows are created one weekend traffic flow and one weekday. For the weekday flow, the historical data used is from April 24, 2019. To create the weekend flow, historical data from April 28, 2019, is used. In the FCS load model, the weekday flow has a $5/7$ probability of being selected and the weekend flow has a $2/7$ probability of being selected.

Figure 9: An overview of the system with yellow circles indicating the traffic nodes. The map is rotated with north being to the right.

The traffic flow going north at $h = 17$, for the weekday flow, is depicted in figure 10. There are a lot of vehicles exiting the system at node 3. This is the area in the system with the biggest population and in the rush hours, the majority of the traffic is likely a result of commuting. The implications of this are implemented in subsection 6.3.3. To model the stochastic nature of the traffic flow and EVs arriving at the FCS. The historic traffic data of hourly arrival rate to the system, at each traffic node, is multiplied with the EV percentage and assumed to be hourly expected traffic flow of EVs. This is used as input in the Poisson process in algorithm 6.

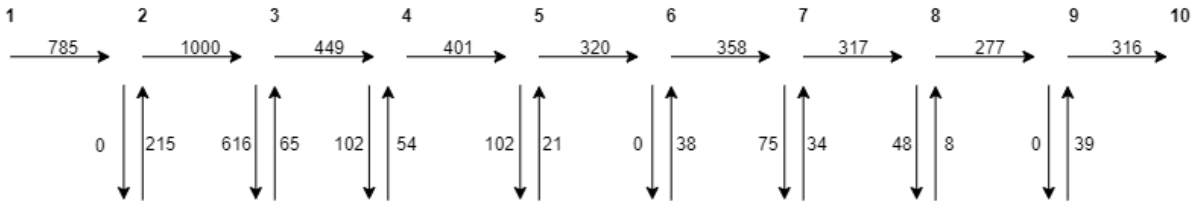

Figure 10: The weekday traffic flow for the system at $h = 17$ in the northern direction.

6.3 FCS load model

The the proposed FCS load model in section 5.2 is implemented in Python. The necessary input used in the load model is described in following subsections 6.3.1 - 6.3.3.

6.3.1 Temperature

The driving efficiency, and therefore also the range of EVs, is highly affected by the outside temperature, as described in subsection 5.2.3. Lower temperatures correlate with a higher driving consumption for the EVs. Thus, more EVs need to charge at FCSs and it results in a higher demand at the FCSs. For the optimization model, the aim is to determine the location of FCSs, the worst-case scenario has to be tested to see ensure grid stability with the proposed FCS network design. Thus, the temperature profile for the coldest day is chosen. The coldest day of 2019 in the system was the 29^{th} of January and the temperature thought the day is depicted in figure 12. For the other scenarios, a temperature profile for a random day is drawn randomly, as described in subsection 5.2.6. There are 12 different temperature profiles one from each month. The temperature profiles are shown in figure 11.

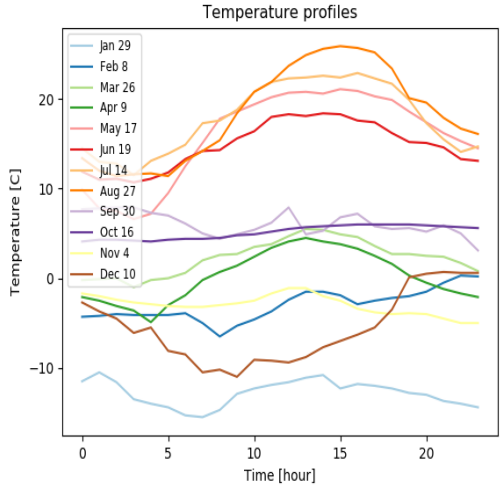

Figure 11: Temperature profile for a random day each month

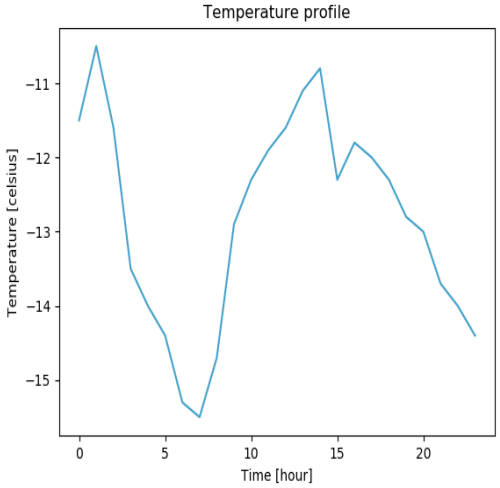

Figure 12: Temperature profile for the coldest day of 2019, 29^{th} of January.

6.3.2 EV fleet

The EVs that are created randomly from the EV fleet in table 2. The table contains the top 10 most common EVs in Norway as of August 24, 2019, [66], and is used as a representation of the current EV fleet. Tesla's are drop from the top 10 most common EVs since Tesla has its own charging network. Although, there are adapters that make Tesla Model X and S compatible with CHAdeMO and CCS, and Tesla Model 3 is compatible with CCS without adapter [67]. Nonetheless, it's assumed that Tesla will not charge at the FCS. Renault Zoe is another EV that is among the top 10 most common in Norway, but Zoe is dropped since it doesn't support charging above 22kW. Each EV has a battery size, maximum charging power, efficiency and charging curve. Appendix B.1 shows the charging curve of the different EVs in table 2. The last column is the adjusted market share of the top 10 EVs. Therefore, the sum of the column will be 100% and the percentage of each EV represent the probability that it will be generated.

Table 2: Battery size, maximum charging power and efficiency for the 10 most common EVs in Norway

Model	**Battery size [kWh]**	**Maximum charging power [kW]**	**Efficiency [kWh/km]**	**Percentage [%]**
Nissan Leaf	40,0	50	0.164	33
Volkswagen e-Golf	35,8	40	0.168	23
BMW i3	33,0	50	0.160	14
Kia Soul	42,0	50	0.171	10
Volkswagen Up!	18,7	40	0.168	5
Hyundai Ioniq	30,5	69	0.144	5
Nissan E-nv200	40,0	46	0.2	3
Mitsubishi I-miev	16,0	40	0.161	2
Jaguar I-pace	90,0	100	0.229	2
Audi E-tron	95,0	150	0.232	2

6.3.3 SOC

The SOC of an EV plays an important role in whether or not the EV will need to charge. Thus, information about the charging habits of EV owners is important to create good assumptions for the arrival SOC of EVs. A survey done by Electromobility Lab Norway [61], found that 90 % of EVs predominantly charge at home. The survey also found that an average EV chargers 4.4 times at home and 1.1 times at work each week. Based on the charging behavior and assumptions for the traffic flow, the $SOC_{arrival}$ of EVs will differ based on if it's a weekday or weekend, and also the time of day.

Table 3 shows the assumptions for the SOC of an EV when it enters the system on a weekday. It tries to describe the user behavior of the EV owners. In the first three time intervals, it's assumed that 10 % of the EVs enters the system with 50 % SOC and 90 % of the EVs with 90 % SOC. This is based on 90% of EVs having the ability to charge at home. As mention in section 6.2, there is likely a lot of commuting in the system on weekdays. It was also mentioned earlier that the majority of charging is done at home and not at work. Therefore, in the fourth time interval, the SOC of arriving EVs try to model EVs commuting back from work. It's assumed that 70% of EVs will have a SOC of 50% when entering the system and 30% of the EVs having a SOC of 90%. Since a substantial amount of EVs will return from work without having charged since the morning. In the last time interval, it's assumed an equal split between EVs having a SOC of 90% and EVs having a SOC of 50% when entering the system. This to model EVs that have returned from work and is driving errands in the afternoon without having charged the EV. All SOC values from table 3 are the mean values of a Gaussian distribution with a standard deviation of 0.05.

Table 3: The distribution of SOC of arriving EVs to the system throughout a weekday.

Time	**Alternative 1**		**Alternative 2**	
	μ_{SOC} **[%]**	**Probability**	μ_{SOC} **[%]**	**Probability**
0-5	50	0.10	90	0.10
6-10	50	0.10	90	0.90
11-14	50	0.10	90	0.90
15-19	50	0.70	90	0.30
20-23	50	0.50	50	0.50

The $SOC_{arrival}$ of the EVs in the system at the weekend shown in table 4. The weekend $SOC_{arrival}$ is based on the assumption that there is no commuting and drive fewer trips at the weekend. Therefore, a constant $SOC_{arrival}$ for the EVs arriving at the system is assumed throughout the day, which is based on 90% of EVs having the ability to charge at home.

Table 4: The distribution of SOC of arriving EVs to the system for a weekend.

Time	**Alternative 1**		**Alternative 2**	
	μ_{SOC} **[%]**	**Probability**	μ_{SOC} **[%]**	**Probability**
0-23	50	0.10	90	0.90

6.4 Grid model

A total of seven distribution grids were created and dimensioned, with the methodology described in section 5.3. The grid model to create and dimension the distribution grids is implemented in Python. After the distribution grids are designed, they were implemented in pandapower [63] in Python, for performing the necessary power flow calculations for the optimization model.

6.4.1 Creating and dimensioning the grid

As mentioned in section 4.4, the optimum cross section is a trade-off between investment cost and cost of power loss. The analysis period for optimum cross section method is long and power loss occurs yearly while the investment cost is a one-time payment. Therefore, the method tends to give a very robust distribution grid with very little power loss and voltage drop. According to [54], less than 40% of the line maximum loading capacity is used at high load, when the lines are designed with an optimum cross section. However, the current distribution grids tend to be old and have been partially upgraded over time. It's assumed that the real distribution is less robust than the distribution grid designed by the optimum cross section method. Thus, the design for the distribution grid given by the optimum cross section method is adjusted to obtain 5% voltage drop at peak load. This is done to try to make a more realistic distribution grid and therefore, highlight the importance of performing grid analysis before placing an FCS.

By using the average temperature in the system for each month [62] and the general load profile for households, the yearly energy consumption of a household in the system calculated to be 18 981 kWh. The empirical coefficients in Velanders formula, are $k_1 = 0.00022$ and $k_2 = 0.019$, for single-family homes in the eastern part of Norway [54]. The peak power for a bus, due to n households, is depicted by the blue line in figure 13. The red line in figure 13, is the peak power per household, as a function of the number of households.

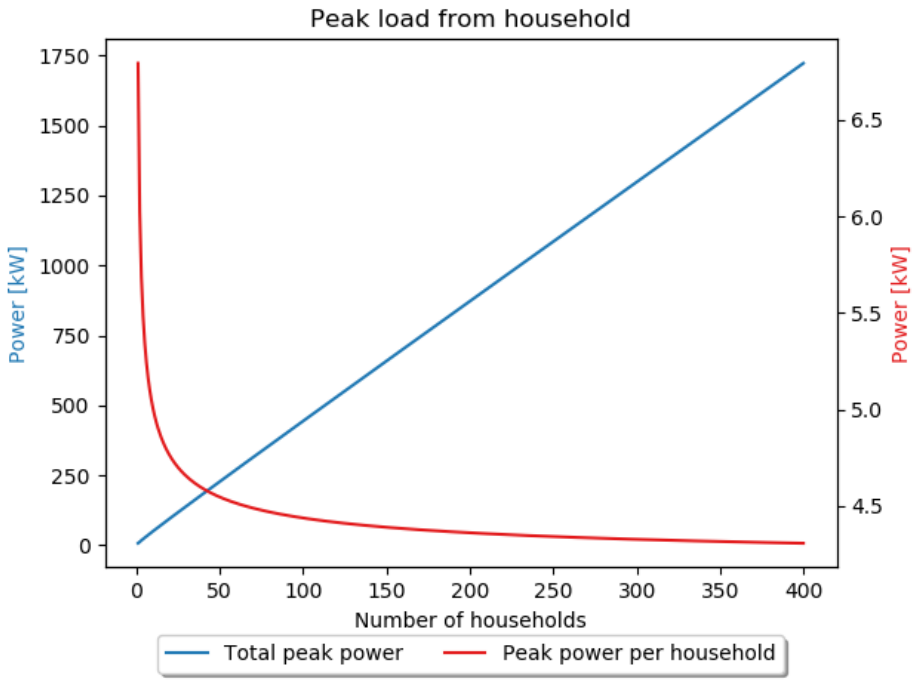

Figure 13: The peak load from households calculated according Velanders formula in equation 32, with $E = 18981kWh$, $k_1 = 0.00022$ and $k_2 = 0.019$. The blue line is the aggregated peak power, while the red line is the peak power per household

FeAl lines with different cross section is used to design the different distribution system. The technical data for the lines are listed in table 5 and are from [64]. Based on the cost per km of line the, c_s was calculated as follows:

$$c_s = \frac{505 - 274}{240 - 25} = 1074,4[kr/km, mm^2]$$

The equivalent cost of power loss was found to be $C_{pekv} = 20700[kr/kW]$, for a 30 year analysis period with discount rate of 4,5% [65]. The specific resistance is $\rho = 18,2[\Omega, mm^2/km]$. In the base load and in the FCS demand model only active power is considered. Thus, a power factor of 1 is used.

Table 5: Line data for FeAl with different cross section used to design the distribution grids

FeAl nr	**Max current at 20 °C [A]**	**Resistance at 20 °C [Ω/km]**	**Reactance [Ω/km]**	**Capacitance [nF/km]**	**Cost [kkr/km]**
10	171	1,791	0,423	5,8	-
16	200	1,126	0,409	5,8	-
25	266	0.721	0.395	5,8	274
50	417	0,359	0,373	5,8	325
70	516	0,257	0,362	5,8	353
95	629	0,191	0,351	5,8	380
120	733	0,151	0,344	6,4	399
150	846	0,121	0,337	6,4	434
185	968	0,098	0,330	6,4	470
240	1143	0,076	0,322	7,6	505

6.4.2 Base load used in simulations

As mention previously in subsection 5.3.2, the household load used to dimensioned the distribution grids is the general household profile from SINTEF Energy Research. However, the household load used in the power flow for optimizing the planning of FCS, are real load profiles for different households. The real load profile data are from a research project at NTNU and the houses are located in a similar climate as in the system. If the general load profile was used for all the houses, the load from each household in the distribution system would be equal and peak at the same time. To avoid this, and get a more realistic base load (distribution system load without FCSs load) for the distribution system, the real load profiles from the NTNU project is used. The coldest day in the year the load profiles where recorded is chosen and, from that day, the load profiles from 20 different households are selected randomly. For the non-household loads in the base load, the general load profiles are used with the temperature profile of the coldest day.

6.4.3 Distribution grid 1: Dal - Hovinmoen

The first distribution grid is between the 66 kV/22 kV substation at Dal to the 66 kV/22 kV substation at Hovinmoen. The potential buses to connect an FCS is bus 6 and bus 12. The topology of the grid is illustrated in figure 14.

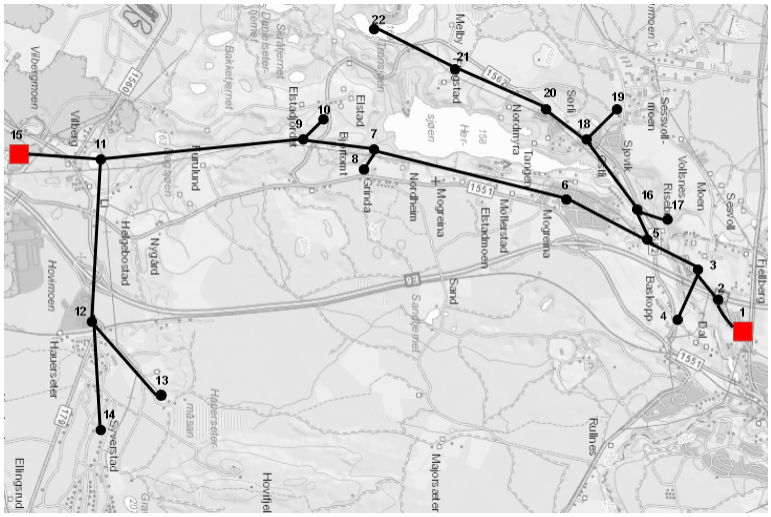

Figure 14: Topology of the distribution grid 1 between Dal and Hovinmoen.

The grid consists of the 22 buses, but there is only load at 13 of the buses. Table 12 in appendix C.1 shows the load at each of the buses. The grid is then is the dimensioned as described in 5.3.2. The distribution grid has two grid connections and the power can flow from both bus 1 and bus 15. Thus, two scenarios are used to dimension the grid, power solely coming for bus 1 and power solely coming from bus 15. In the case of the two scenarios giving different results for the cross section of a line, the biggest of the cross sections are used. Table 11 shows the length of each line in the distribution system and its cross section. For this distribution grid, the goal of a % 5 peak load voltage drop was not reached. This was due to a relatively low peak load in the system, and even with the lowest cross section selected for all the lines the maximum voltage drop in the distribution grid was 4.19 %. However, the 4.19% drop is obtained with power to the branch with bus 22 at the end coming from bus 15. It's assumed in normal operation that the power can flow to branch 22 from both the grid connection at bus 1 and bus 15. During normal operation, the voltage drop in the distribution system is 1.43% at peak load.

The voltage magnitudes at each bus in the distribution system are depicted in 15[3]. The voltage magnitudes are from $h = 15$, when the voltage drop in the distribution system is highest. The base load for the distribution system, and bus 5 and bus 14, is depicted in figure 16. Even though, the load is mainly households the peak load is at $h = 12$. This is due, to the load from offices, businesses and schools, which all have peak load around $h = 12$. This becomes clearer by looking at the base load from bus 14, which consists of 10 households, 1 kindergarten and a medium sized industry load.

[3]The voltage profile of distribution system 1, must be interpreted together the topology of the grid shown in figure 14

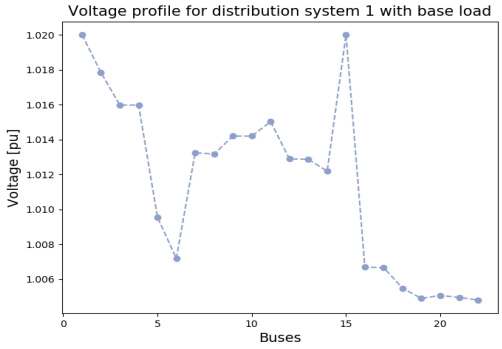

Figure 15: Voltage magnitude in the distribution grid with base load for $h = 15$, when the voltage drop in the system is at its highest.

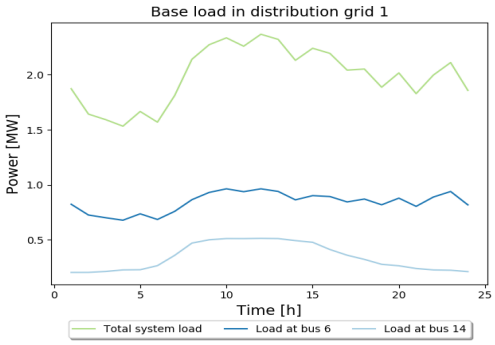

Figure 16: The base load for bus 5, bus 14 and the total system load in distribution grid 1.

6.4.4 Distribution grid 2: Hammerstad - Dal

The second distribution grid is between the 66 kV/22 kV substation at Hammerstad and the 66 kV/22 kV substation at Dal. The potential buses to connect an FCS is bus 3 and bus 15. The topology of the distribution grid is seen in figure 17.

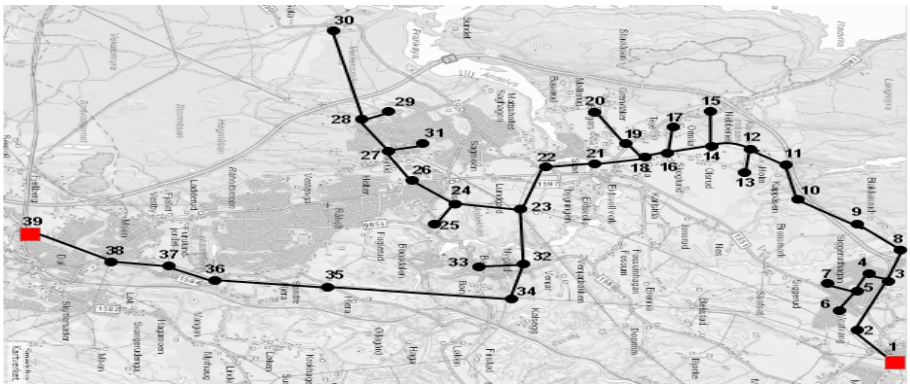

Figure 17: Topology of the distribution grid 2 between Hammerstad and Dal.

There is a total of 39 buses in the distribution grid, with load at 25 of them. The load at each load bus is found in 14 in appendix C.2. The distribution grid is dimensioned with the methodology described in 5.3.2. The distribution grid has two grid connections, at bus 1 and bus 39. Two scenarios are used to dimension the grid, power solely coming for bus 1 and power solely coming from bus 15. In the case of the two scenarios giving different results for the cross section of a line, the biggest of the cross sections are used. Table 13 shows the length of each line in the distribution system and its cross section. As previously mentioned, the aim is to design the grid with a 5% voltage drop at peak load. The design from the optimum cross section method was adjusted. A voltage drop of 5.40 % was achieved with power being delivered from bus 1 and a voltage drop of 5.37% was obtain with power delivered from bus 39. Thus, during normal operation, when power can be delivered from both bus 1 and bus 39 the voltage should be lower. However, due to the real load profiles for households are used for the power flow simulations, and not the peak power from Velanders formula, a higher voltage drop was experienced for with the base load. The reason why this occurred is addressed in section 9.1. The highest voltage drop was 6.21% at $h = 14$, as seen in figure 18[4]. Figure 19 shows the base load of the distribution system, which has a peak of 3.578 MW. The base load at the bus 26 and bus 31, is also seen in figure 19.

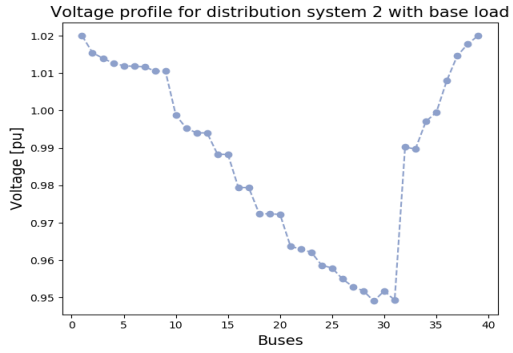

Figure 18: Voltage profile for the distribution system 2 with base load. The voltage profile is for the hour $h = 14$ were the voltage drop is highest

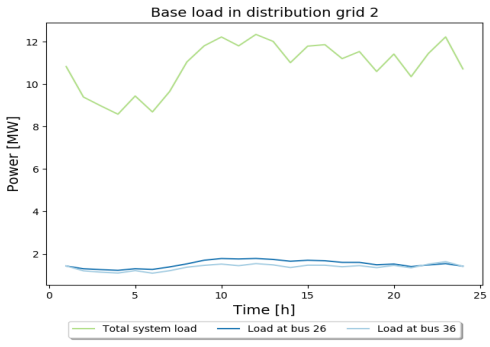

Figure 19: Aggregated base load for the system and base load at bus 26 and 31.

[4]The voltage profile of distribution system 2, must be interpreted together the topology of the grid shown in figure 17

6.4.5 Distribution grid 3: Minnesund - Hammerstad

The third distribution grid consists of a ring distribution grid at the 66 kV/22 kV substation at Minnesund, with a branch to the 66 kV/22 kV substation at Hammerstad. Bus 9 is the only bus where a potential FCS can be connected. The topology of the distribution grid is seen in figure 20.

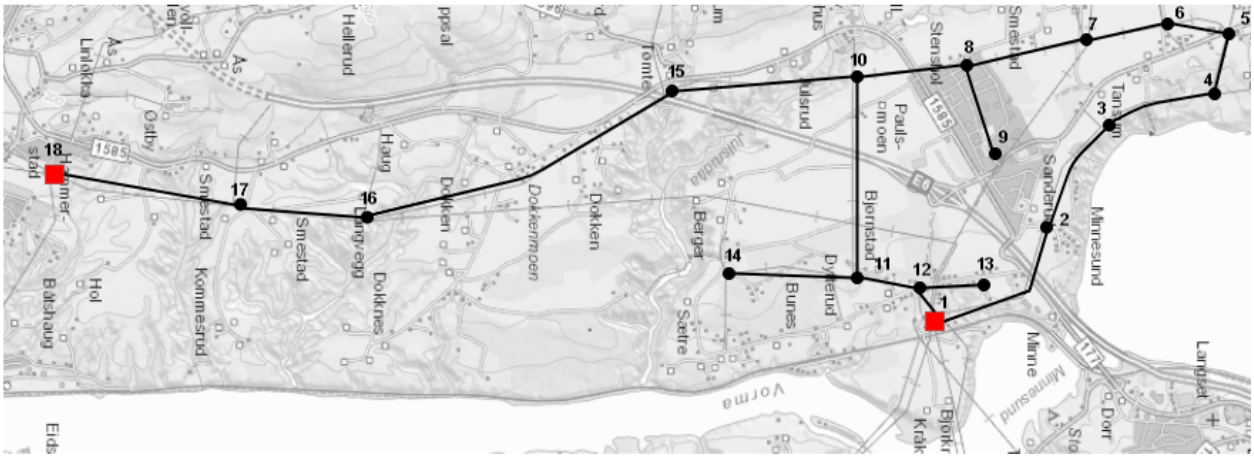

Figure 20: Topology of the distribution grid 3 between Minnesund and Hammerstad.

There is a total of 18 buses in the distribution system, with load at 15 of the buses. The load at each bus, is seen in table 16 in appendix C.3. The grid is dimension after three scenarios, for the ring grid, with the power only flowing in the direction of bus 1 to bus 2 and flowing in the direction of bus 1 to bus 12. Both with the power flowing from bus 10 to 18. For the last scenario, the power is assumed flowing from bus 18 to bus 15. The grid is not dimension for power to the ring grid being delivered from bus 18, due to the n-1 reliability of the ring topology. With power flowing from bus 1, through bus 2, to bus 18 a maximum voltage drop of 5.1 % was obtained with the line as described in table 15 in appendix C.3. For the two other scenarios, the voltage drop is less than 5%. Naturally, during normal operation with power being delivered from bus 1 through both bus 1 and 12, and from bus 18, a lower voltage drop is expected. The voltage drop at peak load was 3.13 %. The voltage magnitudes for all buses in the with base load, are seen in figure 21[5]. The voltage is from $h = 13$ when the voltage drop in the system is at its highest. The base load for the distribution system, as well as bus 4 and bus 9, is seen in figure 22.

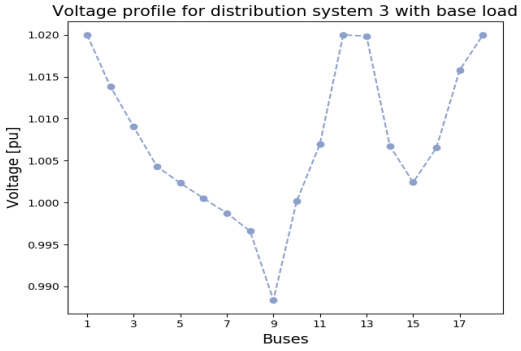

Figure 21: Voltage profile for the distribution system 3 with base load. The voltage profile is for the hour $h = 14$ were the voltage drop is highest

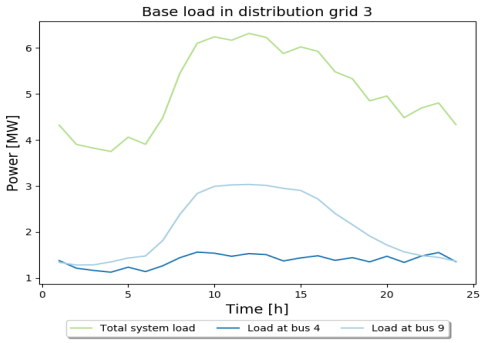

Figure 22: Aggregated base load for the system and base load at bus 4 and 9.

[5]The voltage profile of distribution system 3, must be interpreted together with the topology of the grid shown in figure 20

6.4.6 Distribution grid 4: Skårud - Minnesund

The fourth distribution grid is a radial distribution network. The radial starts at the 66 kV/22 kV substation at Minnesund. Bus 6 is the only bus, where a potential FCS can be connected. The topology of the distribution grid is seen in figure 23.

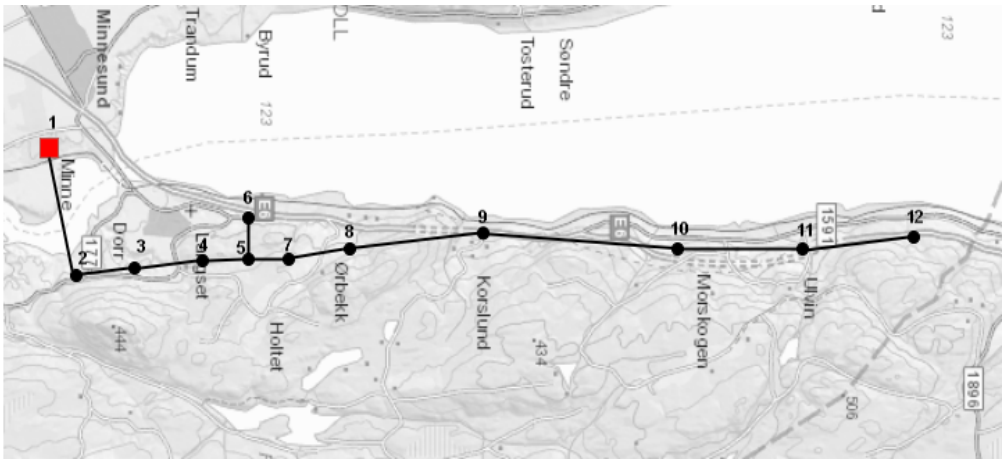

Figure 23: Topology of the distribution grid 4 between Skårud and Minnesund.

There is a total of 12 buses in the distribution system, with load at 9 of the buses. The load at each bus, is seen in table 18 in appendix C.4. The distribution grid is a single radial. Thus, the grid is dimensioned after power flowing from bus 1. The target of 5% voltage drop at peak load was not obtained. This was due to the low load in the system and with the smallest dimension for all the lines, the voltage drop at peak load was 3.98%. The dimension and length of each line are described in table 17. The voltage magnitudes for all buses in the system, with base load, is seen in figure 24. The voltage profile is from $h = 14$, when the voltage drop in the system is highest. The base load for the distribution system, as well as bus 4 and bus 9, is seen in figure 22. The load at bus 4 consist of load from households and a school, as seen in table 18. While the load at bus 9 consists of load from households and farms.

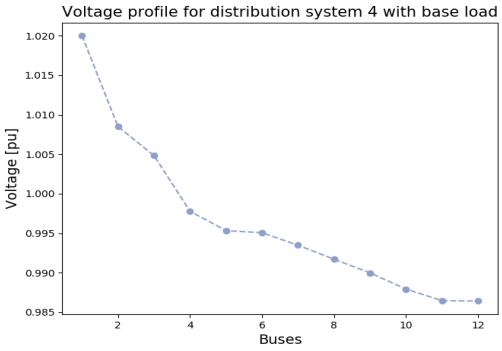

Figure 24: Voltage profile for the distribution system 4 with base load. The voltage profile is for the hour $h = 14$ were the voltage drop is highest

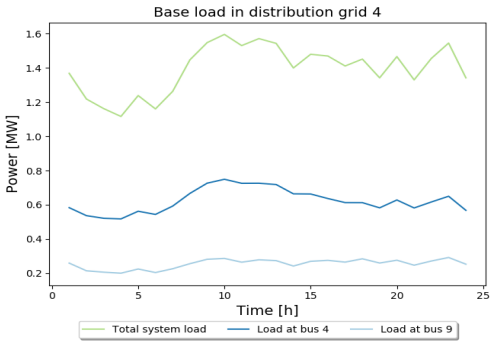

Figure 25: Aggregated base load for the system and base load at bus 4 and 9.

6.4.7 Distribution grid 5: Espa - Strandlykkja

The fifth distribution grid is a radial distribution grid. The radial starts at the 66 kV/22 kV substation at Strandlykkja. The potential location to connect an FCS is buses 2, 5 and 7. The topology of the distribution grid is seen in figure 26.

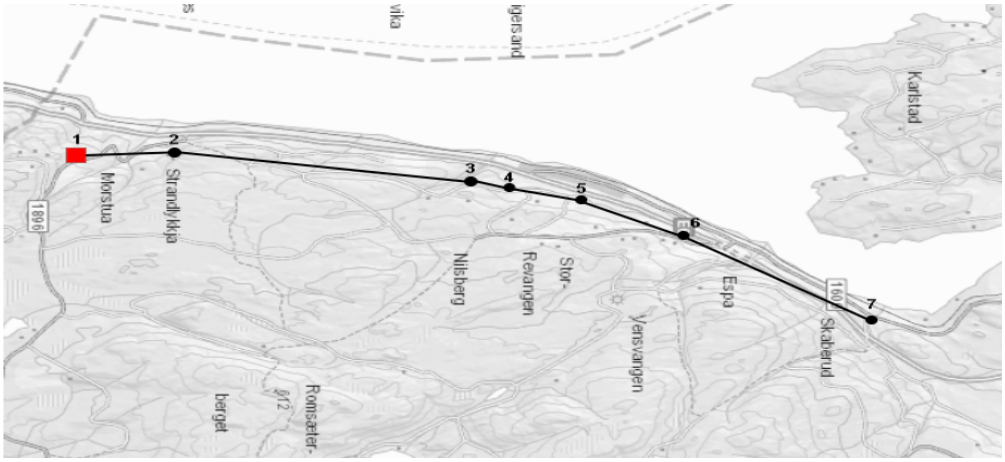

Figure 26: Topology of the distribution grid 5 between Espa and Strandlykkja.

There is a total of 7 buses in the distribution system, with load at every single bus except bus 1, which is the bus connected to the 22kV side of the transformer. The load at each bus, is seen in table 20 in appendix C.5. The distribution grid is a single radial. Thus, the grid is dimensioned after power flowing from bus 1. The target of 5% voltage drop at peak load was obtained. With the smallest dimension for all the lines, the voltage drop at peak load was 5.1%. The dimension and length of each line are described in table 19. The voltage magnitudes for all buses in the system, with base load, is seen in figure 27. The voltage profile is from $h = 14$, when the voltage drop in the system is highest. The base load for the distribution system, as well as bus 5 and bus 6, is seen in figure 28.

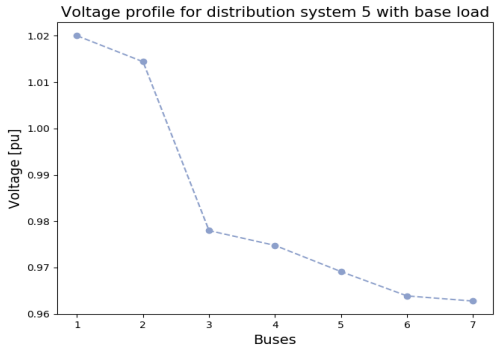

Figure 27: Voltage profile for the distribution system 4 with base load. The voltage profile is for the hour $h = 14$ were the voltage drop is highest

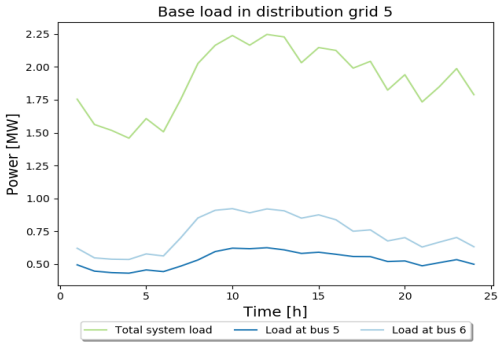

Figure 28: Aggregated base load for the system and base load at bus 5 and 6.

6.4.8 Distribution grid 6: Tangen

The sixth distribution grid has a ring topology with a few radials. The grid connection is at bus 1, which is connected to the low voltage side of a 66kV/22kV substation. The potential location to connect an FCS is buses 3 and 15. The topology of the distribution grid is seen in figure 29.

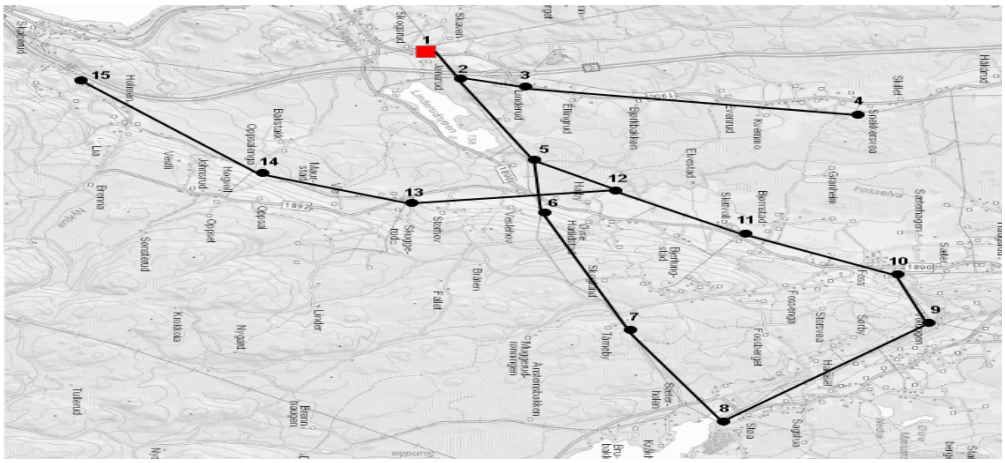

Figure 29: Topology of the distribution grid 6 at Tangen.

There is a total of 15 buses in the distribution system, with load at 12 of the buses. The load at each bus, is seen in table 22 in appendix C.6. Since the distribution grid has a ring topology, two scenarios are studied for the dimensioning of the line. The first scenario, with power flowing from bus 5 to bus 12, and then bus 12 to bus 6 and 15. The second scenario, with power flowing from bus 5 to bus 6, and then from bus 6 to bus 15. For scenarios 1 and 2, the voltage drop at peak load was 4.4% and 5.2 %. The cross section and length of each line is seen in table 21. During normal operation, with power flowing in both directions of the ring, the voltage drop at peak load is 1.98%. The voltage magnitudes for all buses in the system, at peak base load, is seen in figure 30. The base load for the distribution system, as well as bus 8 and bus 11, is seen in figure 31.

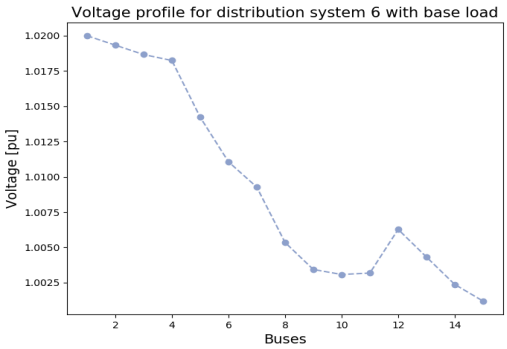

Figure 30: Voltage profile for the distribution system 4 with base load. The voltage profile is for the hour $h = 18$ were the voltage drop is highest

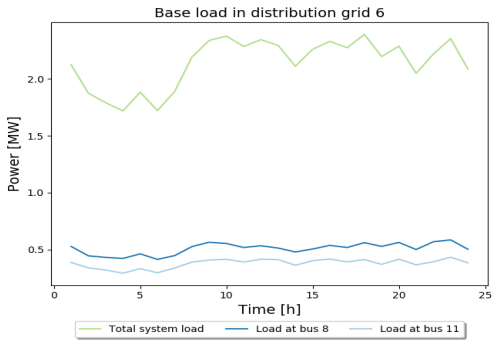

Figure 31: Aggregated base load for the system and base load at bus 8 and 11.

6.4.9 Distribution grid 7: Stange

The last distribution grid has a radial topology. The grid connection is at bus 1, which is connected to the low voltage side of a 66kV/22kV substation. The potential location to connect an FCS is buses 2 and 9. The topology of the distribution grid is seen in figure 32.

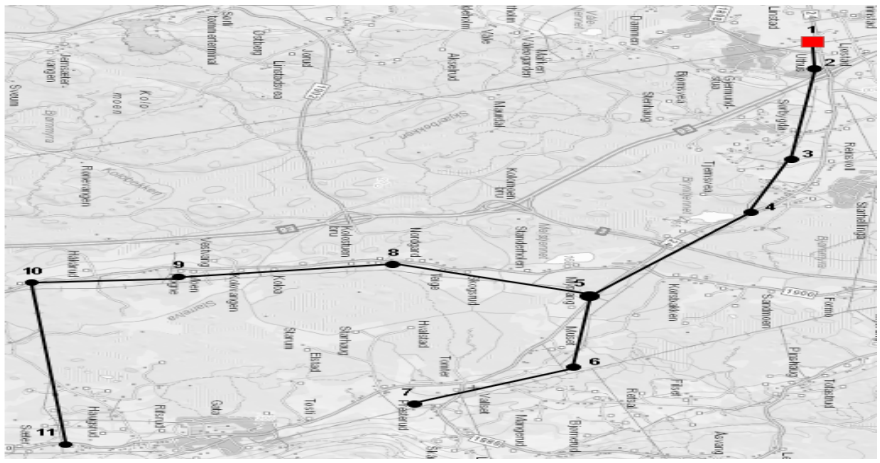

Figure 32: Topology of the distribution grid 7 at Stange.

There is a total of 11 buses in the distribution system, with load at 7 of the buses. The load at each bus, is seen in table 24 in appendix C.7. The distribution grid has a radial topology. Thus, its dimensioned after power flowing from bus 1. With the cross section of the lines, as seen in table 23, a voltage drop of 4.7% was obtained at peak load. The voltage magnitudes for all buses in the system, at peak base load, is seen in figure 33. The base load for the distribution system, as well as bus 3 and bus 7, is seen in figure 34.

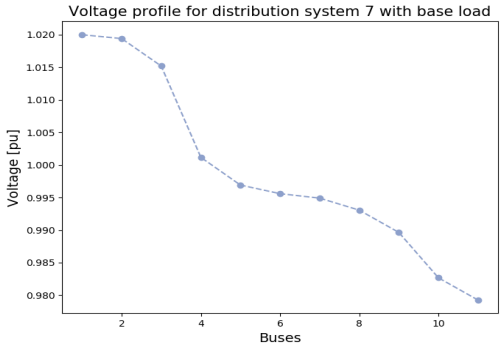

Figure 33: Voltage profile for the distribution system 7 with base load. The voltage profile is for the hour $h = 18$ were the voltage drop is highest

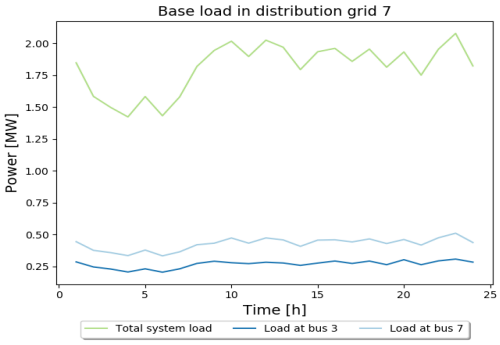

Figure 34: Aggregated base load for the system and base load at bus 3 and 7.

7 Case Studies

7.1 Optimal planning of FCSs

Multiple objective functions are suggested in this thesis to get the placement of the FCS network. The FCS load model also has the number of charging points and its rated power as an input. However, the number of charging points aren't known in the optimal location model. Thus, it's assumed that the FCSs has an unlimited number of charging points, each with a rated power of the EV with the highest charging power. This is a consequence of having a two-step optimization model, and its impact is addressed in section 9.2.

7.1.1 Minimizing grid loss

The aim of the first case study is to optimize the placement of FCSs from a distribution system operator's viewpoint. The objective function is to minimize the energy losses in the distribution system and therefore, minimize the additional power loss from the integration of FCSs. The objective function is presented in 45, subjected to the constraints of equations 36 - 41.

$$\min \quad \Delta P \tag{45}$$

7.1.2 Minimizing grid loss and cost of FCSs

The goal of this case is to minimize the energy loss of the distribution grid and the cost associated with building FCSs. In other words, optimize the position of the FCS with the interest of the DSO and the FCS operator. The cost of an FCS is in the form of equation 46. Where n_{ch} is the number of charging points at the FCS, d is the charging point dependent cost and e is the charging point independent cost.

$$C_{fcs}(n_{ch}) = d \cdot n_{ch} + e \tag{46}$$

However, the number of charging points is determined in the second step of the optimization process. Thus, a flat cost is assumed per FCSs in the BPSO algorithm. Then, after the number of charging points is determined the cost is updated. To be able to compare the two objectives, the power loss is assigned a cost with equation 47, where c_{energy} is the cost of energy.

$$C_{\Delta P} = c_{energy} \cdot \Delta P \tag{47}$$

The objective function is presented in 48, subjected to the constraints of equations 36 - 41.

$$\min \quad C_{\Delta P} + C_{fcs} \tag{48}$$

7.1.3 Minimizing social cost

The last objective functions include the interest of the DSO and FCS operator, but also the EV user. From the DSO's perspective, the cost of energy loss is added and from the FCS operator's perspective, the cost of an FCS is added.

A detour cost is added to illustrate the EV owner's perspective. The detour cost is added if an EV has to drive a detour to charge. If an EV is entering the system at node 3 exiting at node 8, and will need to charge in the system. However, there is no FCS between nodes 3 and 8. Therefore, the EV has to drive in the opposite direction to node 2 to charge. The detour is then defined as the drive from node 3 to node

to, and back. The detour cost is on the form illustrated in equation 49. The first part of the equation is the cost associated with the time of the detour, where d_{detour} is the distance of the detour, v is the speed of the EV and c_t is a time-dependent cost. The latter part, is the cost associated with the energy loss due to the detour. Where η_T is the temperature-dependent driving efficiency introduced in subsection 5.2.3 and $c_{energy,fcs}$ is the energy-dependent cost.

$$C_{detour} = \frac{d_{detour}}{v} \cdot c_t + d_{detour} \cdot \eta_T \cdot c_{energy,fcs} \tag{49}$$

The objective function is presented in 50. The constraints are 36 - 41.

$$\min \quad C_{\Delta P} + C_{fcs} + C_{detour} \tag{50}$$

7.2 Reducing peak power drawn from an FCS

The peak power drawn from an FCS is of great interest. It's dimensioning for the cable or line that is connecting the FCS to the distribution grid. The grid tariffs that the FCS operator pays includes a power tariff that is based on the peak power of the FCS. It can also be of interest from a DSO perspective when planning future grid reinvestments. From the aforementioned perspectives, it's desirable to keep the peak power low. However, it's a trade-off with the serviceability of the FCS and the satisfaction of the customers.

The limit for peak power of an FCS is reduced and its effect on the serviceability of the FCS is studied. The serviceability is measured in the amount of EVs that have to reduce its charging power and percentage of EVs that decide not to charge, due to queue greater than 15 minutes. The EV will share the maximum allowed power of the FCS equally if aggregated the power that the EVs want to charge with exceeds the limit of the FCS. When EVs charging power is limited, it results in EVs having to charge for a longer period to reach its desired SOC. Thus, resulting in longer queues, and therefore more EVs being leaving the FCSs due to excessive queues.

8 Main results

8.1 Optimal planning of FCSs

The input parameters for the BPSO algorithm to decide the location of the FCSs are summarized in table 6. In the BPSO algorithm, 50 particles are created and the algorithm was run for 20 iterations. The possibility for a bit change was limited between 0.25% and 0.9975%, by setting $V_{max} = 6$. The weighting parameters c_1 and c_2 were set to 2. The weight parameter for the inertia, w was varied linearly from 0.9 to 0.2, changing for each iteration. Thus, gradually decreasing exploration of the BPSO.

The input for the FCS load model which is included in the BPSO, is also seen in table 6. Two days were simulated for each tested position. The number of charging points, which is determined in step two, was set to a high number to avoid the possibility of queuing at the FCS. The rated power of the charging points was set to 150 kW, as high as the maximum charging power of any of the EV in the EV fleet. Thus, not limiting the power an EV can charge with. The percentage of cars that are EVs in the system is assumed to 11.5% [6]. The temperature profile used is the temperature profile for the coldest day of 2019. The traffic flow is a stochastic parameter, which can either be weekday and weekend traffic flow.

Table 6: Input for the BPSO algorithm to determine the location of the FCSs

Binary Particle Swarm Input	
Number of particles	50
Number of iterations	20
V_{max}	6
w	0.2-0.9
c_1	2
c_2	2
FCS Demand Model Input	
Deterministic parameters	
Number of simulations	5
Number of charging points	Unlimited
Charging point power rating [kW]	150
EV percentage [%]	11.5
Temperature	Jan 29 2019
Stochastic parameters	
Traffic flow	weekdays, weekends

In the voltage constraint, the limits are set to $V_{min} = 0.95$ pu and $V_{max} = 1.05$ pu. The constraints for the maximum distance between FCSs is determined by the EV with the shortest range, Mitsubishi I-miev. With $SOC_{arr,min} = 0.50$, $SOC_l = 0.2$, $\eta_T = 0.161kWh/km$ and $E_{bat} = 16kWh$, the $d_{fcs,max}$ is calculated by equation 38. Rounding to closest integer, the maximum distance between FCSs is 30 km.

The input parameters for the IPSO algorithm to determine the number of charging points at each FCSs are summarized in table 7. The number of particles used for in the IPSO is 10 and 10 iterations are performed. The IPSO weighting coefficients are the same as for the BPSO. The number of days simulated for each potential solution is increased to 100. This is because the grid model is not included in the IPSO algorithm. Thus, making it computationally less complex. In the IPSO algorithm, the temperature is a stochastic parameter, as the grid model is not included in the IPSO. Therefore, the worst-case scenario is dropped and the temperature is treated as a stochastic input

[6]This is based on personal communication with Vegfinans, which operates the road tolls in the system. At their toll station

Table 7: Input for the BPSO algorithm to determine the location of the FCSs

Integer Particle Swarm Input	
Number of particles	10
Number of iterations	10
V_{max}	6
w	0.9-0.2
c_1	2
c_2	2
FCS Demand Model Input	
Deterministic parameters	
Number of simulations	100
Charging point power rating [kW]	150
EV percentage [%]	11.3
Stochastic parameters	
Temperature	Jan - Dec
Traffic flow	weekdays, weekends

The waiting time constraint 43 of the IPSO is set to a maximum limit of 5% of EVs waiting for more than 5 minutes. The rejection constraint 44, is set to a maximum limit of 1% of EVs leaving due to excessive queues.

at Hovinmoen-Dal, which is located in the system, 11.5% of the cars passing in September 2019 were EVs.

8.1.1 Minimizing grid loss

The total solution space of 8191 combinations of FCSs was simulated to check the performance of the BPSO algorithm. The minimum additional energy loss in the distribution systems, due to the addition of FCS load, is seen in figure 35. The figure shows the minimal additional energy loss as a function of the number of FCSs in the system. There are no valid solutions with one FCS due to the distance constraint being 30 km and the system 74 km. As seen in figure 35, the minimal grid power loss is obtained with 4 FCSs in the system.

The BPSO was simulated with the input of table 6 to decided the locations of the FCSs, with the objective to minimizing the power losses in the system. The lowest cost after each iteration is seen in figure 36. The red line is the optimum solution from figure 35. After six iterations the optimum solution is found. The FCSs are placed at bus 3, bus 2, bus 3 and bus 2, in distribution grids 2, 5, 6 and 7. With the FCSs at the optimum position, the total power loss is 16.776 MWh. The integration of FCS adds an energy loss of 12 kWh. It's important to note that the day simulated is the coldest day of the year with the highest base load. Thus, the daily energy loss is not representative of the average day. The implications of this is addressed in the discussion 9.

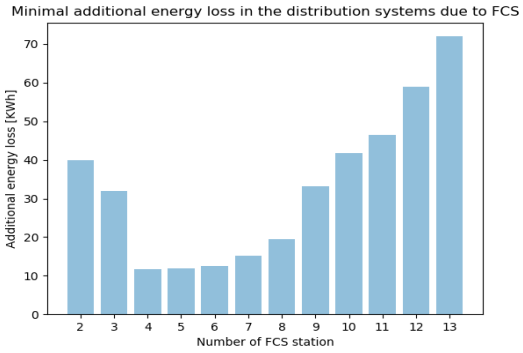

Figure 35: Simulating the total solution space and showing the minimal additional energy loss due to FCS, for each number of FCSs

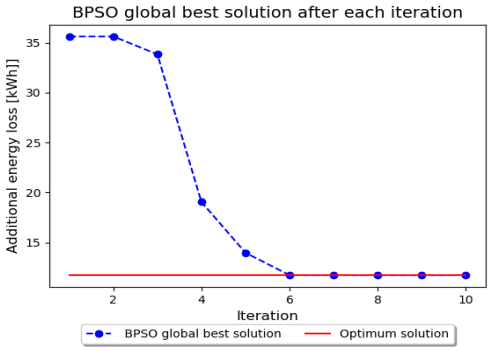

Figure 36: Best solution found by the BPSO algorithm after each iteration. The red line is the optimum solution.

The voltage profiles of the distribution system 2, 5, 6, and 7, deteriorates due to the addition of FCS load. A comparison for the voltage profile, with or without FCS load, is seen in figure 37 and 38, for distribution grid 5 and 6. The comparison is dropped for distribution grid 2 and 7 as the two curves were indistinguishable. Due to both grids having a high base load and the addition of the FCS load had little effect on the voltage profile. The figures show the voltage profiles for both distribution systems, with or without FCS load, in the minute when the voltage profile with FCS load has its minimum value. Thus, confirming that the voltage levels are within the allowed limits.

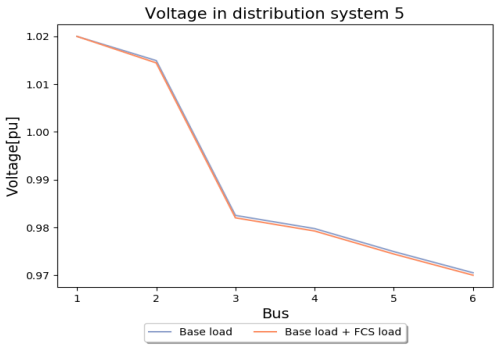

Figure 37: Comparison of the voltage at all the buses in distributions system 5, with an without FCS load. The voltage profile is for a random day, in the minute when the voltage profile with FCS load has its minimum value.

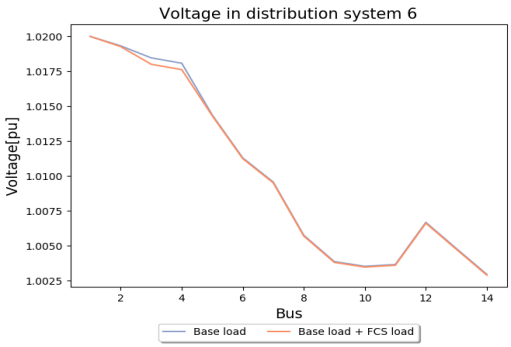

Figure 38: Comparison of the voltage at all the buses in distributions system 6, with an without FCS load. The voltage profile is for a random day, in the minute when the voltage profile with FCS load has its minimum value.

As previously mentioned, the base load is in hourly values while the FCS load has a granularity of a minute. Figure 39a, illustrates how the voltage levels at bus 3 in distribution system 2, fluctuates during for a random day due to the addition of the FCS load. Bus 3 in distribution system 2 is the bus where the FCS is connected. Figure 39b, 39c and 39d, shows the voltage fluctuations at bus 2, 3 and 2, in distribution system distribution system 5, 6 and 7, where the FCS is connected in the respective distribution grid.

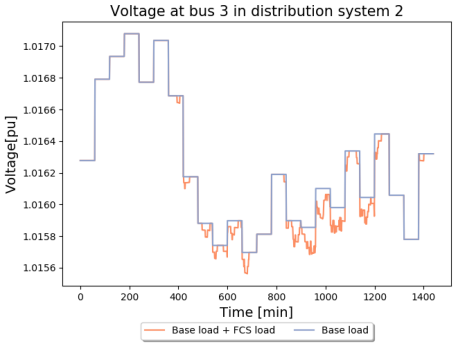

(a) Voltage at bus 3 distribution system 2, with and without FCS load.

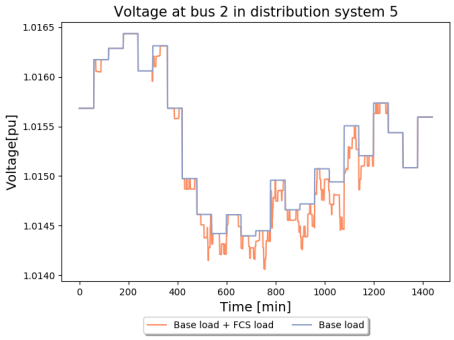

(b) Voltage at bus 2 distribution system 5, with and without FCS load.

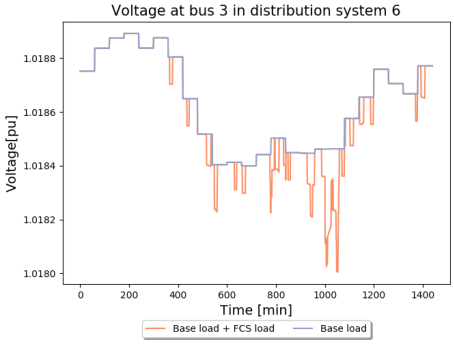

(c) Voltage at bus 3 distribution system 6, with and without FCS load.

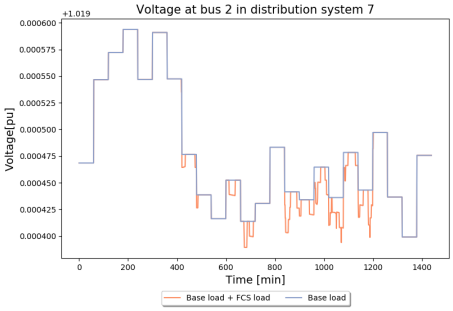

(d) Voltage at bus 2 distribution system 7, with and without FCS load.

Figure 39: Comparison of the voltage at the bus where the FCS is connected, for all the FCSs, with and without FCS load.

8.1.1.1 Optimum size of FCSs

When the optimum location of the FCSs has been determined in the BPSO algorithm. Then, the number of charging points at each FCSs can be determined by the IPSO algorithm. The optimum size of each FCS is shown in table 8. The percentage of EVs leaving the FCS is zero for all the FCSs.

Table 8: Design of the different FCSs for case 1

	FCS 1	**FCS 2**	**FCS 3**	**FCS 4**
Number of charging points	3	3	2	2
EVs wait >5 min [%]	4.47	2.37	4.84	4.14
EVs rejected [%]	0.00	0.00	0.00	0.00

With the load model input from table 6 and the size of the FCSs from table 8, demand profiles for the FCSs are simulated. The load profile for a random day and the average load profile for all the FCSs is seen in figure 40. The random day is a weekday with the temperature profile of December 10, 2019, as input. The average load profiles are based on the simulation of 100 days. For FCS 1 the daily peak power was 166 kW with 48 EVs visiting. The daily peak power of FCS 2 was 151 kW with 27 EVs visiting. For FCS 3 and FCS 4, the daily peak power was 210 kW and 102 kW with 25 and 16 EVs charging at the FCS.

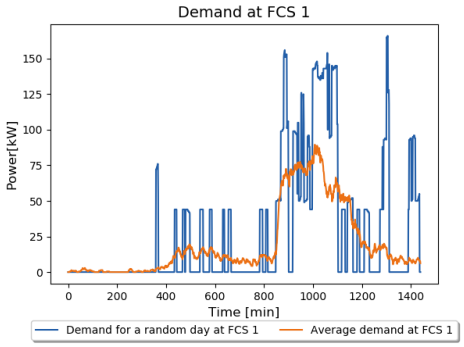

(a) Charging demand for FCS 1

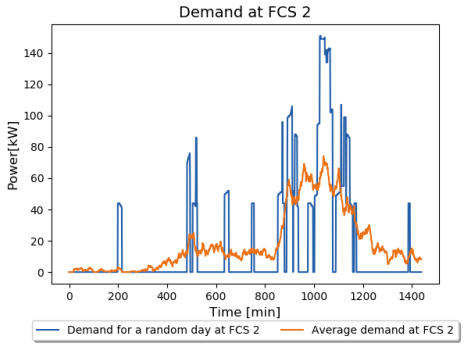

(b) Charging demand for FCS 2

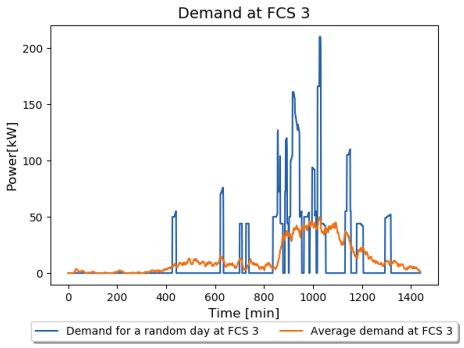

(c) Charging demand for FCS 3

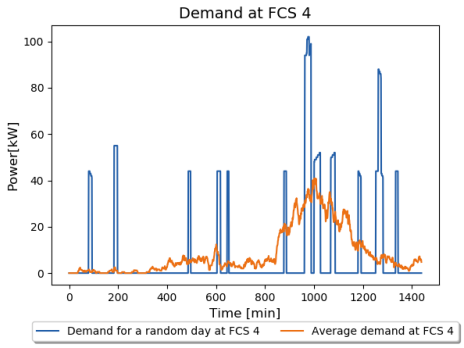

(d) Charging demand for FCS 4

Figure 40: Charging demand at all the four FCSs for the optimum solution.

8.1.2 Minimizing cost of energy loss and cost of FCSs

8.1.2.1 Optimum location of FCSs

The objective function for the BPSO algorithm is changed to minimize the cost of energy loss and the cost of FCSs. The energy loss is assigned a cost of 0.261 kr/kWh [65]. The cost of an FCS is given by equation 46. The charging point dependent cost, d is 1 000 000 kr and based on charging points with a rated power of 150 kW [7]. The constant cost is assumed to be 500 000 kr [69][8]. The number of charging points is not known when deciding the location of the FCSs. Therefore, it's assumed that the number of charging points is constant and the FCSs cost is then transformed to equation 51, with ten charging points in the system. To be able to compare the two costs, the FCS cost is transformed into a yearly cost, by dividing it by the life expectancy of 30 years. The daily energy loss is assumed to be equal for each day and converted into a yearly cost.

$$C_{fcs}(n_{fcs}) = 500000 \cdot n_{fcs} + 10000000 \tag{51}$$

From there previous scenario, four FCSs resulted in minimal grid losses. Thus, the optimum solution for this scenario must be with four or less FCSs, since both costs increases after this point. The BPSO algorithm is then adjusted, so all initial particles have between two and four FCSs. With the aforementioned changes, the BPSO is performed with the input as in table 6. The total solution space is simulated and the minimal cost of FCSs and energy loss for each number of FCSs is seen in figure 41. The FCS cost is the dominating cost. Thus, the optimum solution contains the minimum amount of FCSs needed to not breach the coverage constraint. The BPSO converge quickly and the optimum solution was found after 5 iterations, as seen in figure 42. The two FCSs were placed at bus 3 and bus 2, in distribution grid 2 and 5.

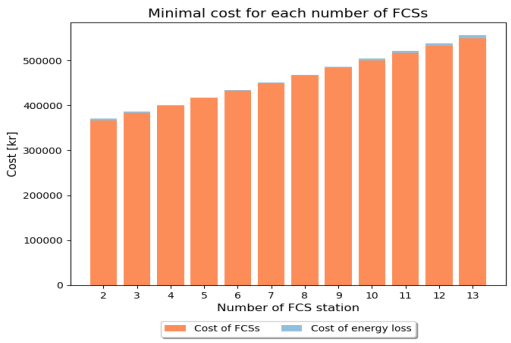

Figure 41: Simulating the total solution space and showing the minimal cost of FCS and cost additional energy loss and due to FCS, for each number of FCSs

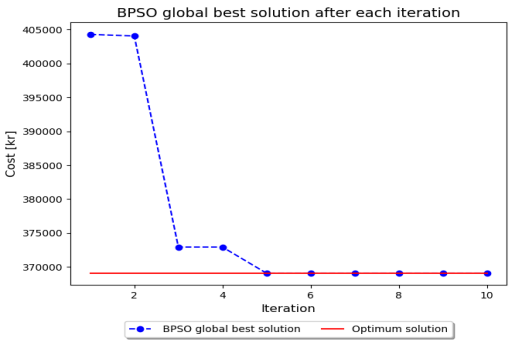

Figure 42: Best solution found by the BPSO algorithm after each iteration. The red line is the optimum solution.

[7] The charging point dependent cost is acquired from the partners of the FuChar project.

[8] This cost is based on a 50 kW charging point costing 250 000 kr and the minimum cost of an FCS with 2 charging points being 1 000 000 kr.

The voltage profiles of the distribution system 2 and 5, deteriorates due to the addition of FCS load. A comparison for the voltage profile, with or without FCS load, is seen in figure 43 and 44. The figures show the voltage profiles for both distribution systems, with or without FCS load, in the minute when the voltage profile with FCS load has its minimum value. Thus, confirming that the voltage levels are within the allowed limits. Distribution gird 2 has a high base load and the addition of the FCS load at bus 3 has little effect on the voltage profile, as seen in figure 43. On the other hand, for distribution grid 5, the addition of the FCS load has a bigger effect on the voltage, as seen in figure 44. This is due to the addition of FCS load, representing a significant addition in the system load of distribution grid 5. However, the voltage profiles for both the distribution grids are well within the limits.

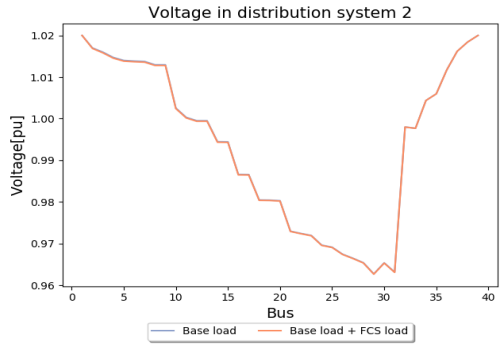

Figure 43: Comparison of the voltage at all the buses in distributions system 2, with an without FCS load. The voltage profile is for a random day, in the minute when the voltage profile with FCS load has its minimum value.

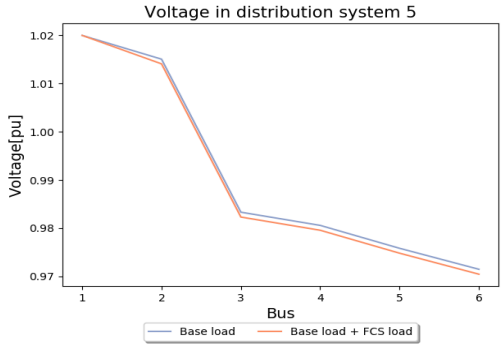

Figure 44: Comparison of the voltage at all the buses in distributions system 5, with an without FCS load. The voltage profile is for a random day, in the minute when the voltage profile with FCS load has its minimum value.

As previously mentioned, the base load is in hourly values while the FCS load has a granularity of a minute. Figure 45, illustrates how the voltage levels at bus 3 in distribution system 2, fluctuates during for a random due to the addition of the FCS load. Bus 3 in distribution system 2 is the bus where the FCS is connected. Figure 46, shows the voltage fluctuations at bus 2 in distribution system 5, for a random day.

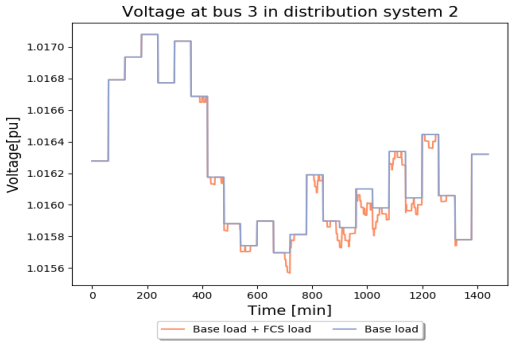

Figure 45: Comparison of the voltage at the bus where the FCS is connected, bus 3 distribution system 2, with and without FCS load.

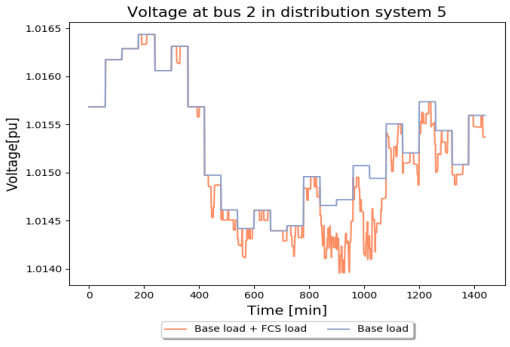

Figure 46: Comparison of the voltage at the bus where the FCS is connected, bus 2 distribution system 5, with and without FCS load.

8.1.2.2 Optimum size of FCSs

When the optimum location for the FCSs has been decided by the BPSO and it's confirmed that the solution is valid with the power flow performed with a time step at 1 minute. Then, the optimum number of charging points at each FCS is then decided by the IPSO algorithm, with the input from table 7. The number of charging points for each FCS is shown in table 9. The percentage of EVs that have to wait longer than 5 minutes before charging and the percentage of EVs that leave the FCS due to excessive waiting time is also seen in table 9. These values are less than the maximum limits for both FCSs.

Table 9: Optimum design of the different FCSs

	FCS 1	**FCS 2**
Number of charging points	4	6
EVs wait <5 min [%]	4.98	2.09
EVs rejected [%]	0.00	0.00

With the load model input from table 6 and the size of the FCSs the same as decided through the IPSO algorithm, load profiles for both the FCSs are simulated. For FCS 1, the load profile for a random day and the average load profile is seen in figure 47. The peak at FCS 1 for the random day is 225 kW and 67 EVs charged at the FCS that day. The demand profile for a random day and the average demand profile for FCS 2, is seen in figure 48. The peak at FCS 2 for the random day is 351 kW and 84 EVs charged at the FCS that day. The random day simulated was a weekday with the temperature profile of November 4, 2019, as input.

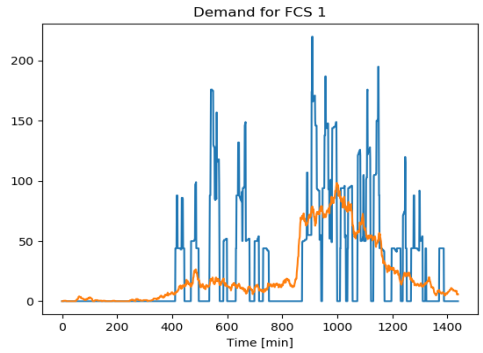

Figure 47: The demand profile for a random day and the average demand profile for FCS 1. The random day simulated is a weekday, with the temperature profile of November 4, 2019, as input.

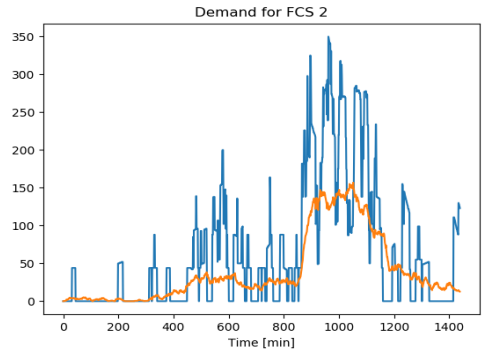

Figure 48: The demand profile for a random day and the average demand profile for FCS 2. The random day simulated is a weekday, with the temperature profile of November 4, 2019, as input.

8.1.3 Minimizing social cost

8.1.3.1 Optimum location of FCSs

When minimizing the social cost connected with the placement of FCSs the objective function is given by equation 50. The cost of energy loss and the cost of FCSs is the same as in the last section. For the detour cost, the time-dependent cost is $c_t = 280$ kr/h. This is based on the cost of queuing from the Norwegian Center for Transport Research [70]. The energy-dependent cost is $c_{energy,fcs} = 8.40$ kr/kWh, which is the cost of energy when charging at an FCS operated by IONITY [71]. Table 8 is used as input for the BPSO.

The total solution space was simulated, and the minimal social cost for each number of FCSs is seen in figure 49. The minimal social cost after each iteration of the BPSO is seen in figure 50. The optimum solution is found after 8 iterations and contains 3 FCSs. The FCSs is placed at bus 12, bus 9 and bus 2, in distribution grid number 1, 3 and 5.

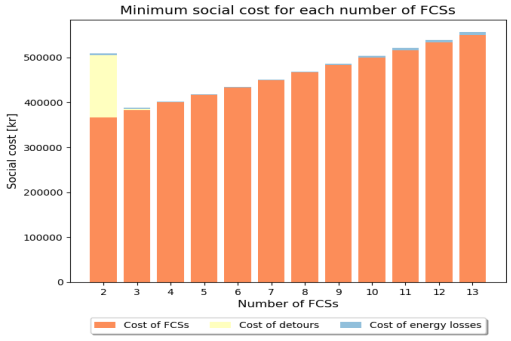

Figure 49: Simulating the total solution space and showing the minimal social cost, for each number of FCSs

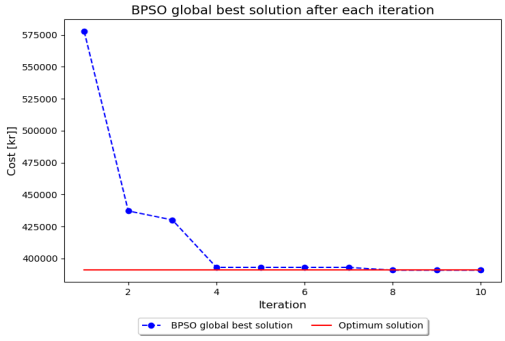

Figure 50: Best solution found by the BPSO algorithm after each iteration. The red line is the optimum solution.

The voltage profiles of the distribution system 1, 3 and 5, deteriorates due to the addition of FCS load. A comparison for the voltage profile, with or without FCS load, is seen in figure 51 and 52. The voltage profile for distribution system 5 is dropped as its indistinguishable from figure 44. The figures show the voltage profiles for both distribution systems, with or without FCS load, in the minute when the voltage profile with FCS load has its minimum value. Thus, confirming that the voltage levels are within the allowed limits.

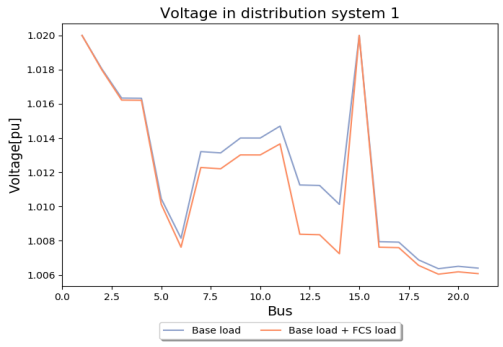

Figure 51: Comparison of the voltage at all the buses in distributions system 1, with an without FCS load. The voltage profile is for a random day, in the minute when the voltage profile with FCS load has its minimum value.

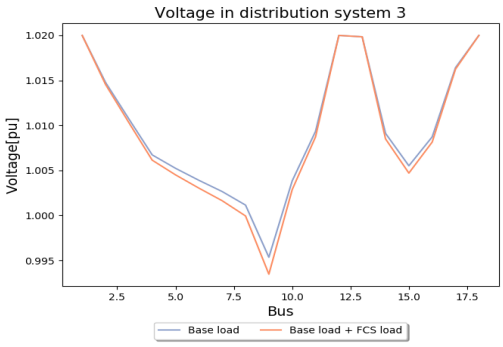

Figure 52: Comparison of the voltage at all the buses in distributions system 5, with an without FCS load. The voltage profile is for a random day, in the minute when the voltage profile with FCS load has its minimum value.

Figure 53, illustrates how the voltage levels at bus 12 in distribution system 1, fluctuates during for a random due to the addition of the FCS load. Bus 3 in distribution system 2 is the bus where the FCS is connected. Figure 54, shows the voltage fluctuations at bus 9 in distribution system 3 for a random day.

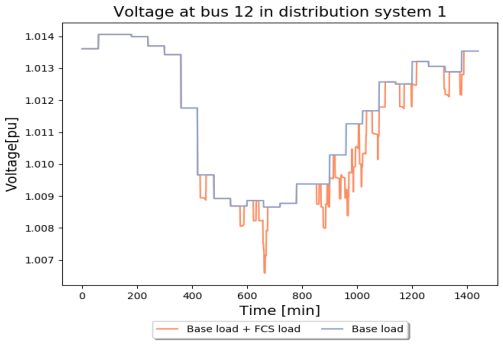

Figure 53: Comparison of the voltage at the bus where the FCS is connected, bus 12 distribution system 1, with and without FCS load.

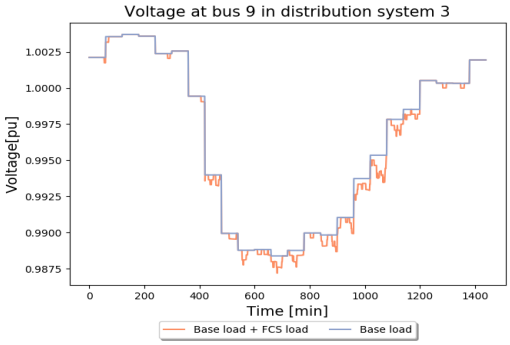

Figure 54: Comparison of the voltage at the bus where the FCS is connected, bus 3 distribution system 9, with and without FCS load.

8.1.3.2 Optimum size of FCSs

The input of the IPSO model is seen in table 7. The IPSO is used to determine the number of charging points at each FCSs and the results are seen in table 10. The optimum number of charging points for FCS 1 and 2 is 3 charging points, while for FCS 3 is 4 charging points. The reason a higher number of charging points is needed at FCS 3, is due to it covering a larger part of the system.

Table 10: Optimum design of the different FCSs

	FCS 1	**FCS 2**	**FCS 3**
Number of charging points	3	3	4
EVs wait <5 min [%]	1.37	3.88	4.96
EVs rejected [%]	0.00	0.00	0.00

With the load model input from table 6 and the size of the FCSs from table 10, load profiles for the FCSs are simulated. For FCS 1, the load profile for a random day and the average demand profile is seen in figure 55. The peak power at FCS 1 for the random day is 144 kW and 39 EVs charged at the FCS that day. The daily load profile and average load profile for FCS 2, is seen in figure 56. The peak power at FCS 2 for the random day is 182 kW and 63 EVs charged at the FCS that day. For FCS 3, the daily and average load profile is seen in figure 57. The peak power at FCS 3 for the random day is 231 kW and 84 EVs charged at the FCS that day. The random day simulated was a weekday with the temperature profile of April 9, 2019, as input.

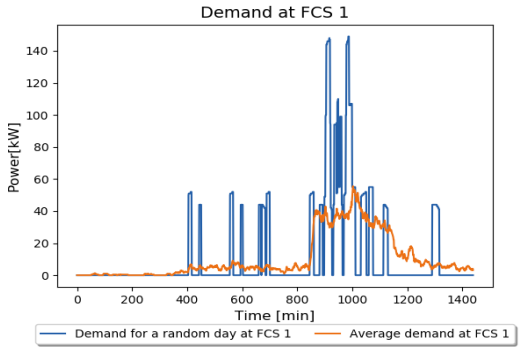

Figure 55: The load profile for a random day and the average load profile for FCS 1. The random day simulated is a weekday, with the temperature profile of April 9, 2019, as input.

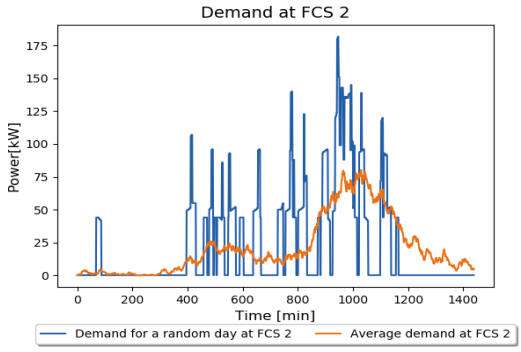

Figure 56: The load profile for a random day and the average load profile for FCS 2. The random day simulated is a weekday, with the temperature profile of April 9, 2019, as input.

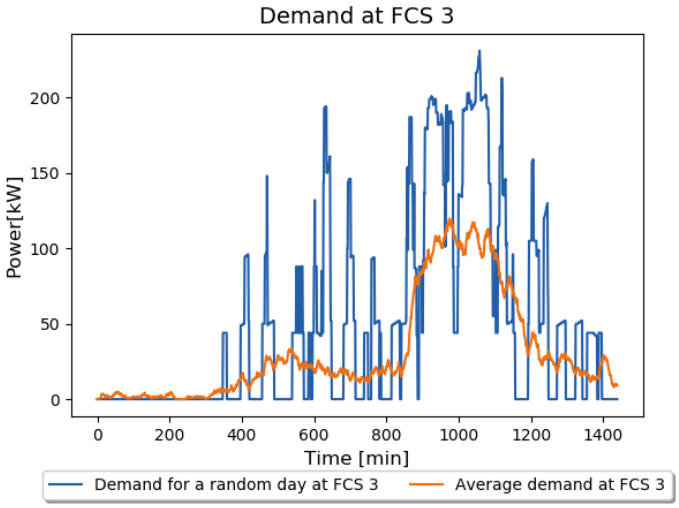

Figure 57: The load profile for a random day and the average load profile for FCS 3. The random day simulated is a weekday, with the temperature profile of April 9, 2019, as input

8.2 Comparing the cases

For each of the three cases, the social cost is computed. This is done to highlight the impact of choosing different objective functions. Figure 58 illustrates the social cost for the different cases. Naturally, the social cost of case 3 is the same as found in subsection 8.1.3. For case two, the detour cost is computed for the optimum solution found in subsection 8.1.2. For the first case, both the cost of FCSs and detour cost is added to the optimum solution found in subsection 8.1.1. The social cost for case 1 and 2, was 21.4% and 25.2% higher the social cost of case 3. Much of this increase is due to the detour cost which was 3327% and 5400% higher for cases 1 and 2, than for case 3.

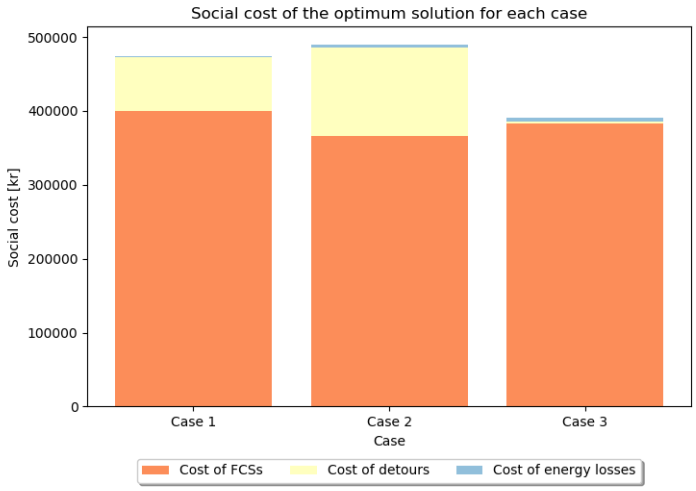

Figure 58: Comparing the social cost of the three case studies. As the two first cases didn't compute the social cost, the missing cost has been added to the optimum solution found in its respective case.

The energy demand of the FCS is not included in any of the objective functions, but for illustrative purposes its depicted in a box plot in figure 59. The daily system fast charging energy demand is calculated for each of the three cases with input to the FCS load model as seen in table 7 and 1000 days is simulated. A box plot is used to illustrate the daily energy demand for its ability to capture both the median demand and its variation. For case 1 with 4 FCSs the median daily fast charging system demand is 1432 kWh, case 2 with 2 FCSs its 1485 kWh and for case 3 with 3 FCS its 1469 kWh.

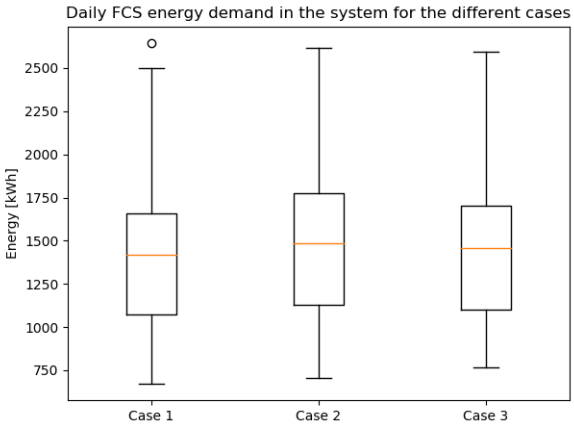

Figure 59: The daily fast charging energy demand for the the system for the different cases.

8.3 Reducing the peak power of an FCS

The FCS 1 in table 10 from the minimal social cost is used to study the effects of reducing the limit for peak power of an FCS. The FCS has three charging points each rated at 150 kW. Thus, the potential peak power of the FCS is 450 kW. The FCS demand model is simulated with input as seen in table 7. The peak power limit of the FCS is varied and for each peak power limit, 100 days is simulated. To study the stochastic impact, the simulations are performed multiple times with different stochastic seeds. Thus, one red dot, in figure 60 and 61, represents a 100 days simulated for constant a peak power limit and stochastic seed.

The percentage of EVs that are capped for each peak power limit of the FCS is seen in figure 60. Capped EVs, are EVs that have to reduce their charging power to not breach the FCS peak power limit. If the allowed peak power of FCS 1 is 180 kW, and two EVs want to charge simultaneously each at 100 kW, then they both are capped and can only charge with 90 kW. Only 1% of the EVs are capped when the FCS's peak power limit is 155 kW, as seen in figure 60. The relationship is nonlinear and with a further reduction to 100 kW, 20.5% of the EVs are capped.

For each simulation, the percentage of EVs leaving the FCS is recorded, creating figure 61. The effects of reducing the peak power of the FCS are not reflected in the rejection rate before the peak power limit is less than 140 kW. When the limit is at 100 kW, about 0.5% of the EVs is rejected due to excessive waiting time.

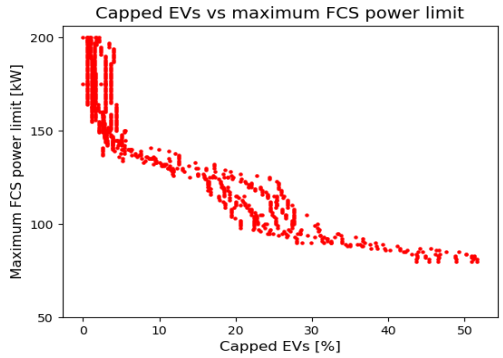

Figure 60: Relationship between maximum allowed peak power at FCS 1 from 10 and percentage of EVs that has there charging power limited. One red dot in represents a 100 days simulated for constant peak power limit and stochastic seed.

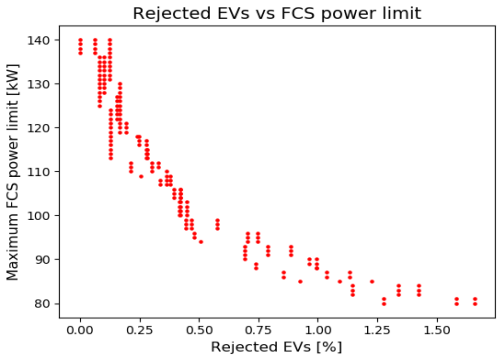

Figure 61: Relationship between maximum allowed peak power at FCS 1 from 10 and percentage of EVs that are decides not to charge due to excessive queues. One red dot in represents a 100 days simulated for constant peak power limit and stochastic seed.

9 Discussion

The main problem of this master thesis was to decide the optimal planning of an FCS network. This is a highly complex problem that requires a detailed distribution grid and the mobility of EVs as an input. However, data about the distribution grid is not open to the public. Thus, a distribution grid model was developed, which creates and dimension distribution grids, specific for the system. The proposed distribution grid model is based on power system planning principles, taking into consideration both economic and power system aspects. The available traffic data was inadequate. Hence, a mobility model was developed to create a more detailed flow of EVs in the system.

9.1 Submodels

The main input to the distribution grid model is the NVE Atlas map tool, which shows the location of overhead distribution lines. The fact that only overhead lines and not cables are shown, resulted in the proposed model is only applicable in areas where the distribution system consists of overhead lines. Due to the geographic and demographic nature of Norway, the distribution grid is complex. In grids that contain long radials, going away from the highway, the load of these radials was aggregated to the origin bus of the radial. The power delivered to the potential FCS would not flow in these radials. Thus, aggregating these the load in these radials would have a minor impact on the energy losses in the grid. In some areas, the distribution grids had a meshed topology. Then, a simpler topology was assumed, for simplicity reasons.

When determining the base load of the distribution grid, the peak of the general load profiles are used for non-household load. The peak load of the non-household load is multiplied with the number of customers from the specific customer group connected to that bus. This method assumes the peak load from customers from the same customer group to happen at the same time, except for households. Generally, this is not through, but since the vast majority of the loads in the system are from households. The household load will contribute most to the peak load at the buses and in Velanders formula a form off coincidence factor is implemented in the calculation of household peak load.

A limitation of the proposed gird model is that is doesn't take into account reactive power, harmonics, or interactions between the distribution grids. Nearly all the distribution grids are connected to each other through a 66kV line. However, for simplicity reasons interactions between the grids are not implemented. The general load profiles only contain real power, and not reactive power. Thus, reactive power wasn't taking into consideration in the base load, and is not modeled in the FCS load model. FCS consists of a lot of power electronics and can introduce unwanted harmonics and consume reactive power. However, as the main focus of this thesis was on the optimization tool and not the grid impacts, this was not accounted for. Nonetheless, this should be improved in future work, especially taking into consideration reactive power.

A total of seven distribution grids was created with the grid model. As previously mentioned in section 5.3, the distribution grids were dimensioned based on the general load profiles, but the load flow was performed with the real load data from households and general load profiles for non-household loads. This was done to create a more realistic base load, with variation in peaks between the different households. However, this can lead to a difference in the peak load used to dimension the grid and the peak of the base load. The Velander formula, which was used to dimension the grid, has a decreasing peak power per household for an increasing number of households. However, by using real data, there is no decrease in the expected peak power per household, when the number of households increases. Thus, the expected mean peak power per household is constant when using the real data, while in the Velander formula is a function of the number of households. If the expected peak power per household for the real load data is somewhere in the middle of the range the Velanders formula. Then, using the Velanders formula might yield a too high peak power for buses with few households and too low for buses with many households. This may explain why, in distribution grid 2, a higher voltage drop was experienced with the base load, than with the load used to dimension the grid. Especially, since distribution grid 2 have buses with a high number of households along the branch starting at bus 23 and ending at bus 30, which is a critical branch of the system. Another explanation, can be due

to statistical variation when drawing real household load data and assigning it to houses in the system.

The proposed mobility model consisted of traffic nodes. The traffic nodes are locations, along the highway, where the traffic flow is measured. The EVs were only able to leave and enter the system at the traffic nodes. It's assumed that this assumption would only have minor impacts as the density of traffic nodes in the system is high. However, if the same methodology is used in a different system, with few traffic nodes, this may result in unrealistic traffic flow. An algorithm was proposed to determine the exit node of the EVs, based on the flow of vehicles in the system. The proposed algorithm only used probability with no assumptions about the driving patterns of the EVs. As there is no data about the route of the individual vehicles, only aggregated traffic flow. Thus, a vehicle that has driven in the system past multiple traffic nodes and a vehicle that just entered the system, is as likely to exit the system at the next traffic node.

With the input from the mobility model, the load at the FCSs was determined using the FCS load model. There is a lot of factors influencing the FCS demand. Thus, to model the load at the FCSs, a few assumptions where needed. The SOC of an EV is the determining factor for whether or not it will charge. However, the SOC of the EVs when they enter the system is not known. Information about EV owners charging habits was used together with the assumption that there was some commuting in the system during the weekdays. This formed the basis for the SOC input used in the model. The accuracy of these assumptions is difficult to determine without researching the charging behavior in the system. Another assumption was taken when creating the EV fleet used in the model. The top 10 most common EVs in Norway is used, as most common EVs in the system is not known. In the case, where an EV has multiple models the newest model is assumed. A limitation of the proposed FCS load model is that it doesn't take into account outside temperature's effect on the charging power, which was pointed out in the literature review. The FCS load model also doesn't take into account the degradation of the EV batteries.

9.2 Optimization model

The proposed optimization model decides the location and size of the FCSs and is a two-step model. The location of the FCS is decided in step 1, while the number of charging points for each FCS is determined in step 2. The motivation for splitting the optimization problem into two parts is to make it less computationally expensive and more transparent. However, the number of charging points at an FCSs will impact the demand profile of the FCS, which is needed to decide the location in step 1. Thus, it was assumed that each FCS had an unlimited number of charging points. This will give the FCSs a higher load in peak hours, since more EVs can charge simultaneously instead of waiting in line. However, as the waiting constraints for step 2 was strict and didn't allow for much queuing, the difference in the charging curves is assumed to be small. Thus, resulting in a negligible impact on average daily energy loss in the distribution system. Nevertheless, as the number of charging points is decided with a stochastic temperature input, the impact will be more significant for a worst-case day.

In step 1 of the optimization problem, the worst-case scenario is assumed. The base load of the distribution system is for the coldest day of the year. In the FCS demand model, the input temperature is the coldest day of the year, resulting in a higher EV power consumption and thus, a high FCS demand. This worst-case scenario is used to ensure grid stability. However, this will lead to an unrepresentative high energy loss compared to an average day. This is not a problem when the goal is to minimize energy loss. As the energy loss might not be the correct value, but the error is assumed equal for all solutions. Thus, not effecting the ranking between different solutions. For the multi objective functions, where there is a trade-off between different costs, this can potentially impact the solution. Nevertheless, the cost of additional energy loss is small compared to the other cost. Therefore, its impact would likely not alter the optimal number of FCS, but could potentially impact the location of the FCS. Ideally, the proposed FCS location should first be tested with the worst case input to ensure grid stability. Then, with the input of an average day, to calculate a representative energy loss. However, for this to be possible, two base load needs to be calculated. With the time restrictions of the master thesis, this was not possible. It would also nearly double the run time of the algorithm, as the most computationally expensive part of the optimization model is the power flow.

As previously mentioned, the load flow in the optimization model is performed with a time step of an hour to make it less computationally expensive. Then, only for the final solution, the power flow calculation is performed with a time step of a minute. As the granularity of the FCS load is 1 minute, hourly averages values are used in the optimization model. This can impact the energy losses in the system, but they are assumed to be minor. It would also not impact the ranking between locations for the single objective function, but could impact the solution for the multi objective function. However, as the cost of energy loss is the smallest, it's therefore unlikely that minor change in it would impact the optimum solution.

The number of charging points for each FCS is decided in step 2 of the optimization model. The FCSs are sized separately and it's assumed that the size of one FCS doesn't impact the size of the other. If an EV leaves an FCS, due to excessive queue, it will not charge at another FCS in the system. However, as the FCSs are designed with a low rejection limit this is seen as a minor flaw with the model. This was also confirmed with the results showing a rejection rate of 0.0% for all the FCSs.

9.3 Main results

In the first scenario, the FCSs were placed to minimize the energy loss in the grids. Generally, the load at an FCS decreases with the amount of FCSs, but this is also dependent on the location of the other FCSs. The total solution space was simulated to check that the algorithm provided the optimum solution. First, the energy loss decreases with the introduction of more FCSs, before it increases again. With four FCSs, the energy loss in the grid was minimized and the proposed BPSO was able to find the optimum solution. When introducing more FCSs to the system the load at each FCS might be reduced. However, the new FCS might be connected to a weak point in the distribution grid, resulting in increased total energy losses in the grids. Thus, its a trade-off between reducing the load at each FCSs and the robustness of the connection points. Its also important to note that with few FCSs in the system, the FCS coverage constraint will narrow the possible locations to place the FCSs. Resulting in FCSs potentially being placed in locations with weak grid connection, to secure coverage.

In the second objective function, the cost of building FCSs was added to the cost of energy losses. Naturally, the cost of FCSs increases with the number of FCSs. With the introduction of the cost of FCS, the optimum solution was shifted from four to two FCSs. Two FCSs is the minimum amount of FCSs in the system, as only a single FCS breaches the coverage constraint. In the optimization problem, the cost of FCSs is only a function of the number of FCSs. Thus, the cost is independent of the location of the FCSs. The optimum solution is therefore in the location with two FCSs that have the lowest energy loss.

In the third scenario, the FCSs were placed to minimize the social cost. A detour cost was added to the objective function from scenario two, which contained the cost of FCSs and the cost of energy losses in the grid. Generally, more EVs need to drive a detour if there are fewer FCSs in the system, but this is also dependent on the location of the FCSs. With the addition of detour cost, the optimum solution was shifted from 2 to 3 FCSs. This was due to the reduction in the cost of energy loss and detour cost, which exceeded the increase in the cost of FCSs, when going from two to three FCSs. The detour cost also outweighed the energy loss cost, so that the optimum solution was not the solution with three FCSs that had the lowest energy cost. Instead, the three FCSs were placed in high traffic areas, to reduce the amount of detour from EVs. This illustrates the importance of taking into consideration the perspective of all the different participants when planning an FCS network.

The social cost was calculated for the optimum solution for the three presented cases. The results showed that the social cost for case 1 and 2, was 21.4% and 25.2% higher the social cost of case 3. A majority of this increase was due to the increase of the detour cost, which was 3327% and 5400% higher for cases 1 and 2, than for case 3. When the FCS network was designed in case 2, taking into consideration the interest of the DSO and FCS operator. The results are a design with the minimum number of FCSs, which placed in the locations to minimize the grid loss. The location with the minimal grid loss isn't necessarily where the most EVs are driving in the system. Therefore, a lot of EVs has to drive detours when they need to charge, resulting in a high detour cost.

To be able to create the multi objective functions in cases 2 and 3, each objective needs to be transformed into monetary values. Thus, additional energy loss, FCSs and detours need to be assigned a cost. The FCS cost will be highly dependent on the location and cost of land, but also the rated power of the charging points. There is also great uncertainty around the cost of detours, as it involves assigned a cost to the time of an EV owner. It's also important to note the objective of the FCSs operator is modeled as wanting to minimize cost. However, it would be more accurate to add their objective as maximize profit. Nonetheless, as the EVs are willing to drive detours to arrive at the FCSs and the energy demand is the highest for the least amount of FCSs, maximize profit and minimize cost yields the same result. If an FCS network or a single FCS is to be placed in an area where there are already existing FCSs. Then, the objective of the FCSs owner has to be changed to maximizing profit. This is a limitation of the proposed objective function that represents the FCS operator's interests.

The daily energy demand of all the FCSs in the system was calculated for each of the three cases. The results showed that energy demand is decreasing with the number of FCSs in the system. This is as expected, since with additional FCSs in the system, the EVs will generally have a shorter drive to the closest FCS when they need to charge. Thus, resulting in a lower energy demand at the FCSs.

For all the three optimization scenarios, the current condition was studied. This includes the current EV fleet, the percentage of vehicles that are EV and base load of the distribution systems. Especially the first two, is expected to change drastically over the coming years. Thus, when planning FCSs with a life expectancy of 30 years, its important to not only consider the current conditions, but future conditions as well. To avoid having to continually upgrade the FCS, when the EV percentage and EV fleet changes enough to make the FCS undersized.

The peak power drawn from an FCS is of great interest to both the FCS operator and DSO. From the DSO and FCS operator perspective, it's desirable to keep the peak power low. However, it's a trade-off with the serviceability of the FCS and the satisfaction of the customers. In section 8.3, the limit for maximal power at an FCS was varied and the effects studied. The FCS studied had 3 charging points and with the current EV fleet, the peak load at the FCS had a theoretical limit of 450 kW. The maximal power at the FCS could be reduced to 155kW, with only 1% of the EVs being effected. The same tendencies were seen when the effects of reducing the peak power of the FCS on the rejection rate of EVs were studied. The peak power of the FCS could be reduced to 100 kW, with less than 0.5% EVs leaving the FCS due to excessive waiting time. The results of section 8.3, indicates a great potential for reducing the peak load at the FCS, with marginal effect of the service rate of the FCS. This is especially relevant when new FCSs are built with charging points rated at 150 kW and above, to handle future demand. As the analysis shows, there are few EVs in the marked able to charge at such high powers. Thus, for the time being, they may be oversized in terms of peak power capacity. A reduction in the peak power of the FCSs can reduce the cost of grid connection and power tariff cost, and also provide flexibility to the DSO, with minimal effect on the serviceability of the FCS. However, simulations with future scenarios as input have to be performed to determine how long this potential exists. As changes in the EV fleet and percentage will impact the effect of reducing the peak load limit at an FCS. The reduction of the FCS peak load will need a control system, and potentially some extra power electronics equipment. This will add a cost of implementing the proposed framework, that must be taken into consideration.

10 Conclusion

In this thesis, multiple models have been developed to find the optimum location and size of an FCS network. The proposed modeling approach includes an EV mobility model, FCS demand model and distribution grid model, which together is incorporated in an optimization model. A real highway case in Norway is considered to test the performance of the models developed. The proposed BPSO model converged quickly and was able to find the optimum solution for all three cases, both for single and multi objective functions.

The results illuminate how the optimal number of FCSs, and their location is highly dependent on the objective function. The three cases studied all got a different optimal number of FCSs. To compare the different objective functions the social cost was computed for all three cases. The results showed that the social cost was highest for case 2, which only considers the DSO and FCS operator perspective. This resulted in a 25.2% higher social cost for case 2 than case 3, with most of the increase due to a 5400% increase in the detour cost.

An algorithm was added in the demand model to keep the aggregated charging power from all the charging points under a certain limit. A reduction in the peak power of the FCSs can reduce the cost of grid connection and power tariff cost, and also provide flexibility to the DSO. The results showed that this could be done with little effect on the serviceability of the FCS.

The versatility of the proposed models has been illustrated by showing how it can be used to determine optimal planning of FCSs, but also deeper analysis such as the impact of reducing the peak power of FCSs. To conclude, the developed optimization model has been able to find the optimum solution, both for single and multi objective functions. To determine the accuracy of the developed sub-models, real data is needed to compere.

11 Further work

To test the accuracy of the proposed model, a comparison with real data is needed. This is especially relevant for the FCS demand model. The proposed optimization model could be improved by letting the worst-case scenario be a screening process to ensure grid stability. Then, for the optimal planning, use a more representative base load and temperature profile to the FCS load model, to get a more accurate grid loss. The number of days simulated for each potential location in the optimization model should be increased to reduce statistical variability.

In this thesis, it has been demonstrated how the peak load from an FCS can be reduced by limiting the power at the charging points. Its effect on the service rate of the FCS has been illustrated. Further analysis, from an FCS operator perspective, could be to determine what this peak power limit should be, taking into consideration grid tariffs and revenue. Analysis from a DSO perspective could be performed, by studying how it could help system stability and reduce or postpone grid investments.

BESS is another way to reduce the grid impacts of FCS integration. A BESS could be integrated at the FCSs to reduce the peak load of the FCS. This would from a grid perspective have the same effect as reducing the peak power limit of the FCS. It also would not impact the serviceability of the FCS as the BESS would supply the remaining power. However, the BESS has a substantial investment cost. Analysis could be performed to compere the two methods, taking into considerations the interests of DSO, FCS operator and EV owners.

In the proposed optimization model, voltage constraints and power flow constraints are implemented as hard constraints. This could be changed, and instead, adding a cost for upgrading the cross section of the line or adding reactive power compensation. This would be particularly valuable when planning FCS networks in areas with a weak distribution grid.

The grid model should be improved taking into reactive power of the base load. The FCS load model should also include reactive power, as well as real power. This would result in more accurate grid impacts when the power flow analysis is performed with base load and FCS load.

EVs has increased rapidly in popularity in recent year, and the same is expected to happen with heavy-duty vehicles, such as semi truck. They are expected to fast charge with the power of a few MW's, as they will need much bigger batteries than the current EVs. Thus, they would potentially present a bigger impact on the distribution grid than the fast charging of EVs. By taking into account electric heavy-duty vehicles in the model. Simulations could be performed to study whether EVs and electric heavy-duty vehicles should have their FCSs in different locations or together.

Bibliography

[1] Eirik Ivarsøy. *Demand modeling of high-power electric vehicle charging,* NTNU, specialization project, Trondheim, Norway, December 2019.

[2] IEA, CO2 Emissions Statistics. Available at: *https://www.iea.org/statistics/co2emissions/* [01.12.2019]

[3] Climate Watch, Global Historical Emissions. Available at: *https://www.climatewatchdata.org/ghg-emissions?breakBy=regions-ABSOLUTE_VALUE&chartType=percentage&gases=177&sectors=518&source=42* [03.12.2019]

[4] EU, CO2 emissions from cars. Available at: *https://www.europarl.europa.eu/news/en/headlines/society/20190313ST031218/co2-emissions-from-cars-facts-and-figures-infographics* [01.12.2019]

[5] UNFCCC, The Paris Agreement *https://unfccc.int/process-and-meetings/the-paris-agreement* [01.12.2019]

[6] IEA, Global EV Outlokk 2019. Available at: *https://www.iea.org/publications/reports/globalevoutlook2019/* [14.11.2019]

[7] European Union, Post-2020 CO2 emission performance standards for cars and vans. Available at: *https://ec.europa.eu/clima/policies/transport/vehicles/regulation_en* [02.12.2019]

[8] Department for Transport, The Road to Zero. Available at: *https://assets.publishing.service.gov.uk/government/uploads/system/uploads/attachment_data/file/739460/road-to-zero.pdf* [06.12.2019]

[9] The New York Times, France Plans to End Sales of Gas and Diesel Cars by 2040. Available at: *https://www.nytimes.com/2017/07/06/business/energy-environment/france-cars-ban-gas-diesel.html* [02.12.2019]

[10] The Irish times, Ireland 2040: 22bn to turn State into low-carbon economy. Available at: *https://www.irishtimes.com/business/energy-and-resources/ireland-2040-22bn-to-turn-state-into-low-carbon-economy-1.3394805* [06.12.2019]

[11] Reuters, Paris plans to banish all but electric cars by 2030. Available at: *https://www.reuters.com/article/us-france-paris-autos/paris-plans-to-banish-all-but-electric-cars-by-2030-idUSKBN1CH0SI* [06.12.2019]

[12] TU.no, EU-kommisær: Ikke lov å forby diesel- og bensinbiler. Available at: *https://www.tu.no/artikler/eu-kommisaer-ikke-lov-a-forby-diesel-og-bensinbiler/470003* [02.12.2019]

[13] Clean Energy Ministerial, EV30@30 Campaign. Available at: *https://www.iea.org/media/topics/transport/3030CampaignDocumentFinal.pdf* [02.12.2019]

[14] Norsk elbilforening, Registered EVs and market share. Available at: *https://elbil.no/elbilstatistikk/* [31.05.2020]

[15] Statistics Norway, Registered vehicles. Available at: *https://www.ssb.no/bilreg* [31.05.2020]

[16] Statistics Norway, Cars and transportation. Available at: *https://www.ssb.no/transport-og-reiseliv/faktaside/bil-og-transport* [31.05.2020]

[17] Regjeringen, Klimaendringer og norsk klimapolitikk. Available at: *https://www.regjeringen.no/no/tema/klima-og-miljo/innsiktsartikler-klima-miljo/klimaendringer-og-norsk-klimapolitikk/id2636812/* [03.12.2019]

[18] Regjeringen, Nasjonal transportplan 2018-2029. Available at: *https://www.regjeringen.no/no/dokumenter/meld.-st.-33-20162017/id2546287/sec1* [03.12.2019]

[19] TU.no, CHAdeMO hurtiglading. Available at: *https://www.tu.no/artikler/de-var-storst-na-kommer-faerre-bilmodeller-med-denne-kontakten/466335* [03.12.2019]

[20] tek.no, Torsdag åpnet Norges første superhurtiglader for elbil. Available at: *https://www.tek.no/nyheter/nyhet/i/Jo3PAX/torsdag-apnet-norges-frste-superhurtiglader-for-elbil* [04.12.2019]

[21] Miljødirektoratet, Greenhouse gas emission from the transport sector. Available at: *https://miljostatus.miljodirektoratet.no/tema/klima/norske-utslipp-av-klimagasser/klimagassutslipp-fra-transport/* [14.11.2019]

[22] Nobil, Hurtigladerstatistikk. Available at: *https://info.nobil.no/statistikk*

[23] Mathias Klingenberg, *Gladnyhet til strømsugne elbilister: I 2019 ble det virkelig fart på byggingen av hurtigladere,* Available at: *https://www.tu.no/artikler/gladnyhet-til-stromsugne-elbilister-i-2019-ble-det-virkelig-fart-pa-byggingen-av-hurtigladere/482582* TU, 10 January, 2020.

[24] Tesla, Supercharging Available at: *https://www.tesla.com/support/supercharging?redirect=no* [03.12.2019]

[25] Stian Strøm, *Elbileiere i nord må fortsatt vente på hurtigladere,*. Available at: *https://www.nrk.no/tromsogfinnmark/elbileiere-i-nord-ma-fortsatt-vente-pa-hurtigladere-1.14796525* NRK, 28 November, 2019.

[26] Martin Thronsen, *Endelig bygges ladenettverket i Troms og Finnmark!* Available at: *https://elbil.no/endelig-bygges-ladenettverket-i-troms-og-finnmark/* Elbil.no, 28 May, 2020.

[27] Norske Elbilforeningen, *Ladeklart Norge 2025* March, 2019.

[28] Q. Deng, S. Tripathy, D. Tylavsky, T. Stowers and J. Loehr, *"Demand Modeling of a dc Fast Charging Station,"* 2018 North American Power Symposium (NAPS), Fargo, ND, 2018, pp. 1-6.

[29] O. Hafez and K. Bhattacharya, *"Queuing Analysis Based PEV Load Modeling Considering Battery Charging Behavior and Their Impact on Distribution System Operation,"* in IEEE Transactions on Smart Grid, vol. 9, no. 1, pp. 261-273, Jan. 2018.

[30] Dr.-Ing. J. Brombach, Dr.-Ing. F. Meyer, Dipl.-Ing C. Strafiel, Dr. J. Winkler, Dipl-Ing. A. Beekmann, *"Grid-integration of high-power charging infrastructure,"* 1st E-Mobility Power System Integration Symposium, Berlin, Germany, 23 October, 2017

[31] W. Alharbi and K. Bhattacharya, *"Electric Vehicle Charging Facility as a Smart Energy Microhub,"* in IEEE Transactions on Sustainable Energy, vol. 8, no. 2, pp. 616-628, April 2017.

[32] W. Alharbi and K. Bhattacharya, *"Impact of mixed charging requests of PEVs on a charging facility load and a distribution grid,"* 2017 IEEE Green Energy and Smart Systems Conference (IGESSC), Long Beach, CA, 2017, pp. 1-5.

[33] F. H. Malik and M. Lehtonen, *"Analysis of power network loading due to fast charging of Electric Vehicles on highways,"* 2016 Electric Power Quality and Supply Reliability (PQ), Tallinn, 2016, pp. 101-106.

[34] L. E. Bremermann, M.Mators, J. A. P. Lopes, M.Rosa, *"Electric vehicle models for evaluating the security of supply,"* Electric Power System Research, vol. 111, pp. 32-39, June 2014

[35] G. Celli, G. G. Soma, F. Pilo, F. Lacu, S. Mocci and N. Natale, *"Aggregated electric vehicles load profiles with fast charging stations,"* 2014 Power Systems Computation Conference, Wroclaw, 2014, pp. 1-7.

[36] Ligen, Yorick, Vrubel, Heron, Girault, *"Local Energy Storage and Stochastic Modeling for Ultrafast Charging Stations,"*, Energies, vol. 12, no. 10, May 2019.

[37] Y. Zhang, Y. He, X. Wang, Y. Wang, C. Fang, H. Xue and C. Fang, *"Modeling of fast charging station equipped with energy storage,"* Global Energy Interconnection, vol. 1, no. 2, pp. 145-152, April 2018.

[38] J.A Domínguez-Navarro, R. Dufo-López, J.M Yusta-Loyo, J.S. Artal-Sevil and J.L. Bernal-Agustín, *"Design of an electric vehicle fast-charging station with integration of renewable energy and storage systems,"* International Journal of Electrical Power and Energy System, vol. 105, pp. 46-58, February 2019.

[39] L. Richard and M. Petit, *"Fast Charging Station with Battery Storage System for EV: Optimal Integration into the Grid,"* 2018 IEEE Power and Energy Society General Meeting (PESGM), August 2018.

[40] AAA, AAA Electric Vehicle Range Testing. Available at: *https://www.aaa.com/AAA/common/AAR/files/AAA-Electric-Vehicle-Range-Testing-Report.pdf* [25.11.2019]

[41] Nissan, Rekkevidde og lading Nissan Leaf. Available at: *https://www.nissan.no/biler/nye-biler/leaf/rekkevidde-lading.html* [20.10.2019]

[42] Opel, Estimer din daglige rekkevidde. Available at: *https://www.opel.no/personbil/ampera-e/modelloversikt/partials/range/range-simulator.html* [20.10.2019]

[43] Y. Motoaki and W. Yi and S. Salisbury, *"Empirical analysis of electric vehicle fast charging under cold temperatures,"* Energy Policy, vol. 122, November 2018, pp. 162-168.

[44] W. Alharbi and K. Bhattacharya, *"Impact of mixed charging requests of PEVs on a charging facility load and a distribution grid,"* 2017 IEEE Green Energy and Smart Systems Conference (IGESSC), Long Beach, CA, 2017, pp. 1-5.

[45] S. Cheng and P. Gao, *"Optimal allocation of charging stations for electric vehicles in the distribution system,"* 2018 3rd International Conference on Intelligent Green Building and Smart Grid (IGBSG), Yi-Lan, 2018, pp. 1-5.

[46] Chen M., Liu Z., Zhou X, *"Optimal Planning of EV Charging Station Based on Gravitational Search Algorithm,"* 2018 2nd IEEE Conference on Energy Internet and Energy System Integration(EI2). IEEE. Beijing. pp. 1-6.

[47] Z. Liu, F. Wen and G. Ledwich, *"Optimal Planning of Electric-Vehicle Charging Stations in Distribution Systems,"* IEEE Transactions on Power Delivery, vol. 28, no. 1, pp. 102-110, Jan. 2013.

[48] A. Shukla, K. Verma and R. Kumar, *"Planning of Fast Charging Stations in Distribution System Coupled with Transportation Network for Capturing EV flow,"* 2018 8th IEEE India International Conference on Power Electronics (IICPE), JAIPUR, India, 2018, pp. 1-6.

[49] M. M. Islam, H. Shareef and A. Mohamed, *"Optimal location and sizing of fast charging stations for electric vehicles by incorporating traffic and power networks,"* IET Intelligent Transport Systems, vol. 12, no. 8, pp. 947-957, 10 2018.

[50] H. Simorgh, H. Doagou-Mojarrad, H. Razmi and G. B. Gharehpetian, *"Cost-based optimal siting and sizing of electric vehicle charging stations considering demand response programmes,"* IET Generation, Transmission & Distribution, vol. 12, no. 8, pp. 1712-1720, 30 4 2018.

[51] R. Eberhart and J. Kennedy, *"A new optimizer using particle swarm theory,"* Proceedings of the Sixth International Symposium on Micro Machine and Human Science, Nagoya, Japan, 1995, pp. 39-43.

[52] J. Kennedy and R. Eberhart, *"Particle swarm optimization,"* International Conference on Neural Networks, Perth, WA, Australia, 1995, pp. 1942-1948 vol.4.

[53] J. Kennedy and R. C. Eberhart, *"A discrete binary version of the particle swarm algorithm,"* 1997 IEEE International Conference on Systems, Man, and Cybernetics. Computational Cybernetics and Simulation, Orlando, FL, USA, 1997, pp. 4104-4108 vol.5.

[54] SINTEG Energi AS, *"Planleggingsbok for kraftnett - Økonomisk optimal tversnitt,"* 2010.

[55] Oliver Ibe (2014). *Fundamentals of Applied Probability and Random Processes, 2nd Edition, Academic Press*

[56] The Norwegian Water Resources and Energy Directorate, NVE Atlas. Available at: *https://atlas.nve.no/Html5Viewer/index.html?viewer=nveatlas#* [07.03.2020]

[57] A. O. Eggen and H. Vefsnmo, *FASIT kravspesifikasjon - versjon 2019,* SINTEF Energi AS, 2018.

[58] Google, Google Maps. Available at: *https://www.google.com/maps* [07.03.2020]

[59] Statens vegvesen, Traffic data. Available at: *https://www.vegvesen.no/trafikkdata/start/kart?lat=63.278206508153588&lon=10.376778391311687&trafikanttype=vehicle&trpids=94210V2411536&zoom=9* [13.11.2019]

[60] Fastned charging curve, *https://support.fastned.nl/hc/en-gb/sections/115000180588-Vehicles-charging-tips*, [Accessed: 11.11.2019]

[61] Ni av ti lader elbilen oftest hjemme nå, *https://www.tu.no/artikler/ni-av-ti-lader-elbilen-oftest-hjemme-na/474372*, [Accessed: 11.11.2019]

[62] *https://www.yr.no/en/statistics/graph/1-86450/Norway/Viken/Ullensaker/Oslo%20Airport,%20Gardermoen?q=2019*, [Accesed: 12.02.2020]

[63] L. Thurner and A. Scheidler and F. Schäfer and J. Menke and J. Dollichon and F. Meier and S. Meinecke and M. Braun, *pandapower — An Open-Source Python Tool for Convenient Modeling, Analysis, and Optimization of Electric Power Systems,* in IEEE Transactions on Power Systems, vol. 33, no. 6, pp. 6510-6521, Nov. 2018.

[64] SINTEG Energi AS, *"Planleggingsbok for kraftnett - Tekniske data,"* 2014.

[65] SINTEG Energi AS, *"Planleggingsbok for kraftnett - Tapskostnader,"* 2014.

[66] elbilstatistikk.no, Elbilstatistikk. Avalible at: *https://elbilstatistikk.no/* [18.11.2019]

[67] Tesla ladekabler, *https://www.tesla.com/no_NO/support/charging-connectors* ,[Accessed: 07.11.2019]

[68] EnergySage, Electric vehicle battery life & warranties. Available at: *https://www.energysage.com/electric-vehicles/buyers-guide/battery-life-for-top-evs/* [05.12.2019]

[69] Karmøy kommune, ETABLERING AV HURTIGLADERE I SENTRUM AV SKUDENESHAVN, ÅKREHAMN OG KOPERVIK - NOTAT TIL FORMANNSKAPET. Available at: *https://www.karmoy.kommune.no/dokumenter/2397920* [05.05.2020]

[70] Transportøkonomisk Institutt, *"Marginale eksterne kostnader ved vegtrafikk med korrigerte ulykkeskostnader,"* 10.2014, revised 2016.

[71] IONITY, Price scheme. Available at: *https://ionity.eu/en/where-and-how.html* [07.05.2020]

[72] Fastned, charging curve Nissan Leaf. Available at: *https://support.fastned.nl/hc/en-gb/articles/204784998-Charging-with-a-Nissan-Leaf-e-or-e-NV200* [01.10.2019]

[73] Fastned, charging curve Volkswagen e-Golf. Available at: *https://support.fastned.nl/hc/en-gb/articles/205205168-Charging-with-a-Volkswagen-e-Golf-or-e-up-* [01.10.2019]

[74] Fastned, charging curve BMW i3. Available at: *https://insideevs.com/news/338777/lets-look-at-fast-charging-curves-for-popular-electric-cars/* [01.10.2019]

[75] Fastned, charging curve Hyundai Ioniq. Available at: *https://support.fastned.nl/hc/en-gb/articles/223715447-Charging-with-a-Hyundai-Ioniq* [01.10.2019]

[76] Fastned, charging curve Nissan E-nv200. Available at: *https://support.fastned.nl/hc/en-gb/articles/204784998-Charging-with-a-Nissan-Leaf-e-or-e-NV200* [01.10.2019]

[77] Fastned, charging curve Jaguar I-pace. Available at: *https://support.fastned.nl/hc/en-gb/articles/360000788848-Charging-with-a-Jaguar-I-PACE* [01.10.2019]

[78] Fastned, charging curve Audi e-Tron. Available at: *https://support.fastned.nl/hc/en-gb/articles/360000815988-Charging-with-an-Audi-e-tron*

[79] Fastned, charging curve Hyundai KONA. Available at: *https://support.fastned.nl/hc/en-gb/articles/360001029367-Charging-with-a-Hyundai-KONA* [01.10.2019]

[80] Fastned, charging curve Opel Ampera-e. Available at: *https://support.fastned.nl/hc/en-gb/articles/115000019368-Charging-with-an-Opel-Ampera-e* [01.10.2019]

Appendices

A Appendix A - FASIT Profiles

Navn	Måned	Dag	AB	01	02	03	04	05	06	07	08	09	10	11	12	13	14	15	16	17	18	19	20	21	22	23	24	SUM
				0000-0100	0100-0200	0200-0300	0300-0400	0400-0500	0500-0600	0600-0700	0700-0800	0800-0900	0900-1000	1000-1100	1100-1200	1200-1300	1300-1400	1400-1500	1500-1600	1600-1700	1700-1800	1800-1900	1900-2000	2000-2100	2100-2200	2200-2300	2300-2400	0000-2400
Jordbruk	høylast	hverdag	A	-0,051	-0,051	-0,051	-0,052	-0,051	-0,050	-0,050	-0,052	-0,061	-0,062	-0,062	-0,066	-0,062	-0,063	-0,065	-0,061	-0,057	-0,064	-0,061	-0,059	-0,063	-0,065	-0,065	-0,067	**-1,411**
Jordbruk	høylast	hverdag	B	2,116	2,100	2,091	2,098	2,068	2,070	2,283	3,076	3,415	2,940	2,579	2,423	2,338	2,270	2,256	2,333	2,711	3,236	3,131	2,581	2,367	2,271	2,189	2,105	**59,047**
Jordbruk	høylast	helg	A	-0,026	-0,026	-0,030	-0,027	-0,028	-0,029	-0,028	-0,026	-0,038	-0,049	-0,043	-0,039	-0,037	-0,035	-0,056	-0,046	-0,046	-0,046	-0,027	-0,031	-0,035	-0,036	-0,038	-0,035	**-0,857**
Jordbruk	høylast	helg	B	2,151	2,149	2,138	2,149	2,120	2,111	2,279	2,846	3,402	3,018	2,573	2,376	2,311	2,217	2,199	2,301	2,623	3,207	3,059	2,604	2,400	2,336	2,248	2,186	**59,003**
Jordbruk	lavlast	hverdag	A	0,003	0,002	0,002	0,002	0,001	0,002	-0,002	-0,002	-0,004	-0,002	0,006	0,009	0,006	0,011	0,014	0,006	-0,004	-0,004	0,007	0,016	0,016	0,008	0,004	0,001	**0,098**
Jordbruk	lavlast	hverdag	B	1,865	1,852	1,841	1,827	1,818	1,795	1,970	2,702	3,108	2,732	2,405	2,237	2,125	2,064	2,044	2,149	2,522	3,014	2,926	2,438	2,195	2,111	2,006	1,914	**53,660**
Jordbruk	lavlast	helg	A	-0,006	-0,007	-0,007	-0,008	-0,010	-0,007	-0,011	-0,009	-0,019	-0,027	-0,018	-0,006	-0,007	-0,007	-0,008	-0,009	-0,016	-0,022	-0,007	-0,004	-0,004	-0,006	-0,010	-0,010	**-0,245**
Jordbruk	lavlast	helg	B	1,873	1,853	1,837	1,831	1,817	1,807	1,944	2,517	3,055	2,779	2,378	2,162	2,093	2,019	1,999	2,106	2,430	3,009	2,825	2,377	2,126	2,047	1,975	1,892	**52,751**
Husholdning	høylast	hverdag	A	-0,056	-0,058	-0,059	-0,061	-0,063	-0,068	-0,068	-0,080	-0,070	-0,066	-0,062	-0,065	-0,061	-0,060	-0,060	-0,060	-0,059	-0,062	-0,061	-0,056	-0,058	-0,054	-0,055	-0,056	**-1,478**
Husholdning	høylast	hverdag	B	2,536	2,442	2,423	2,412	2,458	2,558	2,837	3,038	2,987	2,913	2,887	2,809	2,715	2,668	2,685	2,904	3,201	3,369	3,491	3,536	3,470	3,401	3,191	2,799	**69,730**
Husholdning	høylast	helg	A	-0,056	-0,057	-0,050	-0,054	-0,057	-0,056	-0,054	-0,057	-0,059	-0,054	-0,054	-0,056	-0,049	-0,046	-0,050	-0,048	-0,054	-0,058	-0,057	-0,052	-0,056	-0,057	-0,061	-0,065	**-1,317**
Husholdning	høylast	helg	B	2,643	2,468	2,421	2,404	2,425	2,456	2,520	2,609	2,811	3,093	3,213	3,187	3,132	3,097	3,109	3,237	3,274	3,355	3,464	3,533	3,496	3,338	3,187	2,830	**71,302**
Husholdning	lavlast	hverdag	A	-0,082	-0,085	-0,086	-0,087	-0,089	-0,092	-0,094	-0,101	-0,100	-0,099	-0,099	-0,099	-0,097	-0,098	-0,103	-0,107	-0,109	-0,114	-0,117	-0,116	-0,110	-0,103	-0,096	-0,088	**-2,371**
Husholdning	lavlast	hverdag	B	2,445	2,343	2,315	2,304	2,321	2,389	2,618	2,901	2,945	2,915	2,865	2,793	2,691	2,682	2,753	2,992	3,192	3,341	3,408	3,433	3,409	3,346	3,167	2,793	**68,361**
Husholdning	lavlast	helg	A	-0,087	-0,084	-0,084	-0,086	-0,087	-0,091	-0,091	-0,091	-0,092	-0,096	-0,103	-0,106	-0,104	-0,102	-0,108	-0,112	-0,116	-0,118	-0,120	-0,116	-0,110	-0,100	-0,095	-0,088	**-2,387**
Husholdning	lavlast	helg	B	2,580	2,378	2,324	2,307	2,305	2,342	2,379	2,470	2,680	2,944	3,118	3,147	3,043	3,013	3,121	3,208	3,276	3,337	3,407	3,424	3,397	3,299	3,139	2,816	**69,454**
Industri-1	høylast	hverdag	A	0,000	0,000	0,000	0,000	0,000	0,000	0,000	0,000	0,000	0,000	0,000	0,000	0,000	0,000	0,000	0,000	0,000	0,000	0,000	0,000	0,000	0,000	0,000	0,000	**0,000**
Industri-1	høylast	hverdag	B	107,133	106,377	112,671	125,561	123,883	149,508	210,079	281,420	301,317	304,861	306,550	305,595	303,247	297,228	284,303	241,682	208,777	185,799	157,850	144,596	129,745	118,621	114,933	111,846	**4733,582**
Industri-1	høylast	helg	A	0,000	0,000	0,000	0,000	0,000	0,000	0,000	0,000	0,000	0,000	0,000	0,000	0,000	0,000	0,000	0,000	0,000	0,000	0,000	0,000	0,000	0,000	0,000	0,000	**0,000**
Industri-1	høylast	helg	B	107,286	102,043	100,498	100,635	99,890	99,892	103,752	104,773	110,019	119,227	123,649	126,109	123,465	123,772	119,859	115,739	115,594	115,150	112,861	112,816	111,567	110,379	110,164	108,648	**2677,787**
Industri-1	lavlast	hverdag	A	0,000	0,000	0,000	0,000	0,000	0,000	0,000	0,000	0,000	0,000	0,000	0,000	0,000	0,000	0,000	0,000	0,000	0,000	0,000	0,000	0,000	0,000	0,000	0,000	**0,000**
Industri-1	lavlast	hverdag	B	104,767	97,558	96,979	103,395	103,837	103,557	128,651	190,887	273,450	295,530	300,267	302,200	302,231	299,898	294,786	279,434	224,146	190,067	170,029	151,208	138,950	125,529	113,548	110,230	**4501,134**
Industri-1	lavlast	helg	A	0,000	0,000	0,000	0,000	0,000	0,000	0,000	0,000	0,000	0,000	0,000	0,000	0,000	0,000	0,000	0,000	0,000	0,000	0,000	0,000	0,000	0,000	0,000	0,000	**0,000**
Industri-1	lavlast	helg	B	102,693	95,583	94,579	93,518	93,080	93,274	98,590	99,517	103,657	112,609	116,219	118,420	115,529	115,706	113,198	110,192	109,004	108,388	106,635	105,765	104,348	103,586	103,264	102,731	**2520,085**
Industri-2	høylast	hverdag	A	0,000	0,000	0,000	0,000	0,000	0,000	0,000	0,000	0,000	0,000	0,000	0,000	0,000	0,000	0,000	0,000	0,000	0,000	0,000	0,000	0,000	0,000	0,000	0,000	**0,000**
Industri-2	høylast	hverdag	B	111,846	107,133	106,377	112,671	125,561	123,883	210,079	281,420	301,317	304,861	305,595	305,595	305,595	305,595	305,595	305,595	305,595	305,595	305,595	305,595	305,595	305,595	305,595	284,303	**6042,186**
Industri-2	høylast	helg	A	0,000	0,000	0,000	0,000	0,000	0,000	0,000	0,000	0,000	0,000	0,000	0,000	0,000	0,000	0,000	0,000	0,000	0,000	0,000	0,000	0,000	0,000	0,000	0,000	**0,000**
Industri-2	høylast	helg	B	107,286	102,043	100,498	100,635	99,890	99,892	104,773	110,019	119,227	123,465	123,465	123,465	123,465	123,465	123,465	123,465	123,465	123,465	123,465	123,465	123,465	123,465	123,465	115,739	**2788,512**
Industri-2	lavlast	hverdag	A	0,000	0,000	0,000	0,000	0,000	0,000	0,000	0,000	0,000	0,000	0,000	0,000	0,000	0,000	0,000	0,000	0,000	0,000	0,000	0,000	0,000	0,000	0,000	0,000	**0,000**
Industri-2	lavlast	hverdag	B	104,767	97,558	96,979	103,395	103,837	103,557	190,887	273,450	295,530	300,267	302,231	302,231	302,231	302,231	302,231	302,231	302,231	302,231	302,231	302,231	302,231	302,231	302,231	279,434	**5878,664**
Industri-2	lavlast	helg	A	0,000	0,000	0,000	0,000	0,000	0,000	0,000	0,000	0,000	0,000	0,000	0,000	0,000	0,000	0,000	0,000	0,000	0,000	0,000	0,000	0,000	0,000	0,000	0,000	**0,000**
Industri-2	lavlast	helg	B	102,693	95,583	94,579	93,518	93,080	93,274	99,517	103,657	112,609	116,219	116,219	116,219	116,219	116,219	116,219	116,219	116,219	116,219	116,219	116,219	116,219	116,219	116,219	110,192	**2625,768**
Industri-3	høylast	hverdag	A	0,000	0,000	0,000	0,000	0,000	0,000	0,000	0,000	0,000	0,000	0,000	0,000	0,000	0,000	0,000	0,000	0,000	0,000	0,000	0,000	0,000	0,000	0,000	0,000	**0,000**
Industri-3	høylast	hverdag	B	304,861	304,861	304,861	304,861	304,861	304,861	304,861	304,861	304,861	304,861	304,861	304,861	304,861	304,861	304,861	304,861	304,861	304,861	304,861	304,861	304,861	304,861	304,861	304,861	**7316,664**
Industri-3	høylast	helg	A	0,000	0,000	0,000	0,000	0,000	0,000	0,000	0,000	0,000	0,000	0,000	0,000	0,000	0,000	0,000	0,000	0,000	0,000	0,000	0,000	0,000	0,000	0,000	0,000	**0,000**
Industri-3	høylast	helg	B	123,649	123,649	123,649	123,649	123,649	123,649	123,649	123,649	123,649	123,649	123,649	123,649	123,649	123,649	123,649	123,649	123,649	123,649	123,649	123,649	123,649	123,649	123,649	123,649	**2967,576**
Industri-3	lavlast	hverdag	A	0,000	0,000	0,000	0,000	0,000	0,000	0,000	0,000	0,000	0,000	0,000	0,000	0,000	0,000	0,000	0,000	0,000	0,000	0,000	0,000	0,000	0,000	0,000	0,000	**0,000**
Industri-3	lavlast	hverdag	B	302,231	302,231	302,231	302,231	302,231	302,231	302,231	302,231	302,231	302,231	302,231	302,231	302,231	302,231	302,231	302,231	302,231	302,231	302,231	302,231	302,231	302,231	302,231	302,231	**7253,544**
Industri-3	lavlast	helg	A	0,000	0,000	0,000	0,000	0,000	0,000	0,000	0,000	0,000	0,000	0,000	0,000	0,000	0,000	0,000	0,000	0,000	0,000	0,000	0,000	0,000	0,000	0,000	0,000	**0,000**
Industri-3	lavlast	helg	B	116,219	116,219	116,219	116,219	116,219	116,219	116,219	116,219	116,219	116,219	116,219	116,219	116,219	116,219	116,219	116,219	116,219	116,219	116,219	116,219	116,219	116,219	116,219	116,219	**2789,256**
Varehandel	høylast	hverdag	A	-2,612	-2,617	-2,594	-2,581	-2,696	-2,782	-2,786	-2,751	-2,867	-3,604	-4,008	-3,938	-3,910	-3,873	-3,651	-3,415	-3,589	-3,228	-2,871	-3,149	-2,724	-2,948	-2,639	-2,761	**-74,594**
Varehandel	høylast	hverdag	B	110,838	112,498	110,461	110,690	110,832	113,092	117,935	128,397	144,894	164,127	170,017	167,751	165,096	164,520	164,238	162,386	161,509	152,737	142,092	121,101	114,631	111,380	110,273	109,250	**3240,745**
Varehandel	høylast	helg	A	-1,914	-1,892	-2,094	-1,880	-1,847	-1,745	-1,442	-1,704	-3,217	-3,599	-4,055	-4,110	-3,713	-2,869	-1,773	-2,035	-2,125	-2,122	-2,103	-1,897	-1,934	-1,963	-1,781	-2,058	**-55,872**
Varehandel	høylast	helg	B	109,361	111,910	109,971	111,174	111,817	113,420	117,961	122,651	128,003	132,506	132,730	128,448	126,059	120,693	115,034	106,718	105,483	107,015	111,133	107,470	110,712	110,149	112,517	111,258	**2774,193**
Varehandel	lavlast	hverdag	A	-1,755	-1,756	-1,635	-1,698	-1,706	-1,837	-1,880	-1,934	-1,811	-2,223	-1,625	-1,557	-1,424	-1,191	-1,129	-1,120	-1,401	-1,197	-1,643	-1,573	-1,894	-1,625	-1,609	-1,627	**-38,850**
Varehandel	lavlast	hverdag	B	103,191	104,025	102,465	102,636	103,285	105,903	108,848	119,050	133,031	155,064	163,238	163,159	161,355	159,878	158,227	157,515	156,175	146,592	134,103	115,270	109,813	106,609	103,688	103,144	**3076,264**
Varehandel	lavlast	helg	A	-1,734	-1,696	-1,552	-1,655	-1,752	-1,919	-1,961	-1,818	-1,996	-1,957	-1,622	-1,374	-1,303	-1,189	-1,402	-1,503	-1,467	-1,484	-1,533	-1,479	-1,851	-1,689	-1,737	-1,740	**-39,413**
Varehandel	lavlast	helg	B	101,924	102,297	100,746	101,358	102,657	104,326	107,030	111,590	118,848	126,857	128,552	126,623	125,302	119,634	110,033	101,573	100,982	101,975	103,401	100,893	102,497	103,972	104,275	104,586	**2611,931**
Kontor	høylast	hverdag	A	-0,846	-0,472	-0,333	0,667	1,941	1,612	2,740	2,459	-3,175	-4,386	-4,770	-5,197	-5,173	-5,239	-4,945	-4,526	-1,359	-0,581	-0,176	-1,250	-1,718	-1,181	-1,039	-0,971	**-37,918**
Kontor	høylast	hverdag	B	111,846	107,133	106,377	112,671	125,561	123,883	149,508	210,079	281,420	301,317	304,861	306,550	305,595	303,247	297,228	284,303	241,682	208,777	185,799	157,850	144,596	129,745	118,621	114,933	**4733,582**
Kontor	høylast	helg	A	-0,623	-0,206	-0,234	-0,227	-0,168	-0,147	-0,536	-0,739	-0,940	-1,641	-1,701	-1,667	-1,416	-1,181	-0,783	-0,770	-0,892	-0,818	-0,701	-0,600	-0,615	-0,538	-0,685	-0,700	**-18,528**
Kontor	høylast	helg	B	107,286	102,043	100,498	100,635	99,890	99,892	103,752	104,773	110,019	119,227	123,649	126,109	123,465	123,772	119,859	115,739	115,594	115,150	112,861	112,816	111,567	110,379	110,164	108,648	**2677,787**
Kontor	lavlast	hverdag	A	-1,271	-0,953	-0,846	-0,982	-1,045	-1,070	-1,395	-0,494	-2,470	-2,876	-2,842	-2,777	-2,804	-2,853	-3,021	-3,934	-2,237	-1,476	-1,172	-0,714	-0,738	-0,809	-1,074	-1,381	**-41,234**
Kontor	lavlast	hverdag	B	104,767	97,558	96,979	103,395	103,837	103,557	128,651	190,887	273,450	295,530	300,267	302,200	302,231	299,898	294,786	279,434	224,146	190,067	170,029	151,208	138,950	125,529	113,548	110,230	**4501,134**
Kontor	lavlast	helg	A	-1,348	-0,969	-0,962	-0,915	-0,987	-1,084	-1,432	-1,319	-0,973	-0,902	-0,898	-0,936	-0,930	-0,888	-0,891	-1,057	-1,074	-1,099	-1,166	-1,142	-1,062	-1,022	-1,033	-1,324	**-25,413**
Kontor	lavlast	helg	B	102,693	95,583	94,579	93,518	93,080	93,274	98,590	99,517	103,657	112,609	116,219	118,420	115,529	115,706	113,198	110,192	109,004	108,388	106,635	105,765	104,348	103,586	103,264	102,731	**2520,085**
Hotell	høylast	hverdag	A	-4,106	-4,058	-4,236	-4,330	-4,532	-4,617	-4,234	-4,617	-5,064	-4,488	-4,283	-3,877	-3,787	-3,839	-3,995	-3,668	-3,956	-4,294	-4,744	-4,942	-4,934	-5,009	-4,798	-4,293	**-104,701**
Hotell	høylast	hverdag	B	216,687	209,124	201,458	198,723	199,205	203,251	218,231	244,470	262,273	266,783	267,072	265,913	262,562	261,495	261,050	261,827	264,649	272,076	279,040	279,096	274,564	265,588	250,640	234,789	**5920,566**
Hotell	høylast	helg	A	-4,706	-4,560	-4,646	-4,489	-4,519	-4,758	-4,582	-4,410	-4,839	-4,730	-4,256	-3,748	-3,697	-3,490	-4,035	-3,889	-3,933	-4,721	-5,026	-5,108	-5,050	-5,142	-4,944	-4,119	**-107,397**
Hotell	høylast	helg	B	225,935	217,868	207,254	202,275	200,316	202,241	214,011	234,967	256,995	266,560	265,687	265,389	262,569	261,965	262,643	263,581	265,399	269,624	274,650	273,177	268,588	258,711	245,202	230,078	**5895,685**
Hotell	lavlast	hverdag	A	-5,323	-5,267	-5,115	-5,129	-5,150	-5,104	-5,014	-5,184	-5,333	-5,234	-5,058	-5,145	-5,113	-5,119	-5,125	-5,181	-5,384	-5,467	-5,540	-5,387	-5,385	-5,560	-5,486	-5,486	**-126,289**
Hotell	lavlast	hverdag	B	191,258	182,741	175,994	174,114	175,180	182,153	197,359	220,234	234,579	237,352	237,268	236,398	233,302	233,171	233,139	233,717	236,153	240,649	244,797	243,813	240,310	233,812	220,905	205,791	**5244,189**
Hotell	lavlast	helg	A	-5,864	-5,780	-5,462	-5,372	-5,363	-5,371	-5,310	-5,149	-5,318	-5,421	-5,345	-5,500	-5,468	-5,356	-5,502	-5,378	-5,513	-5,672	-5,584	-5,582	-5,451	-5,494	-5,682	-5,779	**-131,716**
Hotell	lavlast	helg	B	200,431	191,319	181,591	176,715	175,813	181,644	194,863	210,667	227,700	236,132	236,373	235,924	233,558	232,553	234,276	234,023	234,692	238,121	239,328	237,387	230,530	223,295	214,036	201,862	**5202,833**
Skole	høylast	hverdag	A	-2,406	-2,275	-2,520	-2,359	-2,263	-1,573	-0,432	-1,002	-0,808	-1,223	-1,285	-1,267	-1,341	-1,290	-2,398	-3,000	-3,109	-3,291	-3,337	-3,221	-3,126	-2,915	-2,693	-2,611	**-51,745**
Skole	høylast	hverdag	B	90,975	92,555	93,319	97,401	100,160	107,593	118,490	127,714	152,261	152,257	146,396	140,209	140,976	137,878	120,907	106,039	100,785	97,829	100,798	102,293	99,948	96,100	91,335	91,078	**2705,296**
Skole	høylast	helg	A	-2,046	-2,219	-2,129	-2,137	-1,916	-2,097	-2,113	-2,079	-1,831	-2,187	-2,485	-2,561	-2,789	-2,823	-2,900	-2,788	-2,820	-2,820	-2,861	-2,843	-2,522	-2,274	-2,152	-2,380	**-57,772**
Skole	høylast	helg	B	93,737	93,344	94,770	96,034	97,918	97,476	96,776	97,898	97,067	94,645	91,294	89,591	86,184	83,887	81,472	80,833	82,390	86,195	89,821	89,171	88,184	88,463	89,548	90,062	**2176,760**
Skole	lavlast	hverdag	A	-3,289	-3,412	-3,540	-3,592	-4,046	-4,858	-5,068	-5,711	-6,078	-5,733	-5,391	-5,224	-5,203	-4,959	-4,658	-4,732	-4,861	-4,312	-4,144	-3,822	-3,299	-3,275	-3,230	-3,278	**-105,715**
Skole	lavlast	hverdag	B	84,052	84,903	86,994	88,498	95,165	111,333	122,419	135,004	156,726	157,593	152,734	147,327	146,370	142,703	130,443	122,671	116,353	104,874	104,661	101,155	93,028	89,456	85,122	83,330	**2742,914**
Skole	lavlast	helg	A	-3,174	-3,187	-3,259	-3,425	-3,370	-3,612	-3,582	-3,776	-3,765	-3,588	-3,595	-3,489	-3,447	-3,586	-3,184	-3,287	-3,550	-3,562	-3,690	-3,530	-3,096	-3,324	-3,464	-3,443	**-82,985**
Skole	lavlast	helg	B	84,693	84,943	84,586	86,371	86,733	88,448	88,908	90,522	91,141	90,915	89,190	88,167	87,499	86,313	85,602	86,315	88,010	89,817	90,431	89,337	86,423	85,152	84,314	84,520	**2098,350**
Helse og sosial	høylast	hverdag	A	-31,718	-31,907	-32,174	-32,463	-32,419	-33,301	-32,433	-39,244	-34,096	-34,919	-32,243	-31,967	-34,731	-32,266	-37,343	-34,895	-33,017	-34,646	-34,131	-34,149	-34,001	-33,953	-32,634	-32,445	**-807,095**
Helse og sosial	høylast	hverdag	B	1050,539	1043,606	1040,771	1038,470	1043,435	1050,765	1145,913	1420,601	1621,464	1618,141	1683,880	1603,700	1526,940	1513,810	1442,782	1296,273	1211,546	1179,073	1186,771	1152,486	1109,456	1083,735	1058,074	1046,175	**30168,406**
Helse og sosial	høylast	helg	A	-30,022	-30,907	-30,497	-30,624	-31,235	-31,274	-30,235	-34,664	-31,964	-33,849	-31,399	-31,067	-32,771	-30,149	-30,484	-28,418	-28,417	-30,194	-29,921	-31,371	-31,665	-31,547	-30,392	-29,635	**-742,701**
Helse og sosial	høylast	helg	B	1039,390	1029,484	1030,721	1027,828	1025,552	1032,908	1101,055	1230,824	1281,727	1296,001	1306,403	1261,292	1197,546	1189,458	1170,654	1145,819	1127,694	1124,559	1142,658	1116,746	1081,119	1055,262	1034,463	1026,381	**27075,544**
Helse og sosial	lavlast	hverdag	A	-31,226	-31,162	-31,217	-31,315	-31,366	-31,581	-32,462	-36,925	-34,616	-32,223	-33,852	-33,557	-32,432	-33,151	-35,414	-34,425	-34,158	-33,817	-32,966	-32,313	-32,169	-31,939	-31,814	-31,734	**-787,834**
Helse og sosial	lavlast	hverdag	B	1047,507	1037,610	1035,683	1033,279	1035,930	1047,169	1130,662	1446,266	1621,148	1643,134	1701,602	1622,837	1564,323	1552,950	1499,838	1332,750	1239,387	1208,894	1199,303	1161,024	1139,271	1118,694	1092,305	1065,910	**30577,476**
Helse og sosial	lavlast	helg	A	-29,496	-29,856	-29,391	-29,349	-29,517	-30,075	-31,127	-33,476	-32,424	-31,189	-30,931	-29,626	-28,963	-29,541	-29,624	-30,166	-30,902	-31,106	-30,794	-30,278	-30,004	-29,462	-29,143	-29,106	**-725,546**
Helse og sosial	lavlast	helg	B	1039,224	1033,371	1027,648	1023,069	1026,746	1042,150	1094,224	1235,552	1273,124	1307,542	1317,396	1268,146	1226,543	1223,759	1186,703	1152,404	1138,119	1125,825	1134,554	1111,511	1096,046	1079,375	1058,400	1033,577	**27255,008**
Elkjel	høylast	hverdag	A	-17,284	-16,503	-19,098	-20,426	-21,075	-22,487	-22,774	-30,221	-33,447	-31,141	-30,605	-29,259	-27,927	-24,043	-22,417	-22,746	-20,257	-18,875	-19,221	-17,485	-18,361	-18,044	-17,744	-16,849	**-538,289**
Elkjel	høylast	hverdag	B	447,849	441,503	425,235	432,638	436,285	447,855	515,413	589,043	638,532	643,454	639,390	638,104	631,699	616,415	604,132	599,550	586,420	550,348	556,456	533,238	509,749	490,718	467,521	448,024	**12889,571**
Elkjel	høylast	helg	A	-3,924	-3,800	-6,290	-9,357	-10,456	-11,601	-8,443	-9,612	-12,750	-12,313	-17,663	-9,099	-8,365	-4,835	-1,756	0,098	2,143	1,704	-1,596	-4,106	-5,822	-6,207	-7,921	-8,198	**-160,169**
Elkjel	høylast	helg	B	425,988	431,453	415,589	418,182	422,411	423,669	452,001	457,269	472,189	485,759	485,811	503,571	500,573	492,582	465,295	465,527	462,820	464,741	469,174	468,971	460,731	457,984	456,365	452,749	**11011,404**
Elkjel	lavlast	hverdag	A	-20,190	-20,829	-19,613	-20,432	-20,445	-20,301	-20,618	-24,521	-28,737	-30,052	-30,569	-31,194	-31,482	-31,041	-30,251	-30,796	-30,298	-27,853	-26,904	-24,365	-22,993	-21,568	-20,516	-19,796	**-605,364**
Elkjel	lavlast	hverdag	B	420,315	416,822	393,742	399,727	401,357	409,795	479,844	544,315	600,589	620,049	621,963	617,173	609,829	596,422	582,623	583,795	577,699	546,821	538,112	511,956	495,302	476,396	458,466	433,298	**12336,410**
Elkjel	lavlast	helg	A	-18,114	-18,272	-17,438	-18,262	-18,079	-18,437	-18,785	-19,126	-20,399	-21,303	-21,766	-22,782	-22,901	-23,581	-22,038	-22,396	-22,811	-22,649	-22,204	-22,510	-22,039	-21,768	-21,358	-21,645	**-500,663**
Elkjel	lavlast	helg	B	394,262	387,472	370,409	373,321	372,444	377,563	418,830	423,674	439,092	459,483	475,782	487,929	485,269	484,283	460,815	458,179	461,110	461,939	463,260	467,822	462,565	458,246	453,674	443,967	**10541,390**

Navn	Dag	Last	AB	01	02	03	04	05	06	07	08	09	10	11	12	13	14	15	16	17	18	19	20	21	22	23	24	SUM
				0000-0100	0100-0200	0200-0300	0300-0400	0400-0500	0500-0600	0600-0700	0700-0800	0800-0900	0900-1000	1000-1100	1100-1200	1200-1300	1300-1400	1400-1500	1500-1600	1600-1700	1700-1800	1800-1900	1900-2000	2000-2100	2100-2200	2200-2300	2300-2400	0000-2400
Jordbruk	Hverdag	Høylast	A	-0,051	-0,051	-0,051	-0,052	-0,051	-0,050	-0,050	-0,052	-0,061	-0,062	-0,062	-0,066	-0,062	-0,063	-0,065	-0,061	-0,057	-0,064	-0,061	-0,059	-0,063	-0,065	-0,065	-0,067	**-1,411**
Jordbruk	Hverdag	Høylast	B	2,116	2,100	2,091	2,098	2,068	2,070	2,283	3,076	3,415	2,940	2,579	2,423	2,338	2,270	2,256	2,333	2,711	3,236	3,131	2,581	2,367	2,271	2,189	2,105	**59,047**
Jordbruk	Lørdag	Høylast	A	-0,026	-0,026	-0,030	-0,027	-0,028	-0,029	-0,028	-0,026	-0,038	-0,049	-0,043	-0,039	-0,037	-0,035	-0,056	-0,046	-0,046	-0,046	-0,027	-0,031	-0,035	-0,036	-0,038	-0,035	**-0,857**
Jordbruk	Lørdag	Høylast	B	2,151	2,149	2,138	2,149	2,120	2,111	2,279	2,846	3,402	3,018	2,573	2,376	2,311	2,217	2,199	2,301	2,623	3,207	3,059	2,604	2,400	2,336	2,248	2,186	**59,003**
Jordbruk	Søndag	Høylast	A	-0,026	-0,026	-0,030	-0,027	-0,028	-0,029	-0,028	-0,026	-0,038	-0,049	-0,043	-0,039	-0,037	-0,035	-0,056	-0,046	-0,046	-0,046	-0,027	-0,031	-0,035	-0,036	-0,038	-0,035	**-0,857**
Jordbruk	Søndag	Høylast	B	2,151	2,149	2,138	2,149	2,120	2,111	2,279	2,846	3,402	3,018	2,573	2,376	2,311	2,217	2,199	2,301	2,623	3,207	3,059	2,604	2,400	2,336	2,248	2,186	**59,003**
Jordbruk	Hverdag	Lavlast	A	0,003	0,002	0,002	0,002	0,001	0,002	-0,002	-0,002	-0,004	-0,002	0,006	0,009	0,006	0,011	0,014	0,006	-0,004	-0,004	0,007	0,016	0,016	0,008	0,004	0,001	**0,098**
Jordbruk	Hverdag	Lavlast	B	1,865	1,852	1,841	1,827	1,818	1,795	1,970	2,702	3,108	2,732	2,405	2,237	2,125	2,064	2,044	2,149	2,522	3,014	2,926	2,438	2,195	2,111	2,006	1,914	**53,660**
Jordbruk	Lørdag	Lavlast	A	-0,006	-0,007	-0,007	-0,008	-0,010	-0,007	-0,011	-0,009	-0,019	-0,027	-0,018	-0,006	-0,007	-0,007	-0,008	-0,009	-0,016	-0,022	-0,007	-0,004	-0,004	-0,006	-0,010	-0,010	**-0,245**
Jordbruk	Lørdag	Lavlast	B	1,873	1,853	1,837	1,831	1,817	1,807	1,944	2,517	3,055	2,779	2,378	2,162	2,093	2,019	1,999	2,106	2,430	3,009	2,825	2,377	2,126	2,047	1,975	1,892	**52,751**
Jordbruk	Søndag	Lavlast	A	-0,006	-0,007	-0,007	-0,008	-0,010	-0,007	-0,011	-0,009	-0,019	-0,027	-0,018	-0,006	-0,007	-0,007	-0,008	-0,009	-0,016	-0,022	-0,007	-0,004	-0,004	-0,006	-0,010	-0,010	**-0,245**
Jordbruk	Søndag	Lavlast	B	1,873	1,853	1,837	1,831	1,817	1,807	1,944	2,517	3,055	2,779	2,378	2,162	2,093	2,019	1,999	2,106	2,430	3,009	2,825	2,377	2,126	2,047	1,975	1,892	**52,751**
Husholdning	Hverdag	Høylast	A	-0,056	-0,058	-0,059	-0,061	-0,063	-0,068	-0,068	-0,080	-0,070	-0,066	-0,062	-0,065	-0,061	-0,060	-0,060	-0,060	-0,059	-0,062	-0,061	-0,056	-0,058	-0,054	-0,055	-0,056	**-1,478**
Husholdning	Hverdag	Høylast	B	2,536	2,442	2,423	2,412	2,458	2,558	2,837	3,038	2,987	2,913	2,887	2,809	2,715	2,668	2,685	2,904	3,201	3,369	3,491	3,536	3,470	3,401	3,191	2,799	**69,730**
Husholdning	Lørdag	Høylast	A	-0,056	-0,057	-0,050	-0,054	-0,057	-0,056	-0,054	-0,057	-0,059	-0,054	-0,054	-0,056	-0,049	-0,046	-0,050	-0,048	-0,054	-0,058	-0,057	-0,052	-0,056	-0,057	-0,061	-0,065	**-1,317**
Husholdning	Lørdag	Høylast	B	2,643	2,468	2,421	2,404	2,425	2,456	2,520	2,609	2,811	3,093	3,213	3,187	3,132	3,097	3,109	3,237	3,274	3,355	3,464	3,533	3,496	3,338	3,187	2,830	**71,302**
Husholdning	Søndag	Høylast	A	-0,056	-0,057	-0,050	-0,054	-0,057	-0,056	-0,054	-0,057	-0,059	-0,054	-0,054	-0,056	-0,049	-0,046	-0,050	-0,048	-0,054	-0,058	-0,057	-0,052	-0,056	-0,057	-0,061	-0,065	**-1,317**
Husholdning	Søndag	Høylast	B	2,643	2,468	2,421	2,404	2,425	2,456	2,520	2,609	2,811	3,093	3,213	3,187	3,132	3,097	3,109	3,237	3,274	3,355	3,464	3,533	3,496	3,338	3,187	2,830	**71,302**
Husholdning	Hverdag	Lavlast	A	-0,082	-0,085	-0,086	-0,087	-0,089	-0,092	-0,094	-0,101	-0,100	-0,099	-0,099	-0,099	-0,097	-0,098	-0,103	-0,107	-0,109	-0,114	-0,117	-0,116	-0,110	-0,103	-0,096	-0,088	**-2,371**
Husholdning	Hverdag	Lavlast	B	2,445	2,343	2,315	2,304	2,321	2,389	2,618	2,901	2,945	2,915	2,865	2,793	2,691	2,682	2,753	2,992	3,192	3,341	3,408	3,433	3,409	3,346	3,167	2,793	**68,361**
Husholdning	Lørdag	Lavlast	A	-0,087	-0,084	-0,084	-0,086	-0,087	-0,091	-0,091	-0,091	-0,092	-0,096	-0,103	-0,106	-0,104	-0,102	-0,108	-0,112	-0,116	-0,118	-0,120	-0,116	-0,110	-0,100	-0,095	-0,088	**-2,387**
Husholdning	Lørdag	Lavlast	B	2,580	2,378	2,324	2,307	2,305	2,342	2,379	2,470	2,680	2,944	3,118	3,147	3,043	3,013	3,121	3,208	3,276	3,337	3,407	3,424	3,397	3,299	3,139	2,816	**69,454**
Husholdning	Søndag	Lavlast	A	-0,087	-0,084	-0,084	-0,086	-0,087	-0,091	-0,091	-0,091	-0,092	-0,096	-0,103	-0,106	-0,104	-0,102	-0,108	-0,112	-0,116	-0,118	-0,120	-0,116	-0,110	-0,100	-0,095	-0,088	**-2,387**
Husholdning	Søndag	Lavlast	B	2,580	2,378	2,324	2,307	2,305	2,342	2,379	2,470	2,680	2,944	3,118	3,147	3,043	3,013	3,121	3,208	3,276	3,337	3,407	3,424	3,397	3,299	3,139	2,816	**69,454**
Industri-1	Hverdag	Høylast	A	0,000	0,000	0,000	0,000	0,000	0,000	0,000	0,000	0,000	0,000	0,000	0,000	0,000	0,000	0,000	0,000	0,000	0,000	0,000	0,000	0,000	0,000	0,000	0,000	**0,000**
Industri-1	Hverdag	Høylast	B	107,133	106,377	112,671	125,561	123,883	149,508	210,079	281,420	301,317	304,861	306,550	305,595	303,247	297,228	284,303	241,682	208,777	185,799	157,850	144,596	129,745	118,621	114,933	111,846	**4733,582**
Industri-1	Lørdag	Høylast	A	0,000	0,000	0,000	0,000	0,000	0,000	0,000	0,000	0,000	0,000	0,000	0,000	0,000	0,000	0,000	0,000	0,000	0,000	0,000	0,000	0,000	0,000	0,000	0,000	**0,000**
Industri-1	Lørdag	Høylast	B	107,286	102,043	100,498	100,635	99,890	99,892	103,752	104,773	110,019	119,227	123,649	126,109	123,465	123,772	119,859	115,739	115,594	115,150	112,861	112,816	111,567	110,379	110,164	108,648	**2677,787**
Industri-1	Søndag	Høylast	A	0,000	0,000	0,000	0,000	0,000	0,000	0,000	0,000	0,000	0,000	0,000	0,000	0,000	0,000	0,000	0,000	0,000	0,000	0,000	0,000	0,000	0,000	0,000	0,000	**0,000**
Industri-1	Søndag	Høylast	B	107,286	102,043	100,498	100,635	99,890	99,892	103,752	104,773	110,019	119,227	123,649	126,109	123,465	123,772	119,859	115,739	115,594	115,150	112,861	112,816	111,567	110,379	110,164	108,648	**2677,787**
Industri-1	Hverdag	Lavlast	A	0,000	0,000	0,000	0,000	0,000	0,000	0,000	0,000	0,000	0,000	0,000	0,000	0,000	0,000	0,000	0,000	0,000	0,000	0,000	0,000	0,000	0,000	0,000	0,000	**0,000**
Industri-1	Hverdag	Lavlast	B	104,767	97,558	96,979	103,395	103,837	103,557	128,651	190,887	273,450	295,530	300,267	302,200	302,231	299,898	294,786	279,434	224,146	190,067	170,029	151,208	138,950	125,529	113,548	110,230	**4501,134**
Industri-1	Lørdag	Lavlast	A	0,000	0,000	0,000	0,000	0,000	0,000	0,000	0,000	0,000	0,000	0,000	0,000	0,000	0,000	0,000	0,000	0,000	0,000	0,000	0,000	0,000	0,000	0,000	0,000	**0,000**
Industri-1	Lørdag	Lavlast	B	102,693	95,583	94,579	93,518	93,080	93,274	98,590	99,517	103,657	112,609	116,219	118,420	115,529	115,706	113,198	110,192	109,004	108,388	106,635	105,765	104,348	103,586	103,264	102,731	**2520,085**
Industri-1	Søndag	Lavlast	A	0,000	0,000	0,000	0,000	0,000	0,000	0,000	0,000	0,000	0,000	0,000	0,000	0,000	0,000	0,000	0,000	0,000	0,000	0,000	0,000	0,000	0,000	0,000	0,000	**0,000**
Industri-1	Søndag	Lavlast	B	102,693	95,583	94,579	93,518	93,080	93,274	98,590	99,517	103,657	112,609	116,219	118,420	115,529	115,706	113,198	110,192	109,004	108,388	106,635	105,765	104,348	103,586	103,264	102,731	**2520,085**
Industri-2	Hverdag	Høylast	A	0,000	0,000	0,000	0,000	0,000	0,000	0,000	0,000	0,000	0,000	0,000	0,000	0,000	0,000	0,000	0,000	0,000	0,000	0,000	0,000	0,000	0,000	0,000	0,000	**0,000**
Industri-2	Hverdag	Høylast	B	111,846	107,133	106,377	112,671	125,561	123,883	210,079	281,420	301,317	304,861	305,595	305,595	305,595	305,595	305,595	305,595	305,595	305,595	305,595	305,595	305,595	305,595	305,595	284,303	**6042,186**
Industri-2	Lørdag	Høylast	A	0,000	0,000	0,000	0,000	0,000	0,000	0,000	0,000	0,000	0,000	0,000	0,000	0,000	0,000	0,000	0,000	0,000	0,000	0,000	0,000	0,000	0,000	0,000	0,000	**0,000**
Industri-2	Lørdag	Høylast	B	107,286	102,043	100,498	100,635	99,890	99,892	104,773	110,019	119,227	123,465	123,465	123,465	123,465	123,465	123,465	123,465	123,465	123,465	123,465	123,465	123,465	123,465	123,465	115,739	**2788,512**
Industri-2	Søndag	Høylast	A	0,000	0,000	0,000	0,000	0,000	0,000	0,000	0,000	0,000	0,000	0,000	0,000	0,000	0,000	0,000	0,000	0,000	0,000	0,000	0,000	0,000	0,000	0,000	0,000	**0,000**
Industri-2	Søndag	Høylast	B	107,286	102,043	100,498	100,635	99,890	99,892	104,773	110,019	119,227	123,465	123,465	123,465	123,465	123,465	123,465	123,465	123,465	123,465	123,465	123,465	123,465	123,465	123,465	115,739	**2788,512**
Industri-2	Hverdag	Lavlast	A	0,000	0,000	0,000	0,000	0,000	0,000	0,000	0,000	0,000	0,000	0,000	0,000	0,000	0,000	0,000	0,000	0,000	0,000	0,000	0,000	0,000	0,000	0,000	0,000	**0,000**
Industri-2	Hverdag	Lavlast	B	104,767	97,558	96,979	103,395	103,837	103,557	190,887	273,450	295,530	300,267	302,231	302,231	302,231	302,231	302,231	302,231	302,231	302,231	302,231	302,231	302,231	302,231	302,231	279,434	**5878,664**
Industri-2	Lørdag	Lavlast	A	0,000	0,000	0,000	0,000	0,000	0,000	0,000	0,000	0,000	0,000	0,000	0,000	0,000	0,000	0,000	0,000	0,000	0,000	0,000	0,000	0,000	0,000	0,000	0,000	**0,000**
Industri-2	Lørdag	Lavlast	B	102,693	95,583	94,579	93,518	93,080	93,274	99,517	103,657	112,609	116,219	116,219	116,219	116,219	116,219	116,219	116,219	116,219	116,219	116,219	116,219	116,219	116,219	116,219	110,192	**2625,768**
Industri-2	Søndag	Lavlast	A	0,000	0,000	0,000	0,000	0,000	0,000	0,000	0,000	0,000	0,000	0,000	0,000	0,000	0,000	0,000	0,000	0,000	0,000	0,000	0,000	0,000	0,000	0,000	0,000	**0,000**
Industri-2	Søndag	Lavlast	B	102,693	95,583	94,579	93,518	93,080	93,274	99,517	103,657	112,609	116,219	116,219	116,219	116,219	116,219	116,219	116,219	116,219	116,219	116,219	116,219	116,219	116,219	116,219	110,192	**2625,768**
Industri-3	Hverdag	Høylast	A	0,000	0,000	0,000	0,000	0,000	0,000	0,000	0,000	0,000	0,000	0,000	0,000	0,000	0,000	0,000	0,000	0,000	0,000	0,000	0,000	0,000	0,000	0,000	0,000	**0,000**
Industri-3	Hverdag	Høylast	B	304,861	304,861	304,861	304,861	304,861	304,861	304,861	304,861	304,861	304,861	304,861	304,861	304,861	304,861	304,861	304,861	304,861	304,861	304,861	304,861	304,861	304,861	304,861	304,861	**7316,664**
Industri-3	Lørdag	Høylast	A	0,000	0,000	0,000	0,000	0,000	0,000	0,000	0,000	0,000	0,000	0,000	0,000	0,000	0,000	0,000	0,000	0,000	0,000	0,000	0,000	0,000	0,000	0,000	0,000	**0,000**
Industri-3	Lørdag	Høylast	B	123,649	123,649	123,649	123,649	123,649	123,649	123,649	123,649	123,649	123,649	123,649	123,649	123,649	123,649	123,649	123,649	123,649	123,649	123,649	123,649	123,649	123,649	123,649	123,649	**2967,576**
Industri-3	Søndag	Høylast	A	0,000	0,000	0,000	0,000	0,000	0,000	0,000	0,000	0,000	0,000	0,000	0,000	0,000	0,000	0,000	0,000	0,000	0,000	0,000	0,000	0,000	0,000	0,000	0,000	**0,000**
Industri-3	Søndag	Høylast	B	123,649	123,649	123,649	123,649	123,649	123,649	123,649	123,649	123,649	123,649	123,649	123,649	123,649	123,649	123,649	123,649	123,649	123,649	123,649	123,649	123,649	123,649	123,649	123,649	**2967,576**
Industri-3	Hverdag	Lavlast	A	0,000	0,000	0,000	0,000	0,000	0,000	0,000	0,000	0,000	0,000	0,000	0,000	0,000	0,000	0,000	0,000	0,000	0,000	0,000	0,000	0,000	0,000	0,000	0,000	**0,000**
Industri-3	Hverdag	Lavlast	B	302,231	302,231	302,231	302,231	302,231	302,231	302,231	302,231	302,231	302,231	302,231	302,231	302,231	302,231	302,231	302,231	302,231	302,231	302,231	302,231	302,231	302,231	302,231	302,231	**7253,544**
Industri-3	Lørdag	Lavlast	A	0,000	0,000	0,000	0,000	0,000	0,000	0,000	0,000	0,000	0,000	0,000	0,000	0,000	0,000	0,000	0,000	0,000	0,000	0,000	0,000	0,000	0,000	0,000	0,000	**0,000**
Industri-3	Lørdag	Lavlast	B	116,219	116,219	116,219	116,219	116,219	116,219	116,219	116,219	116,219	116,219	116,219	116,219	116,219	116,219	116,219	116,219	116,219	116,219	116,219	116,219	116,219	116,219	116,219	116,219	**2789,256**
Industri-3	Søndag	Lavlast	A	0,000	0,000	0,000	0,000	0,000	0,000	0,000	0,000	0,000	0,000	0,000	0,000	0,000	0,000	0,000	0,000	0,000	0,000	0,000	0,000	0,000	0,000	0,000	0,000	**0,000**
Industri-3	Søndag	Lavlast	B	116,219	116,219	116,219	116,219	116,219	116,219	116,219	116,219	116,219	116,219	116,219	116,219	116,219	116,219	116,219	116,219	116,219	116,219	116,219	116,219	116,219	116,219	116,219	116,219	**2789,256**
Varehandel	Hverdag	Høylast	A	-2,612	-2,617	-2,594	-2,581	-2,696	-2,782	-2,786	-2,751	-2,867	-3,604	-4,008	-3,938	-3,910	-3,873	-3,651	-3,415	-3,589	-3,228	-2,871	-3,149	-2,724	-2,948	-2,639	-2,761	**-74,594**
Varehandel	Hverdag	Høylast	B	110,838	112,498	110,461	110,690	110,832	113,092	117,935	128,397	144,894	164,127	170,017	167,751	165,096	164,520	164,238	162,386	161,509	152,737	142,092	121,101	114,631	111,380	110,273	109,250	**3240,745**
Varehandel	Lørdag	Høylast	A	-1,914	-1,892	-2,094	-1,880	-1,847	-1,745	-1,442	-1,704	-3,217	-3,599	-4,055	-4,110	-3,713	-2,869	-1,773	-2,035	-2,125	-2,122	-2,103	-1,897	-1,934	-1,963	-1,781	-2,058	**-55,872**
Varehandel	Lørdag	Høylast	B	109,361	111,910	109,971	111,174	111,817	113,420	117,961	122,651	128,003	132,506	132,730	128,448	126,059	120,693	115,034	106,718	105,483	107,015	111,133	107,470	110,712	110,149	112,517	111,258	**2774,193**
Varehandel	Søndag	Høylast	A	-1,914	-1,892	-2,094	-1,880	-1,847	-1,745	-1,442	-1,704	-3,217	-3,599	-4,055	-4,110	-3,713	-2,869	-1,773	-2,035	-2,125	-2,122	-2,103	-1,897	-1,934	-1,963	-1,781	-2,058	**-55,872**
Varehandel	Søndag	Høylast	B	109,361	111,910	109,971	111,174	111,817	113,420	117,961	122,651	128,003	132,506	132,730	128,448	126,059	120,693	115,034	106,718	105,483	107,015	111,133	107,470	110,712	110,149	112,517	111,258	**2774,193**
Varehandel	Hverdag	Lavlast	A	-1,755	-1,756	-1,635	-1,698	-1,706	-1,837	-1,880	-1,934	-1,811	-2,223	-1,625	-1,557	-1,424	-1,191	-1,129	-1,120	-1,401	-1,197	-1,643	-1,573	-1,894	-1,625	-1,609	-1,627	**-38,850**
Varehandel	Hverdag	Lavlast	B	103,191	104,025	102,465	102,636	103,285	105,903	108,848	119,050	133,031	155,064	163,238	163,159	161,355	159,878	158,227	157,515	156,175	146,592	134,103	115,270	109,813	106,609	103,688	103,144	**3076,264**
Varehandel	Lørdag	Lavlast	A	-1,734	-1,696	-1,552	-1,655	-1,752	-1,919	-1,961	-1,818	-1,996	-1,957	-1,622	-1,374	-1,303	-1,189	-1,402	-1,503	-1,467	-1,484	-1,533	-1,479	-1,851	-1,689	-1,737	-1,740	**-39,413**
Varehandel	Lørdag	Lavlast	B	101,924	102,297	100,746	101,358	102,657	104,326	107,030	111,590	118,848	126,857	128,552	126,623	125,302	119,634	110,033	101,573	100,982	101,975	103,401	100,893	102,497	103,972	104,275	104,586	**2611,931**
Varehandel	Søndag	Lavlast	A	-1,734	-1,696	-1,552	-1,655	-1,752	-1,919	-1,961	-1,818	-1,996	-1,957	-1,622	-1,374	-1,303	-1,189	-1,402	-1,503	-1,467	-1,484	-1,533	-1,479	-1,851	-1,689	-1,737	-1,740	**-39,413**
Varehandel	Søndag	Lavlast	B	101,924	102,297	100,746	101,358	102,657	104,326	107,030	111,590	118,848	126,857	128,552	126,623	125,302	119,634	110,033	101,573	100,982	101,975	103,401	100,893	102,497	103,972	104,275	104,586	**2611,931**
Kontor	Hverdag	Høylast	A	-0,846	-0,472	-0,333	0,667	1,941	1,612	2,740	2,459	-3,175	-4,386	-4,770	-5,197	-5,173	-5,239	-4,945	-4,526	-1,359	-0,581	-0,176	-1,250	-1,718	-1,181	-1,039	-0,971	**-37,918**
Kontor	Hverdag	Høylast	B	111,846	107,133	106,377	112,671	125,561	123,883	149,508	210,079	281,420	301,317	304,861	306,550	305,595	303,247	297,228	284,303	241,682	208,777	185,799	157,850	144,596	129,745	118,621	114,933	**4733,582**
Kontor	Lørdag	Høylast	A	-0,623	-0,206	-0,234	-0,227	-0,168	-0,147	-0,536	-0,739	-0,940	-1,641	-1,701	-1,667	-1,416	-1,181	-0,783	-0,770	-0,892	-0,818	-0,701	-0,600	-0,615	-0,538	-0,685	-0,700	**-18,528**
Kontor	Lørdag	Høylast	B	107,286	102,043	100,498	100,635	99,890	99,892	103,752	104,773	110,019	119,227	123,649	126,109	123,465	123,772	119,859	115,739	115,594	115,150	112,861	112,816	111,567	110,379	110,164	108,648	**2677,787**
Kontor	Søndag	Høylast	A	-0,623	-0,206	-0,234	-0,227	-0,168	-0,147	-0,536	-0,739	-0,940	-1,641	-1,701	-1,667	-1,416	-1,181	-0,783	-0,770	-0,892	-0,818	-0,701	-0,600	-0,615	-0,538	-0,685	-0,700	**-18,528**
Kontor	Søndag	Høylast	B	107,286	102,043	100,498	100,635	99,890	99,892	103,752	104,773	110,019	119,227	123,649	126,109	123,465	123,772	119,859	115,739	115,594	115,150	112,861	112,816	111,567	110,379	110,164	108,648	**2677,787**
Kontor	Hverdag	Lavlast	A	-1,271	-0,953	-0,846	-0,982	-1,045	-1,070	-1,395	-0,494	-2,470	-2,876	-2,842	-2,777	-2,804	-2,853	-3,021	-3,934	-2,237	-1,476	-1,172	-0,714	-0,738	-0,809	-1,074	-1,381	**-41,234**
Kontor	Hverdag	Lavlast	B	104,767	97,558	96,979	103,395	103,837	103,557	128,651	190,887	273,450	295,530	300,267	302,200	302,231	299,898	294,786	279,434	224,146	190,067	170,029	151,208	138,950	125,529	113,548	110,230	**4501,134**
Kontor	Lørdag	Lavlast	A	-1,348	-0,969	-0,962	-0,915	-0,987	-1,084	-1,432	-1,319	-0,973	-0,902	-0,898	-0,936	-0,930	-0,888	-0,891	-1,057	-1,074	-1,099	-1,166	-1,142	-1,062	-1,022	-1,033	-1,324	**-25,413**
Kontor	Lørdag	Lavlast	B	102,693	95,583	94,579	93,518	93,080	93,274	98,590	99,517	103,657	112,609	116,219	118,420	115,529	115,706	113,198	110,192	109,004	108,388	106,635	105,765	104,348	103,586	103,264	102,731	**2520,085**
Kontor	Søndag	Lavlast	A	-1,348	-0,969	-0,962	-0,915	-0,987	-1,084	-1,432	-1,319	-0,973	-0,902	-0,898	-0,936	-0,930	-0,888	-0,891	-1,057	-1,074	-1,099	-1,166	-1,142	-1,062	-1,022	-1,033	-1,324	**-25,413**
Kontor	Søndag	Lavlast	B	102,693	95,583	94,579	93,518	93,080	93,274	98,590	99,517	103,657	112,609	116,219	118,420	115,529	115,706	113,198	110,192	109,004	108,388	106,635	105,765	104,348	103,586	103,264	102,731	**2520,085**
Hotell	Hverdag	Høylast	A	-4,106	-4,058	-4,236	-4,330	-4,532	-4,617	-4,234	-4,617	-5,064	-4,488	-4,283	-3,877	-3,787	-3,839	-3,995	-3,668	-3,956	-4,294	-4,744	-4,942	-4,934	-5,009	-4,798	-4,293	**-104,701**
Hotell	Hverdag	Høylast	B	216,687	209,124	201,458	198,723	199,205	203,251	218,231	244,470	262,273	266,783	267,072	265,913	262,562	261,495	261,050	261,827	264,649	272,076	279,040	279,096	274,564	265,588	250,640	234,789	**5920,566**
Hotell	Lørdag	Høylast	A	-4,706	-4,560	-4,646	-4,489	-4,519	-4,758	-4,582	-4,410	-4,839	-4,730	-4,256	-3,748	-3,697	-3,490	-4,035	-3,889	-3,933	-4,721	-5,026	-5,108	-5,050	-5,142	-4,944	-4,119	**-107,397**
Hotell	Lørdag	Høylast	B	225,935	217,868	207,254	202,275	200,316	202,241	214,011	234,967	256,995	266,560	265,687	265,389	262,569	261,965	262,643	263,581	265,399	269,624	274,650	273,177	268,588	258,711	245,202	230,078	**5895,685**
Hotell	Søndag	Høylast	A	-4,706	-4,560	-4,646	-4,489	-4,519	-4,758	-4,582	-4,410	-4,839	-4,730	-4,256	-3,748	-3,697	-3,490	-4,035	-3,889	-3,933	-4,721	-5,026	-5,108	-5,050	-5,142	-4,944	-4,119	**-107,397**
Hotell	Søndag	Høylast	B	225,935	217,868	207,254	202,275	200,316	202,241	214,011	234,967	256,995	266,560	265,687	265,389	262,569	261,965	262,643	263,581	265,399	269,624	274,650	273,177	268,588	258,711	245,202	230,078	**5895,685**
Hotell	Hverdag	Lavlast	A	-5,323	-5,267	-5,115	-5,129	-5,150	-5,104	-5,014	-5,184	-5,333	-5,234	-5,058	-5,145	-5,113	-5,119	-5,125	-5,181	-5,384	-5,467	-5,540	-5,387	-5,385	-5,560	-5,486	-5,486	**-126,289**
Hotell	Hverdag	Lavlast	B	191,258	182,741	175,994	174,114	175,180	182,153	197,359	220,234	234,579	237,352	237,268	236,398	233,302	233,171	233,139	233,717	236,153	240,649	244,797	243,813	240,310	233,812	220,905	205,791	**5244,189**
Hotell	Lørdag	Lavlast	A	-5,864	-5,780	-5,462	-5,372	-5,363	-5,371	-5,310	-5,149	-5,318	-5,421	-5,345	-5,500	-5,468	-5,356	-5,502	-5,378	-5,513	-5,672	-5,584	-5,582	-5,451	-5,494	-5,682	-5,779	**-131,716**
Hotell	Lørdag	Lavlast	B	200,431	191,319	181,591	176,715	175,813	181,644	194,863	210,667	227,700	236,132	236,373	235,924	233,558	232,553	234,276	234,023	234,692	238,121	239,328	237,387	230,530	223,295	214,036	201,862	**5202,833**
Hotell	Søndag	Lavlast	A	-5,864	-5,780	-5,462	-5,372	-5,363	-5,371	-5,310	-5,149	-5,318	-5,421	-5,345	-5,500	-5,468	-5,356	-5,502	-5,378	-5,513	-5,672	-5,584	-5,582	-5,451	-5,494	-5,682	-5,779	**-131,716**
Hotell	Søndag	Lavlast	B	200,431	191,319	181,591	176,715	175,813	181,644	194,863	210,667	227,700	236,132	236,373	235,924	233,558	232,553	234,276	234,023	234,692	238,121	239,328	237,387	230,530	223,295	214,036	201,862	**5202,833**
Skole	Hverdag	Høylast	A	-2,406	-2,275	-2,520	-2,359	-2,263	-1,573	-0,432	-1,002	-0,808	-1,223	-1,285	-1,267	-1,341	-1,290	-2,398	-3,000	-3,109	-3,291	-3,337	-3,221	-3,126	-2,915	-2,693	-2,611	**-51,745**
Skole	Hverdag	Høylast	B	90,975	92,555	93,319	97,401	100,160	107,593	118,490	127,714	152,261	152,257	146,396	140,209	140,976	137,878	120,907	106,039	100,785	97,829	100,798	102,293	99,948	96,100	91,335	91,078	**2705,296**
Skole	Lørdag	Høylast	A	-2,046	-2,219	-2,129	-2,137	-1,916	-2,097	-2,113	-2,079	-1,831	-2,187	-2,485	-2,561	-2,789	-2,823	-2,900	-2,788	-2,820	-2,820	-2,861	-2,843	-2,522	-2,274	-2,152	-2,380	**-57,772**
Skole	Lørdag	Høylast	B	93,737	93,344	94,770	96,034	97,918	97,476	96,776	97,898	97,067	94,645	91,294	89,591	86,184	83,887	81,472	80,833	82,390	86,195	89,821	89,171	88,184	88,463	89,548	90,062	**2176,760**
Skole	Søndag	Høylast	A	-2,046	-2,219	-2,129	-2,137	-1,916	-2,097	-2,113	-2,079	-1,831	-2,187	-2,485	-2,561	-2,789	-2,823	-2,900	-2,788	-2,820	-2,820	-2,861	-2,843	-2,522	-2,274	-2,152	-2,380	**-57,772**
Skole	Søndag	Høylast	B	93,737	93,344	94,770	96,034	97,918	97,476	96,776	97,898	97,067	94,645	91,294	89,591	86,184	83,887	81,472	80,833	82,390	86,195	89,821	89,171	88,184	88,463	89,548	90,062	**2176,760**
Skole	Hverdag	Lavlast	A	-3,289	-3,412	-3,540	-3,592	-4,046	-4,858	-5,068	-5,711	-6,078	-5,733	-5,391	-5,224	-5,203	-4,959	-4,658	-4,732	-4,861	-4,312	-4,144	-3,822	-3,299	-3,275	-3,230	-3,278	**-105,715**
Skole	Hverdag	Lavlast	B	84,052	84,903	86,994	88,498	95,165	111,333	122,419	135,004	156,726	157,593	152,734	147,327	146,370	142,703	130,443	122,671	116,353	104,874	104,661	101,155	93,028	89,456	85,122	83,330	**2742,914**
Skole	Lørdag	Lavlast	A	-3,174	-3,187	-3,259	-3,425	-3,370	-3,612	-3,582	-3,776	-3,765	-3,588	-3,595	-3,489	-3,447	-3,586	-3,184	-3,287	-3,550	-3,562	-3,690	-3,530	-3,096	-3,324	-3,464	-3,443	**-82,985**
Skole	Lørdag	Lavlast	B	84,693	84,943	84,586	86,371	86,733	88,448	88,908	90,522	91,141	90,915	89,190	88,167	87,499	86,313	85,602	86,315	88,010	89,817	90,431	89,337	86,423	85,152	84,314	84,520	**2098,350**
Skole	Søndag	Lavlast	A	-3,174	-3,187	-3,259	-3,425	-3,370	-3,612	-3,582	-3,776	-3,765	-3,588	-3,595	-3,489	-3,447	-3,586	-3,184	-3,287	-3,550	-3,562	-3,690	-3,530	-3,096	-3,324	-3,464	-3,443	**-82,985**
Skole	Søndag	Lavlast	B	84,693	84,943	84,586	86,371	86,733	88,448	88,908	90,522	91,141	90,915	89,190	88,167	87,499	86,313	85,602	86,315	88,010	89,817	90,431	89,337	86,423	85,152	84,314	84,520	**2098,350**
Helse og sosial	Hverdag	Høylast	A	-31,718	-31,907	-32,174	-32,463	-32,419	-33,301	-32,433	-39,244	-34,096	-34,919	-32,243	-31,967	-34,731	-32,266	-37,343	-34,895	-33,017	-34,646	-34,131	-34,149	-34,001	-33,953	-32,634	-32,445	**-807,095**
Helse og sosial	Hverdag	Høylast	B	1050,539	1043,606	1040,771	1038,470	1043,435	1050,765	1145,913	1420,601	1621,464	1618,141	1683,880	1603,700	1526,940	1513,810	1442,782	1296,273	1211,546	1179,073	1186,771	1152,486	1109,456	1083,735	1058,074	1046,175	**30168,406**
Helse og sosial	Lørdag	Høylast	A	-30,022	-30,907	-30,497	-30,624	-31,235	-31,274	-30,235	-34,664	-31,964	-33,849	-31,399	-31,067	-32,771	-30,149	-30,484	-28,418	-28,417	-30,194	-29,921	-31,371	-31,665	-31,547	-30,392	-29,635	**-742,701**
Helse og sosial	Lørdag	Høylast	B	1039,390	1029,484	1030,721	1027,828	1025,552	1032,908	1101,055	1230,824	1281,727	1296,001	1306,403	1261,292	1197,546	1189,458	1170,654	1145,819	1127,694	1124,559	1142,658	1116,746	1081,119	1055,262	1034,463	1026,381	**27075,544**
Helse og sosial	Søndag	Høylast	A	-30,022	-30,907	-30,497	-30,624	-31,235	-31,274	-30,235	-34,664	-31,964	-33,849	-31,399	-31,067	-32,771	-30,149	-30,484	-28,418	-28,417	-30,194	-29,921	-31,371	-31,665	-31,547	-30,392	-29,635	**-742,701**
Helse og sosial	Søndag	Høylast	B	1039,390	1029,484	1030,721	1027,828	1025,552	1032,908	1101,055	1230,824	1281,727	1296,001	1306,403	1261,292	1197,546	1189,458	1170,654	1145,819	1127,694	1124,559	1142,658	1116,746	1081,119	1055,262	1034,463	1026,381	**27075,544**
Helse og sosial	Hverdag	Lavlast	A	-31,226	-31,162	-31,217	-31,315	-31,366	-31,581	-32,462	-36,925	-34,616	-32,223	-33,852	-33,557	-32,432	-33,151	-35,414	-34,425	-34,158	-33,817	-32,966	-32,313	-32,169	-31,939	-31,814	-31,734	**-787,834**
Helse og sosial	Hverdag	Lavlast	B	1047,507	1037,610	1035,683	1033,279	1035,930	1047,169	1130,662	1446,266	1621,148	1643,134	1701,602	1622,837	1564,323	1552,950	1499,838	1332,750	1239,387	1208,894	1199,303	1161,024	1139,271	1118,694	1092,305	1065,910	**30577,476**
Helse og sosial	Lørdag	Lavlast	A	-29,496	-29,856	-29,391	-29,349	-29,517	-30,075	-31,127	-33,476	-32,424	-31,189	-30,931	-29,626	-28,963	-29,541	-29,624	-30,166	-30,902	-31,106	-30,794	-30,278	-30,004	-29,462	-29,143	-29,106	**-725,546**
Helse og sosial	Lørdag	Lavlast	B	1039,224	1033,371	1027,648	1023,069	1026,746	1042,150	1094,224	1235,552	1273,124	1307,542	1317,396	1268,146	1226,543	1223,759	1186,703	1152,404	1138,119	1125,825	1134,554	1111,511	1096,046	1079,375	1058,400	1033,577	**27255,008**
Helse og sosial	Søndag	Lavlast	A	-29,496	-29,856	-29,391	-29,349	-29,517	-30,075	-31,127	-33,476	-32,424	-31,189	-30,931	-29,626	-28,963	-29,541	-29,624	-30,166	-30,902	-31,106	-30,794	-30,278	-30,004	-29,462	-29,143	-29,106	**-725,546**
Helse og sosial	Søndag	Lavlast	B	1039,224	1033,371	1027,648	1023,069	1026,746	1042,150	1094,224	1235,552	1273,124	1307,542	1317,396	1268,146	1226,543	1223,759	1186,703	1152,404	1138,119	1125,825	1134,554	1111,511	1096,046	1079,375	1058,400	1033,577	**27255,008**
Elkjel	Hverdag	Høylast	A	-17,284	-16,503	-19,098	-20,426	-21,075	-22,487	-22,774	-30,221	-33,447	-31,141	-30,605	-29,259	-27,927	-24,043	-22,417	-22,746	-20,257	-18,875	-19,221	-17,485	-18,361	-18,044	-17,744	-16,849	**-538,289**
Elkjel	Hverdag	Høylast	B	447,849	441,503	425,235	432,638	436,285	447,855	515,413	589,043	638,532	643,454	639,390	638,104	631,699	616,415	604,132	599,550	586,420	550,348	556,456	533,238	509,749	490,718	467,521	448,024	**12889,571**
Elkjel	Lørdag	Høylast	A	-3,924	-3,800	-6,290	-9,357	-10,456	-11,601	-8,443	-9,612	-12,750	-12,313	-17,663	-9,099	-8,365	-4,835	-1,756	0,098	2,143	1,704	-1,596	-4,106	-5,822	-6,207	-7,921	-8,198	**-160,169**
Elkjel	Lørdag	Høylast	B	425,988	431,453	415,589	418,182	422,411	423,669	452,001	457,269	472,189	485,759	485,811	503,571	500,573	492,582	465,295	465,527	462,820	464,741	469,174	468,971	460,731	457,984	456,365	452,749	**11011,404**
Elkjel	Søndag	Høylast	A	-3,924	-3,800	-6,290	-9,357	-10,456	-11,601	-8,443	-9,612	-12,750	-12,313	-17,663	-9,099	-8,365	-4,835	-1,756	0,098	2,143	1,704	-1,596	-4,106	-5,822	-6,207	-7,921	-8,198	**-160,169**
Elkjel	Søndag	Høylast	B	425,988	431,453	415,589	418,182	422,411	423,669	452,001	457,269	472,189	485,759	485,811	503,571	500,573	492,582	465,295	465,527	462,820	464,741	469,174	468,971	460,731	457,984	456,365	452,749	**11011,404**
Elkjel	Hverdag	Lavlast	A	-20,190	-20,829	-19,613	-20,432	-20,445	-20,301	-20,618	-24,521	-28,737	-30,052	-30,569	-31,194	-31,482	-31,041	-30,251	-30,796	-30,298	-27,853	-26,904	-24,365	-22,993	-21,568	-20,516	-19,796	**-605,364**
Elkjel	Hverdag	Lavlast	B	420,315	416,822	393,742	399,727	401,357	409,795	479,844	544,315	600,589	620,049	621,963	617,173	609,829	596,422	582,623	583,795	577,699	546,821	538,112	511,956	495,302	476,396	458,466	433,298	**12336,410**
Elkjel	Lørdag	Lavlast	A	-18,114	-18,272	-17,438	-18,262	-18,079	-18,437	-18,785	-19,126	-20,399	-21,303	-21,766	-22,782	-22,901	-23,581	-22,038	-22,396	-22,811	-22,649	-22,204	-22,510	-22,039	-21,768	-21,358	-21,645	**-500,663**
Elkjel	Lørdag	Lavlast	B	394,262	387,472	370,409	373,321	372,444	377,563	418,830	423,674	439,092	459,483	475,782	487,929	485,269	484,283	460,815	458,179	461,110	461,939	463,260	467,822	462,565	458,246	453,674	443,967	**10541,390**
Elkjel	Søndag	Lavlast	A	-18,114	-18,272	-17,438	-18,262	-18,079	-18,437	-18,785	-19,126	-20,399	-21,303	-21,766	-22,782	-22,901	-23,581	-22,038	-22,396	-22,811	-22,649	-22,204	-22,510	-22,039	-21,768	-21,358	-21,645	**-500,663**
Elkjel	Søndag	Lavlast	B	394,262	387,472	370,409	373,321	372,444	377,563	418,830	423,674	439,092	459,483	475,782	487,929	485,269	484,283	460,815	458,179	461,110	461,939	463,260	467,822	462,565	458,246	453,674	443,967	**10541,390**

B Appendix B - Charging curves

To accurately model the load from each EV, individual charging curves from each EV model has been used. Most EV companies doesn't publish charging curves for their EV. The majority of the curves used in this thesis are from the Fastned. Fastned builds and operates FCS in Netherlands. All the charging curves are plotted with charging power dependent on SOC.

B.1 EV fleet

B.1.1 Nissan Leaf

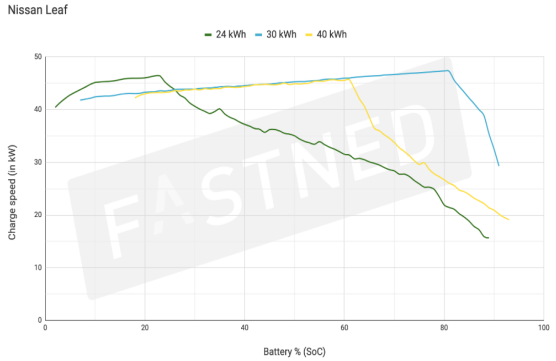

Figure 62: Measured charging curve for Nissan Leaf from [72]

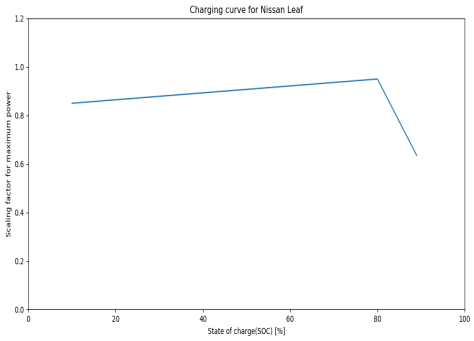

Figure 63: Modeled charging curve for Nissan Leaf.

B.1.2 Volkswagen e-Golf

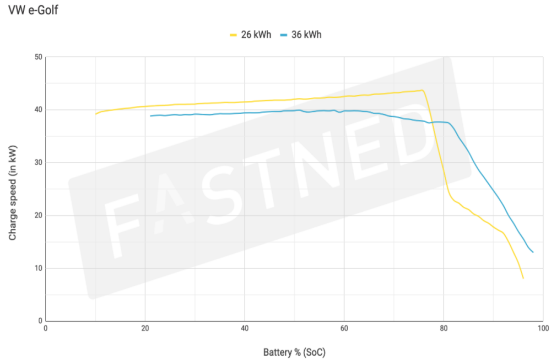

Figure 64: Measured charging curve for Volkswagen e-Golf from [73]

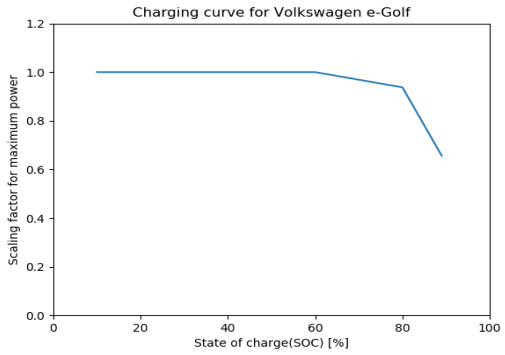

Figure 65: Modeled charging curve for Volkswagen e-Golf

B.1.3 BMW i3

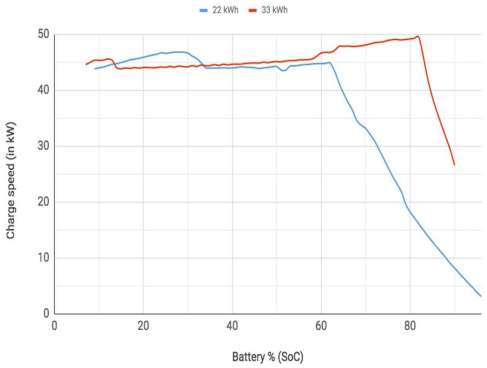

Figure 66: Measured charging curve for BMW i3 from [74]

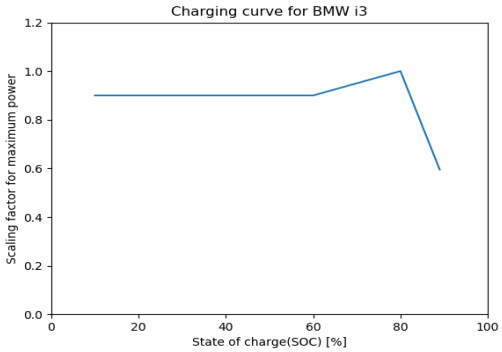

Figure 67: Modeled charging curve for BMW i3

B.1.4 Kia e-Soul

Kia e-Soul has no published charging curve. Therefore, due to the low maximum charging power, constant charging at maximum power is assumed.

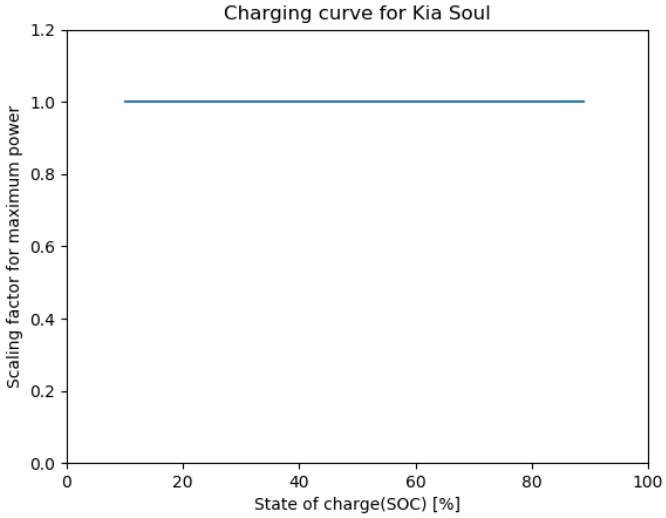

Figure 68: Modeled charging curve for Kia e-Soul.

B.1.5 Volkswagen Up!

Volkswagen Up! has no published charging curve. Therefore, due to the low maximum charging power, constant charging at maximum power is assumed.

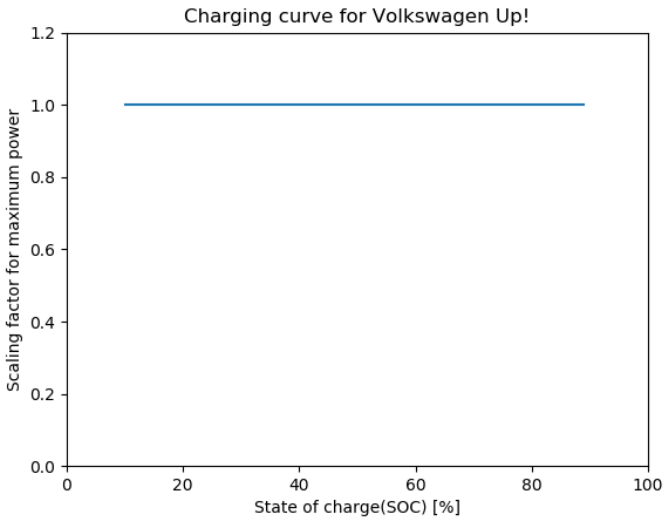

Figure 69: Modeled charging curve for Volkswagen Up!l

B.1.6 Hyundai Ioniq

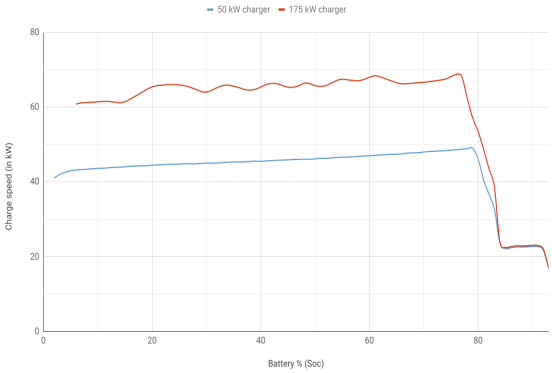

Figure 70: Measured charging curve for Hyundai Ioniq from [75]

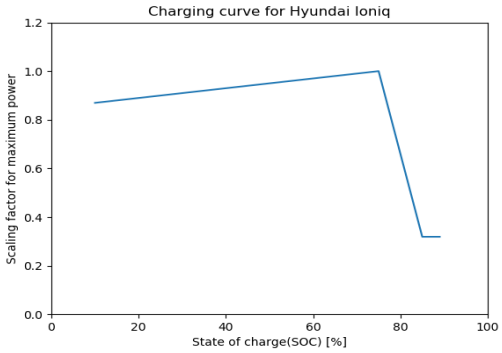

Figure 71: Modeled charging curve for Hyundai Ioniq.

B.1.7 Nissan E-nv200

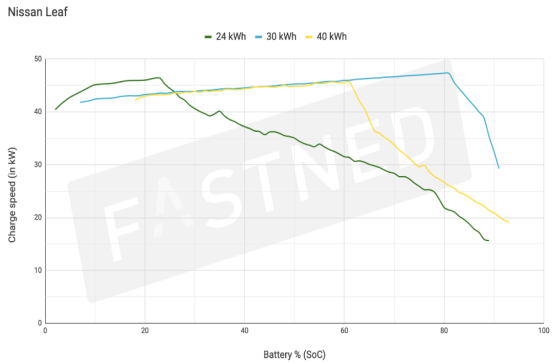

Figure 72: Measured charging curve for Nissan e-NV200 form [72]

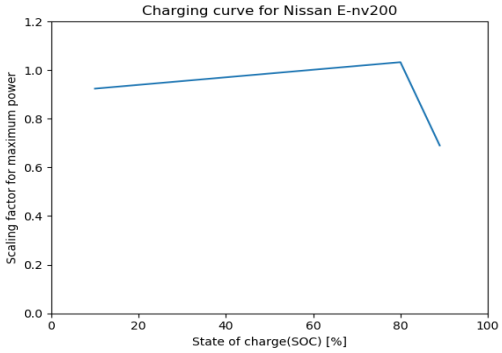

Figure 73: Modeled charging curve for Nissan e-NV200.

B.1.8 Mitsubishi I-miev

Mitsubishi I-miev has no published charging curve. Therefore, due to the low maximum charging power, constant charging at maximum power is assumed.

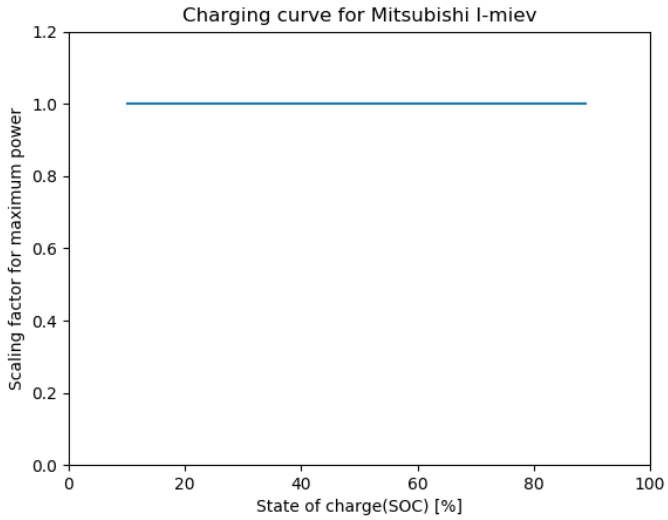

Figure 74: Modeled charging curve for Mitsubishi I-miev.

B.1.9 Jaguar I-pace

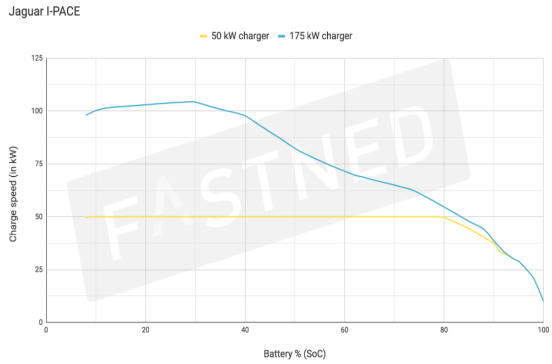

Figure 75: Measured charging curve for Jaguar I-pace from [77]

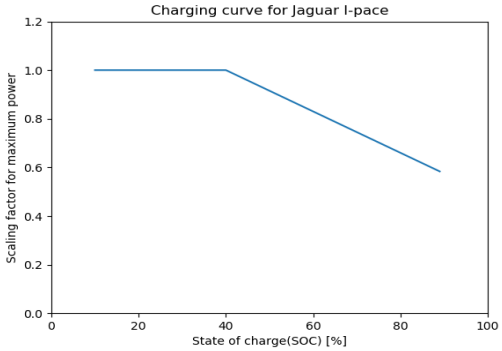

Figure 76: Modeled charging curve for Jaguar I-pace.

B.1.10 Audi e-tron

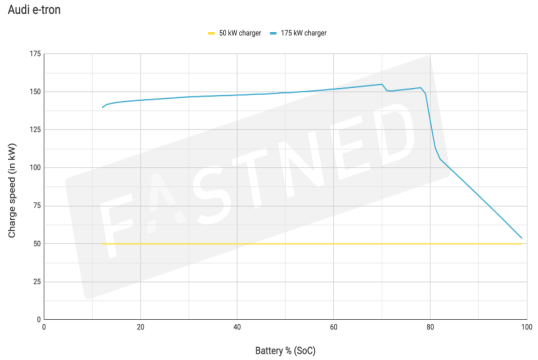

Figure 77: Measured charging curve for Audi e-tron [78]

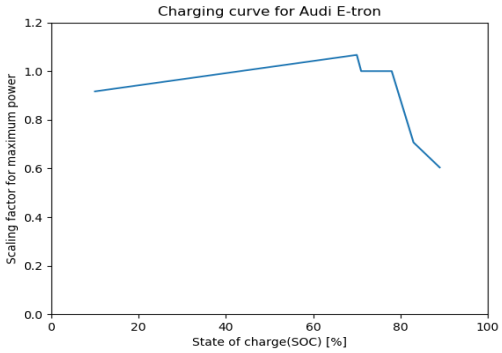

Figure 78: Modeled charging curve for Audi e-tron.

B.1.11 Opel Ampera-e

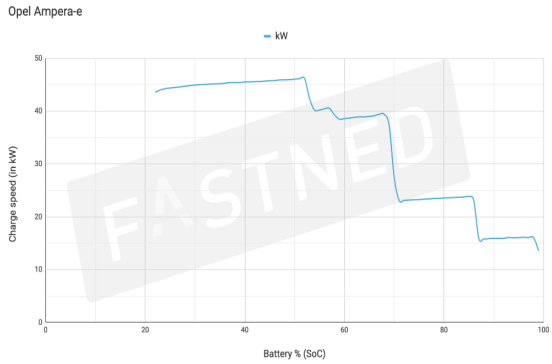

Figure 79: Measured charging curve for Opel Ampera-e from [80]

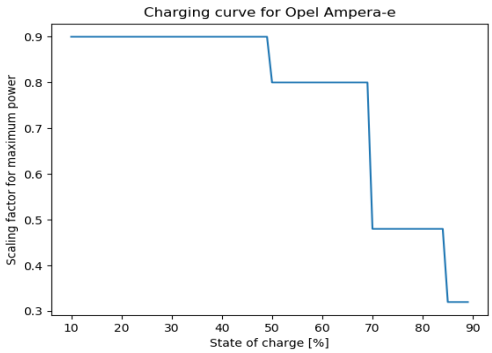

Figure 80: Modeled charging curve for Opel Ampera-e.

C Appendix C - Distribution grids

C.1 Distribution grid 1: Dal - Hovinmoen

Table 11: Information about the lines of distribution system 1

Line nr.	Line length [m]	FeAl nr.	From bus	To bus
1	370	10	1	2
2	370	10	2	3
3	540	10	3	4
4	1280	10	4	5
5	2600	10	5	6
6	540	10	6	7
7	380	10	7	8
8	130	10	7	9
9	330	10	9	10
10	2050	10	9	11
11	360	10	11	12
12	710	10	12	13
13	1400	10	12	14
14	900	10	11	15
15	210	10	5	16
16	400	10	16	17
17	610	10	16	18
18	480	10	18	19
19	500	10	18	20
20	510	10	20	21
21	1070	10	21	22

Table 12: Information about the load of distribution system 1

Distribution grid 1	
Bus	**Load**
2	50 housholds
4	1 farm, 1 nursing home
5	190 households, 1 school, 2 grocery shops
6	15 households, 1 nursing home
8	11 households, 1 farm
10	1 household, 1 farm
13	1 households, 3 farms, 1 auto shop
14	10 households, 1 kindergarten, 1 medium industry load
17	8 households, 1 farm
19	140 households
20	40 households
21	5 households, 1 farm
22	7 households, 2 farms

C.2 Distribution grid 2: Hammerstad - Dal

Table 13: Information about the lines of distribution system 2

Line nr.	Line length [m]	FeAl nr.	From bus	To bus
1	1300	70	1	2
2	480	70	2	3
3	320	10	3	4
4	270	10	4	5
5	180	10	5	6
6	200	10	5	7
7	330	70	3	8
8	690	10	8	9
9	1490	70	8	10
10	530	70	10	11
11	480	70	11	12
12	340	10	12	13
13	400	70	12	14
14	560	10	14	15
15	470	70	14	16
16	470	10	16	17
17	260	70	17	18
18	300	10	18	19
19	640	10	19	20
20	540	70	18	21
21	540	50	21	22
22	690	50	22	23
23	650	50	23	24
24	300	16	24	25
25	460	25	24	26
26	560	10	26	27
27	590	10	27	28
28	300	10	28	29
29	1600	10	28	30
30	230	10	27	31
31	880	50	23	32
32	340	10	32	33
33	570	50	32	34
34	1940	50	34	35
35	1150	50	35	36
36	680	40	36	37
37	460	40	37	38
38	990	40	38	39

Table 14: Information about the load of distribution system 2

Distribution grid 2	
Bus	**Load**
2	130 housholds
3	90 households
4	100 households
5	150 households
6	40 households
7	100 households
9	3 households, 5 farms
10	1 household, 1 farm
11	3 households, 2 farms
13	1 household, 3 farms
15	2 shops
16	28 households, 1 farm
17	39 households
19	60 households
20	30 households, 2 farms
22	160 households, 1 farm, 2 schools, 1 kindergarten
25	320 households, 2 offices
26	270 households, 3 shops, 3 offices, 1 school
29	310 housesholds
30	4 households, 3 farms
31	370 households, 1 nursing home
33	130 households, 1 nursing home
35	40 households, 2 auto shops
36	430 households, 1 school, 1 kindergarten
37	200 households
38	130 households

C.3 Distribution grid 3: Minnesund - Hammerstad

Table 15: Information about the lines of distribution system 3

Line nr.	Line length [m]	FeAl nr.	From bus	To bus
1	1050	25	1	2
2	830	25	2	3
3	820	25	3	4
4	430	16	4	5
5	460	16	5	6
6	570	16	6	7
7	950	16	7	8
8	610	10	8	9
9	820	10	8	10
10	1410	10	10	11
11	430	10	11	12
12	420	10	12	13
13	890	10	12	14
14	1300	10	10	15
15	2290	10	15	16
16	920	10	16	17
17	1260	10	17	18

Table 16: Information about the load of distribution system 3

Distribution grid 3	
Bus	**Load**
2	14 housholds
3	2 households, 1 farm
4	380 households, 16 farms, 2 schools, 1 kindergarten
5	43 households
6	35 households, 5 farms
7	10 households, 3 farms
8	110 households
9	90 households, 3 shops, 1 small-size industry, 1 medium-size industry, 2 auto shops, 5 offices
10	11 households, 1 farm, 1 kindergarten, 1 hotel
11	24 households
13	27 households
14	34 households, 6 farms
15	38 households, 3 farms
16	57 households, 7 farms
17	36 households, 4 farms

C.4 Distribution grid 4: Skrårud - Minnesund

Table 17: Information about the lines of distribution system 4

Line nr.	Line length [m]	FeAl nr.	From bus	To bus
1	1600	10	1	2
2	510	10	2	3
3	1030	10	3	4
4	700	10	4	5
5	600	10	5	6
6	630	10	5	7
7	730	10	7	8
8	1900	10	8	9
9	2600	10	9	10
10	1230	10	10	11
11	2250	10	11	12

Table 18: Information about the load of distribution system 4

Distribution grid 4	
Bus	**Load**
3	25 housholds
4	130 households, 1 school
5	25 households, 2 farms
7	19 households
8	31 households
9	84 households, 3 farms
10	36 households, 2 farms
11	31 households, 7 farms
12	3 farms

C.5 Distribution grid 5: Espa - Strandlykkja

Table 19: Information about the lines of distribution system 5

Line nr.	Line length [m]	FeAl nr.	From bus	To bus
1	450	10	1	2
2	3760	10	2	3
3	380	10	3	4
4	1020	10	4	5
5	1280	10	5	6
6	1030	10	6	7

Table 20: Information about the load of distribution system 5

Distribution grid 5	
Bus	**Load**
2	45 housholds, 8 farms
3	15 households, 2 farns
4	94 households, 3 farms
5	88 households, 1 school, 2 businesses
6	155 households, 3 farms, 1 medium-size industry
7	58 households, 1 farm

C.6 Distribution grid 6: Tangen

Table 21: Information about the lines of distribution system 6

Line nr.	Line length [m]	FeAl nr.	From bus	To bus
1	440	70	1	2
2	460	10	2	3
3	2220	10	3	4
4	1400	25	2	5
5	800	25	5	6
6	1840	25	6	7
7	1770	25	7	8
8	2430	16	8	9
9	750	10	9	10
10	1500	10	10	11
11	1320	10	11	12
12	1530	10	12	13
13	1500	10	13	14
14	2240	10	14	15
15	900	16	5	12

Table 22: Information about the load of distribution system 6

Distribution grid 6	
Bus	**Load**
3	3 housholds, 1 farm, 1 grocery shop
4	14 households, 3 farns
6	3 households, 2 farms
7	14 households, 3 farms
8	165 households, 15 farms
9	130 households, 40 farms
10	20 households, 5 farms
11	117 households, 15 farms
13	25 households, 4 farms
14	14 households, 4 farms
15	50 households, 5 farms

C.7 Distribution grid 7: Stange

Table 23: Information about the lines of distribution system 7

Line nr.	Line length [m]	FeAl nr.	From bus	To bus
1	200	25	1	2
2	1670	25	2	3
3	1020	25	3	4
4	1720	16	4	5
5	1260	10	5	6
6	850	10	6	7
7	1860	16	5	8
8	1720	10	8	9
9	960	10	9	10
10	2690	10	10	11

Table 24: Information about the load of distribution system 7

Distribution grid 7	
Bus	**Load**
3	85 housholds, 5 farms
4	27 households, 4 farns
6	15 households, 2 farms
7	145 households, 8 farms
8	24 households, 5 farms
9	12 households, 4 farms
11	220 households, 4 farms, 1 school, 1 kindergarten, 1 grocery shop

Eirik Ivarsøy

Optimal planning of fast charging stations for EVs – A Norwegian case study

NTNU
Norwegian University of
Science and Technology